A DYNAMIC SIMULATION MODEL OF CARBON CIRCULATION AND METHANE FEEDBACKS IN ANTHROPOGENIC CLIMATE CHANGE

by

YEŞİM ATAĞ AKPINAR

B.S., in Civil Engineering, Boğaziçi University, 1992

Submitted to the Institute of Environmental Sciences in partial fulfillment of the requirements for the degree of

Master of Science

in

Environmental Technology

Boğaziçi University

2010

A DYNAMIC SIMULATION MODEL OF CARBON CIRCULATION AND METHANE FEEDBACKS IN ANTHROPOGENIC CLIMATE CHANGE

APPROVED BY:

Assoc. Prof. Dr. Ali Kerem Saysel (Thesis Supervisor)	.....
Assoc. Prof. Dr. Nadim Copty	.....
Prof. Dr. Nüzhet Dalfes	.....

DATE OF APPROVAL: 02/02/2010

ACKNOWLEDGEMENTS

First and foremost, I offer my sincerest gratitude to my supervisor, Assoc. Prof. Dr. Ali Kerem Saysel, for his valuable support, continuous guidance and patience on the way to completion of my thesis. It is a pleasure to pay tribute also to the esteemed academic and administrative staff of the Institute of Environmental Sciences for their meaningful contribution and assistance.

I am thankful to my dear friends Özlem and Tanyeli, who motivated me immensely on taking the decision of pursuing a master's degree after 15 years of my university graduation and, continued to support me during the times I lacked energy and enthusiasm.

I especially want to express my gratitude to my dear friend Feza, for her enormous support in the final editing and formatting process of this dissertation.

Finally, I would like to thank my beloved husband for the positive attitude and patience he has provided during my graduate studies, my little son, who always kept my spirit high with his joy, my parents and all the members of my beautiful family, and, my precious friends, for their constant support and encouragement.

ABSTRACT

The human induced climate change is the most serious and difficult environmental issue to manage that has emerged in the recent decades. The complexity of this problem lies in the fact that if the increase in atmospheric greenhouse gas concentrations continue in an uncontrolled manner, its potential damage can be very severe but the costs associated with the mitigation activities are very high. Although the severity of the problem and the need for urgent action are unquestionable today, people usually prefer 'wait and see' policies instead of prompt action. One reason of this tendency is inherent difficulties of understanding the dynamics of anthropogenic climate change and anticipating the possible future results of today's actions. Climate change is a good example of a dynamic systems problem. It embodies several delays, feedbacks, nonlinearities and uncertainties in its dynamically complex structure. Therefore, the need for and the usefulness of descriptive and simpler models that explain these dynamic complexities are undisputed.

The aim of this study is to construct such a dynamic simulation model. The method used is system dynamics, which is a powerful approach to model and analyze complex dynamic systems to create hypotheses on structure and to predict future behavior. The model integrates several components of the climate system. It includes the carbon cycle, radiative forcing of CO_2, CH_4, N_2O and induced temperature change as well as the temperature feedback affecting terrestrial carbon absorption rates. It also proposes a representation of the permafrost melting and methane feedback process. The model aims at enabling the user to test the effects of these feedbacks, the emission scenarios and parameter uncertainty on greenhouse gas concentrations and average surface temperature change. The simulation length is 240 years from 1860 to 2100. Model structure is validated with indirect structure tests. Historical emissions and temperature change data are used to calibrate the model behavior. Model reference behavior is based on IS92a emission scenario of IPCC.

The model can be transformed to an interactive learning environment and be used as a tool to improve the public understanding about dynamics of climate change and to increase awareness. It is also possible to develop it and to transform to a web application that enables the users to test different policy options and observe the results.

ÖZET

İnsan kaynaklı iklim değişimi, yakın geçmişte ortaya çıkan en ciddi ve kontrolü zor çevresel sorunlardan biridir. Sorunun karmaşıklığı; atmosferdeki sera gazı yoğunluklarındaki artış kontrolsüz bir şekilde devam ettiği takdirde zararının çok ciddi olacağı, fakat bunu azaltma çalışmalarının maliyetinin de çok yüksek olduğu gerçeğinden kaynaklanmaktadır. Bugün sorunun ciddiyeti ve acil eylem gerekliliği sorgulanamaz olmasına rağmen, genellikle acil eylem yerine 'bekle-gör' politikaları tercih edilmektedir. Bu eğilimin nedeni insanoğlunun, insan kaynaklı iklim değişiminin dinamiklerini anlaması ve bugünkü eylemlerinin gelecekteki sonuçlarını öngörmesindeki yapısal güçlüklerdir. İklim değişimi iyi bir 'dinamik sistem problemi' örneğidir. Karmaşık dinamik yapısı içinde birçok gecikme, geribildirim ve belirsizlikler barındırır. Bu nedenle bu dinamik karmaşıklıkları açıklayan betimleyici ve basit modellerin yararı ve bunlara olan ihtiyaç tartışılmaz bir gerçekliktir.

Bu çalışmanın amacı böyle bir dinamik simulasyon modeli oluşturmaktır. Bunun için karmaşık dinamik sistemleri kavramsallaştırmak, modellemek ve yapıları üzerine varsayımlar oluşturup gelecekteki davranışlarını öngörmek için güçlü bir araç olan 'sistem dinamiği' yaklaşımı kullanılmıştır. Model, iklim sisteminin farklı bileşenlerini biraraya getirmekte ve karbon döngüsü, CO_2, CH_4, N_2O gazlarının ısınımsal zorlamaları ve bunun neden olduğu sıcaklık değişimi ile birlikte karasal karbon emilim oranlarını etkileyen sıcaklık geribildirimini de içermektedir. Ayrıca permafrost erimesi ve metan geribildirim döngüleri için de bir gösterim şekli önermektedir. Model, kullanıcıya bu geribildirimler, emisyon senaryoları ve parametre belirsizliklerinin sera gazı yoğunlukları ve ortalama yüzey sıcaklığı değişimi üzerindeki etkilerini test edebilme imkanını sunmaktadır. Simulasyonun uzunluğu 1860'tan 2100'e 240 yıldır. Model yapısının geçerliliği dolaylı yapısal testlerle sınanmıştır. Model davranışını kalibre etmek için geçmişe ait emisyon ve sıcaklık verileri, modelin referans davranışında ise IPCC'nin IS92a emisyon senaryosu kullanılmıştır.

Model bir interaktif öğrenme ortamına dönüştürülebilir ve kişilerin iklim değişiminin dinamikleri hakkındaki anlayışını geliştirmek ve farkındalıklarını arttırmak için bir araç olarak kullanılabilir. Ayrıca geliştirilerek, kullanıcıların farklı politika seçeneklerini test edip sonuçlarını gözlemleyebilecekleri bir web uygulamasına da dönüştürülebilir.

TABLE OF CONTENTS

LIST OF FIGURES

LIST OF TABLES

LIST OF SYMBOLS and ABBREVIATIONS

Symbol	Explanation	Units used
BAU	Business as Usual	
CH_4	methane	Gt or ppbv
CO_2	Carbon dioxide	Gt or ppm
N_2O	Nitrous Oxide	Tg or ppbv
CDIAC	Carbon Dioxide Information Analysis Center	
EMIC	Earth System Model of Intermediate Complexity	
GCM	General Circulation Model	
GHG	Greenhouse gas	
GISS	Goddard Institute for Space Studies	
GPP	Gross Primary Production	Gt/year or ppm/year
Gt	gigaton	10^9 tons
IPCC	Intergovernmental Panel on Climate Change	
K	Eddy diffusion coefficient	m^2/year
LUC	Land Use Change	
MIT	Massachusetts Institute of Technology	
NBP	Net Biome Production	Gt/year or ppm/year
NPP	Net Primary Production	Gt/year or ppm/year
OH	Hydroxyl ion	

ppmv	part per million by volume	
ppbv	part per billion by volume	
Q_{10}	Temperature coefficient	unitless
RF	radiative forcing	W/m^2
TAR	Third Assessment Report	
TBM	Terrestrial Biosphere Model	
Tg	teragram	$10^{12}g$
WPO	World Public Opinion	
α	radiative forcing coefficient	W/m^2
β	Biostimulation coefficient	unitless
ζ	Buffer factor	unitless

1. INTRODUCTION

Of all the environmental issues that have emerged in the past few decades, global climate change is the most serious, and the most difficult to manage (Dessler and Parson, 2007). Although climate change in IPCC usage refers to "any change in climate over time, whether due to natural variability or as a result of human activity", activities of mankind have surely precipitated it with disastrous results. Today, increased emissions of greenhouse gases are known to be the main cause of this increase. According to IPCC, global average concentration of CO_2, the main greenhouse gas in the atmosphere, rose by about 35% since the beginning of industrial revolution in 1800's while it was almost constant during eight centuries before 1800's. The reality of this CO_2 increase is unquestioned, and virtually all climatologists agree that the cause is human activity, predominantly burning of fossil fuels and to a lesser extent deforestation and other land use changes, along with industrial activities such as cement production (Schneider et al., 2002).

Today, the World is facing hazard, vulnerability and risk by climate change and whilst some of the possible hazards are not even known to us, it has become an imperative to create policies to contain them. Consequently, climate change carries higher stakes than other environmental issues, both in the severity of potential harms if the changes go unchecked, and in the apparent cost and difficulty of reducing the changes. In this sense, climate change is the first of a new generation of harder environmental problems that human society will face over the 21st century, as the increasing scale of our activities puts pressure on evermore basic planetary-scale processes.

Climate change presents a classical dynamic systems problem. The effects of changes in emission and absorption processes of greenhouse gases (GHGs) can only be observed with very long time delays. There are uncertain destabilizing feedbacks, such as methane, water vapor, soil decomposition and sea ice/albedo processes (Ford, 2007). There are nonlinearities in GHG transfer between ecosystem compartments such as photosynthesis. Nevertheless, many detailed climate models lack the integrity of aquatic, oceanic and terrestrial systems which play a fundamental role in time delays and feedbacks. Many large scale atmospheric circulation models (Global Circulation Models:GCMs) focus on the

details of spatial processes but ignore the possible effects of those highly uncertain feedback mechanisms (Claussen at al., 2002). Therefore, it would be useful to explore these individual elements of dynamic complexity on a simpler integrated anthropogenic climate change simulator.

2. PROBLEM DESCRIPTION AND PURPOSE OF THE STUDY

The fact that human induced climate change and related global warming is a serious problem requiring very urgent action is unquestioned today. However, polls worldwide show that, people prefer to apply 'wait and see' policies instead of taking prompt action albeit they believe climate change poses serious risks (WPO, 2005). Most people believe that reducing GHG emissions can be delayed until there is greater evidence that climate change is dangerous and, until they begin to feel uncomfortable with existing climatic conditions. Governments also prefer 'wait and see' policies because they do not want to take costly actions to reduce emissions today for results that will occur decades after.

Wait and see policies, however, often don't work in systems with flows, stocks that accumulate the flows, long time delays, (slow accumulations), multiple feedback processes, nonlinearities, and other elements of dynamic complexity (Sterman, 1994). A feedback means when the result of a process affects its origin thereby intensifying (positive or reinforcing feedback) or reducing (negative or counteracting feedback) the original effect (Baede et. al., 2001). A common example of feedback in climate science is ice-albedo positive feedback: Melting snow causes a lower surface albedo that causes more heat absorption and more snow melting. Delays in a system declare how fast/slow a system variable responds to an external forcing. For instance the coupled land-atmosphere system responds relatively quickly to an increase in heat content of the system while deep ocean responds to the same in far slower manner due to its huge heat capacity compared to land-atmosphere system. Non-linearity in system dynamics means that the relation between cause and effect is not proportional. This unproportionality, often causes the dynamic feedback systems to exhibit abrupt behavior and, makes hard to analyze these systems. A well-known example of such behavior in climate science is carbon uptake of land and ocean from the atmosphere.

The climate change problem, even when reduced to its simplest representation (as a stock of CO_2 gas accumulating the difference between emissions and absorptions), creates great difficulties for people trying to manage the emissions with respect to a target

concentration level (Moxnes and Saysel, 2009). Adults' mental models of climate change violate even the most basic principle of physics: conservation of matter (Sterman and Sweeney, 2006). The main reason of these misperceptions is that, humans have big difficulties in perceiving and conceptualizing dynamic systems in general and complex dynamics of the climate system in particular. In addition to this, the climate system contains several uncertainties due to its chaotic dynamic structure. All these facts together, lead people to misinterpret the basic behavioral dynamics of the system and to make erroneous predictions about its behavior under different GHG emission scenarios. In this context, the need for adequately descriptive, yet simple and easily understandable models seems obvious.

A wide variety of models have been built to describe dynamics of climate system and to make forecasts for changes due to anthropogenic emissions. These models are classified by Claussen (2000) as simple, intermediate and comprehensive models according to their degree of complexity. Also a spectrum is proposed by Claussen et al. (2002) to classify the models, the three dimensions of which are integration, detail of description and processes.

Simple models, also called box type models, are composed of aggregated global stocks, have high degree of parameterization, easy to simulate and easier to understand and interpret. Their outputs are generally non spatial but global. On the other hand, the comprehensive models, also called General Circulation Models (GCMs), include much more details and have high degree of spatial resolution, but have computational difficulties even by very powerful computers and, are hard to understand by people having no scientific background (Ford 2007). Intermediate models, also known as Earth System Models of Intermediate Complexity (EMICs), are located in between, in the spectrum of climate system models. They have less spatial resolution than GCMs, thus computationally easier. They represent the processes described in GCMs in a more reduced fashion (Claussen at al., 2002). However both GCMs and EMICs lack representation of delays and feedbacks.

According to Ford (2007), the best line of improvement in climate modeling studies would be to expand along the "processes" dimension of the Claussens's climate models classification spectrum by retaining the emphasis on integration. In this sense, it is clear that dynamic systems modelers have a long way to go from simple towards intermediate

climate model construction including as much feedbacks as possible to decrease uncertainty but without sacrificing integrity. Besides their contribution to climate science, such simple but scientifically significant system dynamics models of the climate system would also be helpful for people having no scientific background, to understand better the severity of climate change problem and the urgency of action.

There are several climate change simulators that can readily be used by citizens to observe the results produced by different emission scenarios, for developing insights about the implied urgencies of the climate change problem (see www.climateinteractive.org for examples). However, they do not enable the user to explore the elements of dynamic complexity but give direct results of applied emission scenarios instead. Therefore, it would be useful to build a climate change simulator comprising selected elements of dynamic complexity, yet simple and convenient for exploration of the effects of different parametric and structural uncertainties on climate system.

The aim of this study is to build such a coupled, simple, dynamic simulation model. The model is intended to comprise basic feedback structures like temperature-CO_2 circulation, temperature-methane emissions and, temperature-permafrost melting feedbacks, and, to couple major elements of climate system, i.e. atmospheric, terrestrial and oceanic carbon as well as the heat transfer between Earth's surface layer and the deep ocean. Carbon cycle modules of climate-economy models, the system dynamics climate models and some GCMs are investigated and, an integrated model is constituted. STELLA software (v9.0.2, isee systems) is used as the modeling platform. The model is validated with indirect structure tests (Barlas, 1996), with respect to the data created by large scale simulators reported in IPCC Technical Paper II (Houghton[(2)] et. al., 1997) and, with respect to several historical data provided by various IPCC reports, Carbon Dioxide Information Analysis Center (CDIAC) and NASA Goddard Institute for Space Studies (GISS).

The model also allows the user to observe the effects of some non-CO_2 gases on climate change and the effects of some variables such as biostimulation coefficient or temperature coefficient on major processes such as photosynthesis, respiration or wetland methane emissions, and, to test parameter uncertainty and observe the results through sensitivity tests.

3. METHODOLOGY

The earth's climate, with, delays, feedbacks and non-linearities is a complex dynamic system. Dynamic systems, while solving complex problems, simultaneously create other complex challenges that make hard or even impossible to predict their behavior correctly. For this reason their structure and complex dynamics need to be well understood and analyzed (Barlas, 2002). However, it is often hard to understand a dynamic system problem with the limited capacity of human brain because of its dynamically complex nature. Anthropogenic climate change is such a dynamic systemic feedback problem. It contains interactions of various subsystems, large delays in responses of these subsystems to changing greenhouse gas (GHG) emissions and, numerous positive and negative feedbacks. One of the best tools to investigate a systemic problem is to build a descriptive model of its selected aspects related to the problem. Modeling allows to simulate and to analyze the behavior of the system.

The system dynamics methodology is used in this study to construct a model of anthropogenic global climate change. System dynamics is a powerful methodology to understand, model and analyze complex systems, to create and test hypotheses and to constitute policies. It was created in 1950's by a group of researchers lead by Professor Jay W. Forrester at M.I.T. to analyze dynamic socio-economic problems. Since then it is widely used in a variety of fields. One of these fields is the climate science. The climate system is very suitable to be analyzed with the principles of dynamic system modeling due to its structural properties.

The main steps of approaching a problem from system dynamics perspective are:

- to define a dynamic feedback problem,
- to develop a dynamic hypothesis, i.e. to define existing feedbacks, delays, non-linearities and stock-flow structures,
- to construct a formal dynamic simulation model,
- to test the validity, i.e. structural and behavioral adequacies of the model, and,
- to analyze the model, to observe the system behavior and to develop policies (Barlas, 2002).

The main characteristic property of the system dynamics approach is its feedback structure. The system dynamics models are focused on circular causality instead of direct causality between the system variables. For instance, in a study to estimate the global temperature increase, the plant photosynthesis can be identified as a factor affecting the atmospheric CO_2 level. The representation of the problem with the direct causality approach is shown in Figure 3-1, the arrows representing the direction and the arithmetical signs representing the polarity of the relationships between the variables.

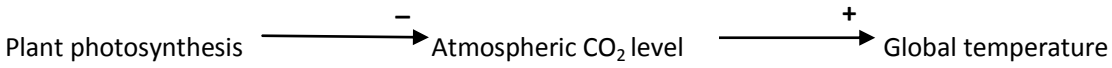

Figure 3.1 Direct causal representation of the relationships between the factors affecting global temperature

Hence, other things being equal, more plant photosynthesis decreases global temperature.

However, when the same problem is analyzed with the feedback approach, temperature increase stimulates the photosynthesis creating a negative circular causality (negative feedback loop) and less temperature increase. But, it also stimulates the plant respiration and, creates a positive circular causality (positive feedback loop) and more temperature increase. The increase in atmospheric CO_2 level itself stimulates the photosynthesis too (positive feedback loop). Thus, complex systems are constructed by defining the interactions between several feedback loops. The resulting behavior of the system depends on which feedback loop dominates. The feedback loops can be represented on a causal-loop diagram (Figure 3.2).

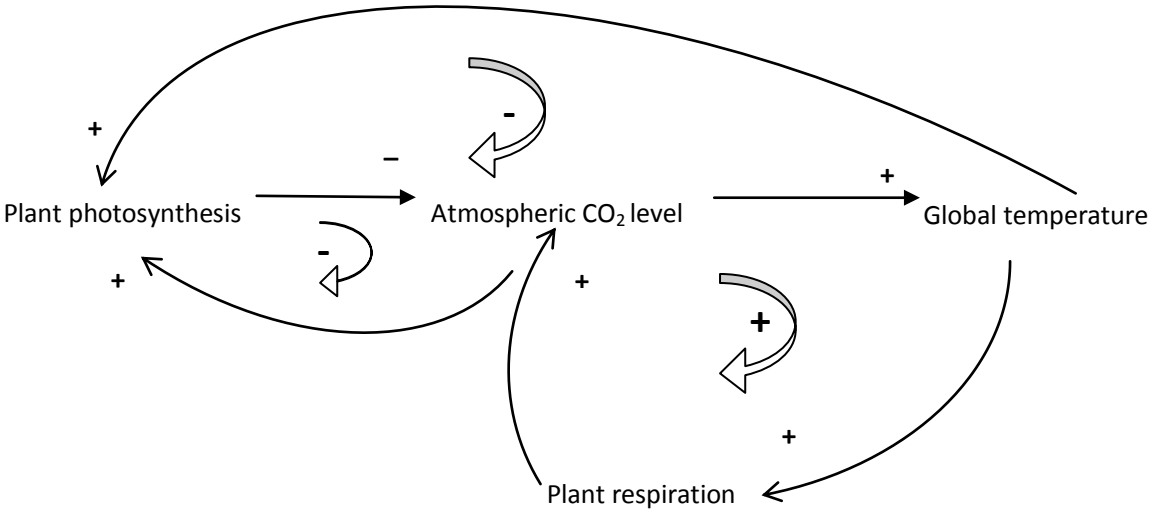

Figure 3.2 Causal loop diagram representing land biota-atmospheric CO_2 relationship

A system dynamics model is composed of interacting feedback loops, numerous variables embedded in these feedback loops and equations defining the relationships between these variables. The variables of a system dynamics model are stocks, flows and converters. The stocks variables and flow variables can be described as main building blocks of system dynamics models. Stocks, also called states, represent entities that accumulate or deplete over time. Flows represent the rate of change of stocks. Carbon in atmosphere and heat stored in deep ocean are examples of stocks while carbon uptake of land biota is an example of flow. Converters are all other variables used to define the relationships between the elements of the model. As an example, the stock-flow structure of the land biota-atmospheric CO_2 relationship described in Figure 3.2 is depicted below:

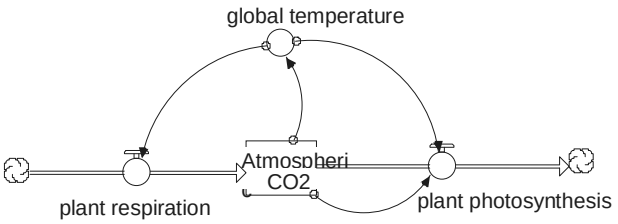

Figure 3.3 Stock-flow structure of the land biota-atmospheric CO_2 relationship

Stock equations are differential equations of the form:

$$S(t+dt)=S(t)+(\sum flows)*dt \quad (3.1.)$$

Flows are functions of stocks, and/or other flows and converters, i.e.

$$Flow=f(stock, flow, converter) \quad (3.2.)$$

The behaviors of stock variables, which are the state variables of a system dynamics model, determine the general behavior patterns of the system. For instance, the behavior of the atmospheric CO_2 level and of the temperature, which is the consequence of the behavior of the former, are depicted in Figure 3.4.

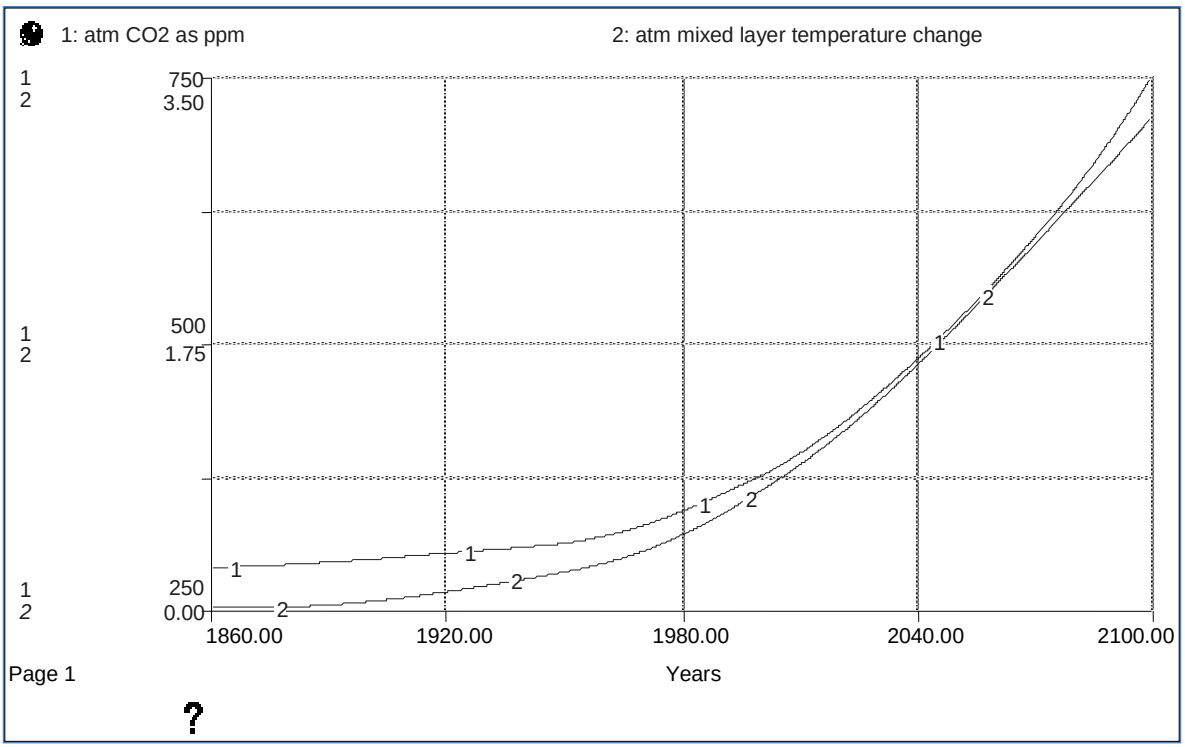

Figure 3.4 Behavior of atmospheric CO_2 level and atmosphere-mixed layer temperature

4. MODEL DESCRIPTION

4.1. Overview of the Model

A system dynamics model investigating the circulation of most important greenhouse gases and their effect on climate system is constructed. The effect of greenhouse gases on climate system is analyzed by their effect on radiative forcing and the global temperature increase they caused. The most important greenhouse gas, CO_2, and the two most important non-CO_2 greenhouse gases, CH_4 and N_2O are studied. The model is a non-spatial, coupled box model of the atmosphere, ocean and terrestrial system. The time horizon of the model is 1860-2100. The year 1860 is assumed as the beginning of industrial age. The model consists of 23 stocks in 7 sectors. The overview of the model structure is depicted in Figure 4.1.

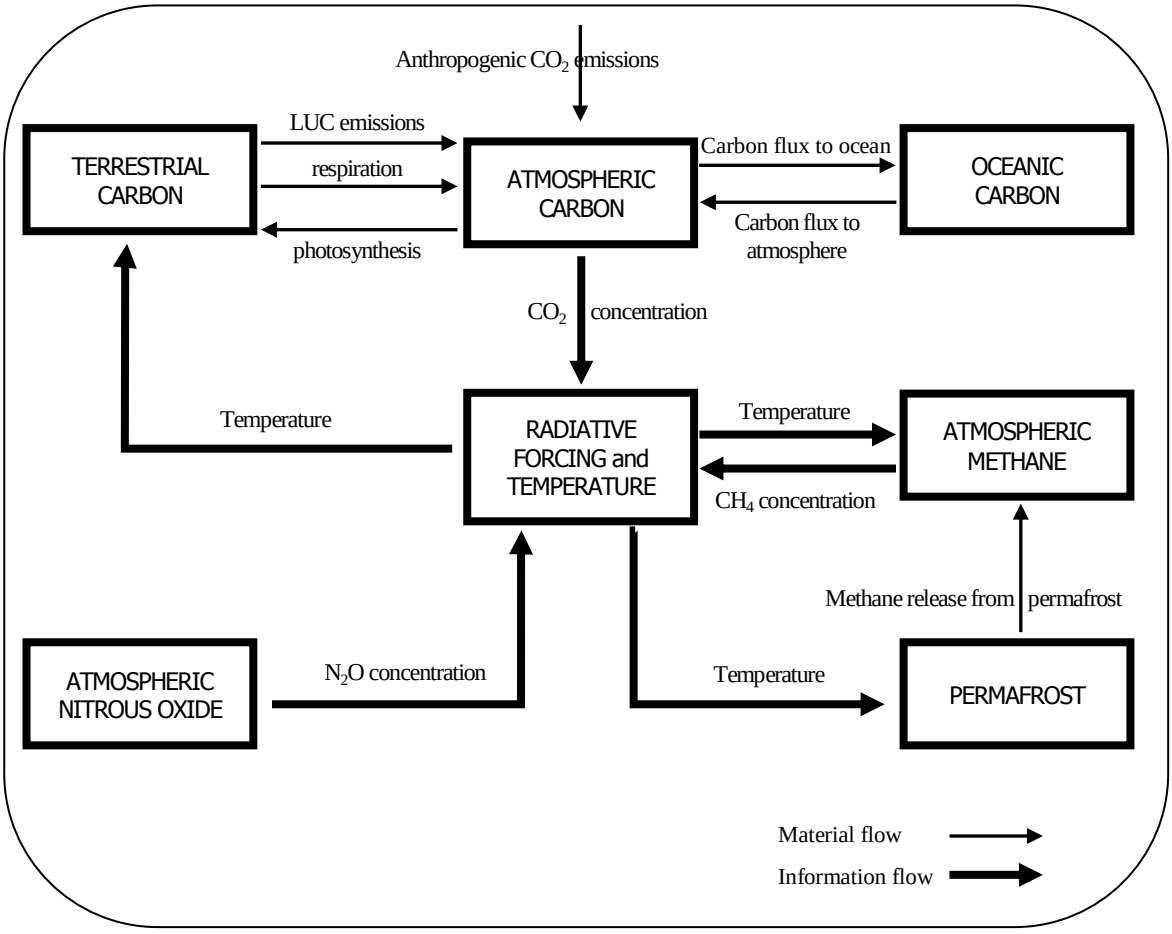

Figure 4.1 Model overview

The ‘terrestrial carbon’ sector contains various carbon stocks of the terrestrial ecosystem and their interactions with each other and with the atmosphere. It exchanges carbon with atmosphere through photosynthesis and respiration of biosphere and, through land-use change emissions. Carbon transfers between the stocks of the sector are represented with linear relationships while the carbon absorptions of the green elements of the sector, the photosyntheses, are represented with logarithmic non-linear equations. Both photosynthesis and respiration are affected by temperature change.

The ‘oceanic carbon’ sector contains the carbon stocks of mixed layer and deep ocean layers. Mixed layer of ocean exchanges carbon with atmosphere according to the partial pressure difference between atmospheric and oceanic carbon dioxide.

The ‘atmospheric carbon’ sector represents the carbon stored as CO_2 in the atmosphere. Increasing CO_2 concentration of the atmosphere causes global temperature to rise through increasing radiative forcing hence stimulating plant respiration and photosynthesis.

The main driving forces of the anthropogenic climate change are GHG emissions. They are exogenous to the model structure as LUC emissions are.

The ‘atmospheric methane’ sector represents the methane stored in the atmosphere. Increasing methane concentration in atmosphere increases the radiative forcing and then the temperature, thereby causing an increase in methane emissions from wetlands and in permafrost melting, thus, carbon release as CH_4 from permafrost to the atmosphere.

The ‘permafrost’ sector comprises the stocks representing global permafrost area and the carbon contained in permafrost. Increasing global temperature causes permanent permafrost melting and carbon release to the atmosphere as methane. This methane release increases radiative forcing and the temperature and, creates a positive feedback by causing further permafrost melting.

The ‘atmospheric nitrous oxide’ sector represents the nitrous oxide retained in the atmosphere. It contributes to global warming by means of its additive effect on radiative forcing.

Finally, the ‘radiative forcing and temperature change’ sector includes the radiative forcing calculations and, the two atmosphere-mixed layer and deep ocean heat stocks. These stocks represent the change in heat contents of the reservoirs since preindustrial times. They receive and release heat through different processes like radiative forcing, feedback cooling and heat transfer from mixed layer to the deep ocean. The global temperature change is calculated via the change in the heat content of the atmosphere-mixed layer stock.

4.2. Description of the Sectors

4.2.1. Terrestrial Carbon Sector

4.2.1.1. Background Information. The terrestrial ecosystem is an integral part of the global carbon cycle. Carbon is assimilated from atmosphere with photosynthesis and given back to the atmosphere with respiration of living biomass and decomposition of dead biomass. Human perturbation to this flow is through land-use change (Foley and Ramankutty, 2003). The autotrophic part of living biomass assimilates carbon through photosynthesis. This process is called ‘Gross Primary Production’ (GPP). Release of carbon to the atmosphere through respiration of photosynthesizing biomass is called ‘Autotrophic respiration’. The difference between GPP and the autotrophic respiration is called ‘Net primary production’ (NPP). The net exchange of carbon between the terrestrial biosphere and the atmosphere is then the difference between NPP and, heterotrophic respiration and other perturbations (Denman et. al., 2007). There is a consensus in scientific community that this net exchange, currently, points out to a flux from atmosphere to land, i.e. the terrestrial biosphere acts as a sink for carbon (Foley and Ramankutty, 2003). However, the size of this sink and the future pattern of the exchange are not easy to estimate on a global scale due to several restrictions like large heterogeneity of ecosystems, spatial and temporal differences in ecosystems, insufficiency of observational data, etc. (Denman et. al., 2007). Nevertheless, efforts for modeling the terrestrial ecosystems are continuing despite such restrictions and uncertainties. Existing models in the literature range from simple box models to complex process-based global vegetation models (Köhler and Fischer, 2004, Prentice et. al., 2001). In box models, which is the type adopted in this study, the ecosystem types and the soils are represented with several different

compartments exchanging carbon with each other. The number of compartments changes according to the purpose and the degree of complexity of the model. Several micro processes causing carbon exchange between two reservoirs add up to a single linear relationship with its unique rate coefficient. However, the fluxes representing photosynthesis, which is a process having more complex dynamics, are represented with non-linear relationships.

4.2.1.2. Description of the Terrestrial Carbon Sector. For flow of carbon in terrestrial ecosystems the study of Emanuel et al. (1981), which is an old but a fundamental example of the box type terrestrial biosphere models (TBMs), is adopted. The model consists of a globally aggregated terrestrial biosphere with five stocks. The stocks represent carbon in different ecosystems with different turnover times. Estimating the initial and actual carbon contents of the globally averaged stocks is a hard issue to resolve because of the areal heterogeneity of vegetation types, scarcity of available data on global basis, difficulty of integrating regional data to global scale and the poor information about carbon inventories in preindustrial times (Emanuel et al., 1981). However, the quantities assigned by Emanuel et al. (1981) for preindustrial steady state conditions are used as initial values of the stocks. The flows between the stocks are represented with linear equations except respiration and photosynthesis fluxes. Some of the rate coefficients in Emanuel et al. (1981) are slightly adjusted to calibrate the model. Being different from the model of Emanuel et al. (1981), temperature dependence of photosynthesis and respiration is included in the model. Land use change (LUC) emissions are defined as time series and represented with flows from terrestrial stocks to the atmosphere.

Three stocks of the sector represent the carbon in the living part of the terrestrial ecosystems while two stocks represent the carbon in the non-living part. The living part of the system is composed of ground vegetation and trees.

The simplified stock-flow structure of the sector can be seen below:

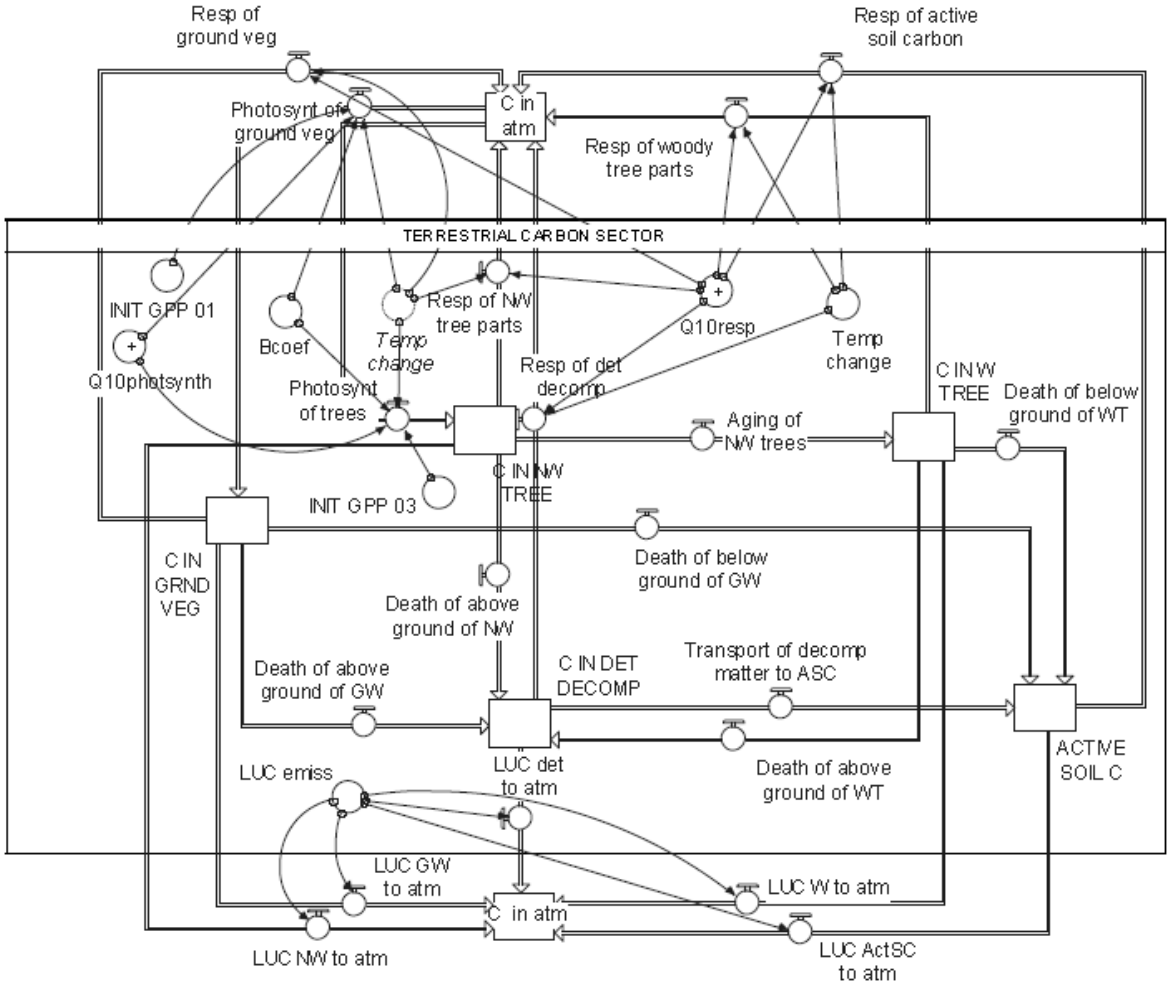

Figure 4.2 Simplified stock-flow structure of the terrestrial carbon sector

The ‘carbon in ground vegetation’ stock represents the carbon in all photosynthesizing vegetation types other than trees. Ground vegetation absorbs carbon from atmosphere through photosynthesis and releases carbon to the atmosphere through respiration and LUC emissions. Carbon is also transferred to the ‘detritus-decomposers’ reservoir by death of above ground parts of ground vegetation and, to the ‘active soil carbon’ reservoir by death and initial decomposition of below-ground parts of ground vegetation. Thus the stock has one inflow and four outflows.

The stock equation of the ‘carbon in ground vegetation’ is:

C_IN_GRND_VEG(t) = C_IN_GRND_VEG(t - dt) + (Photosynt_of_ground_veg - Death_of_below_ground_of_GW - Resp_of_ground_veg - Death_of_above_ground_of_GW - LUC_GW_to_atm) * dt (4.1.)

where ‘Photosynt of ground veg’ is photosynthesis of ground vegetation, ‘Resp of ground veg’ is respiration of ground vegetation, ‘Death of below ground of GW’ is death of below-ground parts and, ‘Death of above ground of GW’ is death of above ground parts of ground vegetation and, ‘LUC GW to atm’ is carbon release through LUC emissions from ground vegetation to the atmosphere.

The ‘carbon in nonwoody tree parts’ stock represents the carbon in all photosynthesizing parts and nonwoody parts like flowers, fruits of trees. Nonwoody parts of trees absorb carbon from atmosphere through photosynthesis and release carbon to the atmosphere through respiration and LUC emissions. They also transfer carbon to the ‘detritus-decomposers’ pool by death of above ground parts and, to the ‘woody tree parts’ pool by aging of nonwoody tree parts and becoming woody tree parts. Thus the stock has one inflow and four outflows. The stock equation of the ‘Carbon in nonwoody tree parts’ is:

C_IN_NW_TREE(t) = C_IN_NW_TREE(t - dt) + (Photosynt_of_trees - Resp_of_NW_tree_parts - LUC_NW_to_atm - Death_of_above_ground_of_NW - Aging_of_NW_trees) * dt (4.2.)

where ‘Photosynt of trees’ is photosynthesis, ‘Resp of NW tree parts’ is respiration, ‘Death of above ground of NW’ is death of above ground parts, ‘Aging of NW trees’ is aging of nonwoody tree parts, and, ‘LUC NW to atm’ is carbon release through LUC emissions from nonwoody tree parts to the atmosphere.

The ‘carbon in woody tree parts’ stock represents the carbon in all non-photosynthesizing woody parts of trees as boles, branches and, in roots. Woody parts of trees accumulate carbon through aging of nonwoody tree parts and becoming woody tree parts and, release carbon to the atmosphere through respiration and LUC emissions. They

also transfer carbon to the detritus pool through death of their above ground parts and to the active soil carbon pool through death of their below ground parts. Thus the stock has one inflow and four outflows. The stock equation of the ‘Carbon in woody tree parts’ is:

C_IN_W_TREE(t) = C_IN_W_TREE(t - dt) + (Aging_of_NW_trees - LUC_W_to_atm - Resp_of_woody_tree_parts - Death_of_below_ground_of_WT - Death_of_above_ground_of_WT) * dt (4.3.)

where ‘Resp of woody tree parts’ is respiration, ‘Death of above ground of WT’ and ‘Death of below ground of WT’ are deaths of above and below ground parts of woody tree parts respectively, ‘Aging of NW trees’ is aging of nonwoody tree parts and, ‘LUC W to atm’ is carbon release to the atmosphere through LUC emissions from woody tree parts to the atmosphere.

The other two stocks representing the carbon contained in the dead parts of the terrestrial ecosystem are ‘carbon in detritus/decomposers’ and ‘active soil carbon’.

The ‘carbon in detritus/decomposers’ stock represents the carbon contained in the litter and its decomposer organisms intermixed with soil, also known as humus altogether. This pool receives carbon from ground vegetation and trees through death of their above ground parts. It gives carbon to the atmosphere by respiration and through LUC emissions, and, to the active soil carbon reservoir by transport of decomposed material from the actively decaying litter layer. The stock having three inflows and three outflows is defined with the following equation:

C_IN_DET_DECOMP(t) = C_IN_DET_DECOMP(t - dt) + (Death_of_above_ground_of_GW + Death_of_above_ground_of_WT + Death_of_above_ground_of_NW - Resp_of_det_decomp - Transport_of_decomp_matter_to_ASC - LUC_det_to_atm) * dt (4.4.)

where ‘Resp of det decomp’ is respiration of detritus/decomposers, ‘Transport of decomp matter to ASC’ is transport of decomposed material from the actively decaying litter layer and ‘LUC det to atm’ is carbon release to the atmosphere through LUC emissions from detritus/decomposers.

The final stock of the terrestrial system, ‘active soil carbon’ stock, represents the carbon in soils and its decomposers that undergo relatively rapid decomposition compared to fossil carbon. The accumulation of carbon to this pool occurs through death of below grounds parts of ground vegetation and woody tree parts and, transport of decomposed material from the actively decaying litter layer. The pool releases carbon to the atmosphere through respiration of the organisms decomposing it and through LUC emissions. Actually, it also releases carbon to a much less active pool that decomposes very slowly, the fossil carbon pool. However this pool is not represented in the model as a stock since its turnover time is in the order of thousands of years and thus is not significant within the time horizon of this study. Instead, the transfer to this pool is represented in the model by a non-conserved flow with a value of zero. The stock equation for ‘active soil carbon’ is:

ACTIVE_SOIL_C(t) = ACTIVE_SOIL_C(t - dt) + (Death_of_below_ground_of_GW + Transport_of_decomp_matter_to_ASC + Death_of_below_ground_of_WT - Fossilization - Resp_of_active_soil_carbon - LUC_ActSC_to_atm) * dt (4.5.)

where ‘Resp of active soil carbon’ is respiration of the organisms decomposing the active soil carbon, ‘LUC ActSC to atm’ is carbon release to the atmosphere through LUC emissions from active soil carbon and, ‘Fossilization’ is flow to fossil carbon pool.

All respiration, death and decomposition fluxes that outflow from the stocks are defined by the product of the stock with related rate coefficient. The general form of the linear equation for these outflows is:

$$\text{Flux} = \text{Stock} * \text{rate coef.} \quad (4.6.)$$

where ‘Flux’ is the respiration, death or decomposition outflow from a stock and ‘rate coef.’ is the empirical rate coefficient that represents the effect of all the micro processes contained in the related process.

LUC emissions flows from the terrestrial stocks are fractionated among the stocks according to the ratio of the carbon content of the related stock to the terrestrial sum.

For temperature dependence of photosynthesis and respiration, a Q_{10} formulation is used. Among several formulations describing temperature dependence of biochemical reaction rates, the Q_{10} relationship (van't Hoff, 1898) is frequently used in literature (Kaetterer et al. 1998). The Q_{10} temperature coefficient is a measure of the rate of change of a biological or chemical process by an increase of 10°C in temperature. It can be stated as:

$$M = M_0 Q_{10}^{\left(\frac{\Delta T}{10}\right)} \tag{4.7.}$$

where;

M_0 is the initial rate of a process

M is the rate of a process after a ΔT°C increase in temperature

Q_{10} is the temperature coefficient, the fractional increase in M_0 when temperature increases by 10°C

Q_{10} values for respiration and photosynthesis are chosen from the values proposed in literature (Foley, 1995, Kwon and Schnoor, 1994, Köhler and Fischer, 2004). Due to the uncertainty associated with Q_{10} values, a sensitivity analysis is performed to test the effect of different Q_{10} values to photosynthesis and respiration.

Finally, the carbon assimilation of the biosphere, the photosynthesis, is modeled with a nonlinear formulation. It is suggested in almost all modeling studies that carbon assimilation of plants is stimulated by increasing atmospheric CO_2 concentration and increasing temperature (Denman et. al., 2007). However, the dynamics of this stimulation are not well known. There exist also some hypotheses that state the increase in carbon assimilation rate is not infinite but has some limitations like nutrient availability, moisture, etc., so, some asymptotic limits exist. However, this approach is not considered in this study. A formulation similar to one given by Goudriaan and Ketner (1984) is proposed. But, gross primary production (GPP) is calculated instead of net primary production (NPP) since respirations are separately represented with different functions.

The formula proposed for GPP is:

$$GPP_t = GPP_0 * \left(1 + \beta \ln \frac{C}{C_0}\right) * Q_{10}^{\left(\frac{\Delta T}{10}\right)} \tag{4.8.}$$

where;

GPP_0 is the GPP at preindustrial times, the beginning of simulation

GPP_t is the GPP at time 't'

β is biostimulation coefficient, the coefficient for response of GPP to increasing CO_2

C_0 is the preindustrial atmospheric quantity of carbon

C is the current atmospheric quantity of carbon

$Q_{10}^{\left(\frac{\Delta T}{10}\right)}$ is the temperature effect described previously.

The major uncertain parameter of this formulation is the biostimulation coefficient, β. The value is chosen as 0.5 after Goudriaan and Ketner (1984). However a sensitivity analysis is performed to observe the effects of different values on model behavior.

As exemplary of formulations of the terrestrial system flows, the photosynthesis, respiration and LUC emissions flows of nonwoody parts of trees respectively, are given below:

Photosynt_of_trees =
INIT_GPP_03*(1+Bcoef*LOGN(C_IN_ATM/Preindustrial_C_in_atmosphere))*
$Q_{10photsynth}$^(atm_mixed_layer_temperature_change/10) (4.9.)

Resp_of_NW_tree_parts =
C_IN_NW_TREE*Rate_coef_07*Q_{10resp}^(atm_mixed_layer_temperature_change/10) (4.10)

LUC_NW_to_atm =
(LUC_emissions_2)*(C_IN_NONWOODY_TREE_PARTS/terrestrial_stocks_sum) (4.11)

Complete set of equations of the sector can be found in Appendix A.

4.2.2. Oceanic Carbon Sector

4.2.2.1. Background Information. The oceans cover 70 percent of the Earth's surface area and, with a soluble inorganic carbon content of about 60 times more than the atmosphere, constitute an important sink for atmospheric carbon dioxide. The carbon exchange between atmosphere and the ocean is governed by solubilization of CO_2 in water in decadal timescales,

whereas in centennial to millennial timescales biological and physico-chemical processes, i.e. photosynthesis, respiration, death and decay of marine biota, come to scene. (Raven and Falkowski, 1999). The exchange of gaseous CO_2 between atmosphere and the surface ocean is a rapid process compared to deep ocean mixing and, is driven by the difference in partial pressures of atmospheric and surface ocean CO_2 (Kwon and Schnoor, 1994, Siegenthaler and Sarmiento, 1993, Peng et al., 1987, Sundquist and Plummer, 1981). Gas exchange occurs until the partial pressure of the atmospheric CO_2 is equilibrated with the partial pressure of CO_2 dissolved in surface ocean. The equation describing the process is:

$$F=c*(pCO_{2,a}-pCO_{2,s}) \quad (4.12)$$

where;

F is the air-sea CO_2 flux

$pCO_{2,s}$ is the equilibrium partial pressure of CO_2 in surface ocean

$pCO_{2,a}$ is the partial pressure of atmospheric CO_2

c is the gas exchange coefficient.

The CO_2 taken up by the surface ocean enters several different chemical reactions to produce HCO_3^- and CO_3^{2-} ions and leaving less than 1% as dissolved CO_2 gas. Thus the chemical equilibrium is shifted such that the increase in partial pressure of CO_2 in water is about 10 times larger than the increase in total CO_2 concentration. This buffer mechanism limits the uptake capacity of the ocean and, causes it to behave as if it had only ~6.5 times larger carbon capacity than the atmosphere in preindustrial times while it had 65 times larger. However, even this uptake capacity is not immediately available but reached when the whole ocean is in chemical equilibrium with atmospheric CO_2, which takes hundreds of years. Thus, the governing step of the air-ocean carbon flux is not the surface interaction but the slow downward transport of water into the deep ocean (Siegenthaler and Sarmiento, 1993).

4.2.2.2. Description of the Oceanic Carbon Sector. The structure of the sector is based on the model of Oeschger et al. (1975). It is a box Eddy diffusion model with 11 stocks; one representing the carbon in mixed layer and ten representing carbon in deep ocean layers. Thickness of the mixed layer is 75 m. The deep ocean has upper five layers of 200 meter thickness and deeper five layers of 560 meter thickness.

The simplified stock-flow structure of the sector can be seen in Figure 4.3.

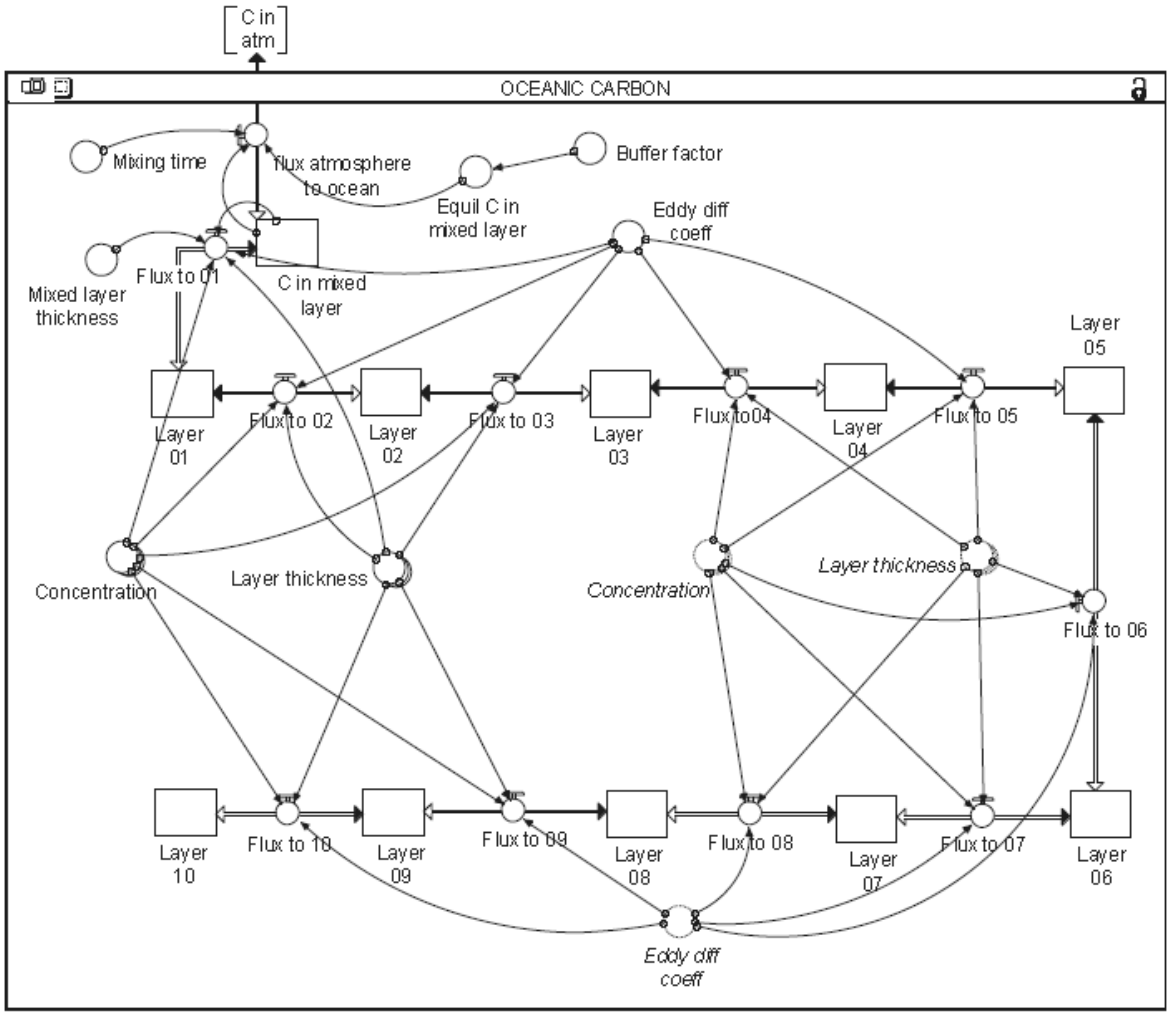

Figure 4.3 Simplified stock-flow structure of the oceanic carbon sector

The ‘carbon in mixed layer’ stock has one inflow, ‘flux atmosphere to ocean’, and one outflow, ‘flux to layer 01’, which represents the carbon transfer to the first layer of deep ocean. The stock equation is:

C_in_mixed_layer(t) = C_in_mixed_layer(t - dt) + (flux_atmosphere_to_ocean - Flux_to_01) * dt (4.13)

For convenience, the gas flux between atmosphere and the mixed layer is not represented in the model by using partial pressure differences but through equilibrium carbon content of the mixed layer instead.

The equation defining the gas flux between atmosphere and the mixed layer is:

flux_atmosphere_to_ocean = (Equil_C_in_mixed_layer-C_in_mixed_layer)/Mixing_time (4.14)

'Equilibrium carbon in mixed layer' is the carbon in mixed layer when its partial pressure is equal to the partial pressure of atmospheric CO_2. Gas exchange occurs between atmosphere and mixed layer until this equilibrium is reached. It is defined with the following equation:

$$C_m = C_{m,0}\left(1 + \frac{C_a - C_{a,0}}{C_{a,0} * \zeta}\right) \quad (4.15)$$

where;

C_m is the equilibrium carbon in mixed layer

$C_{m,0}$ is the preindustrial carbon in mixed layer

C_a is the carbon in atmosphere

$C_{a,0}$ is the preindustrial carbon in atmosphere

ζ is Buffer or Revelle factor.

Mixing time is the adjustment time of the atmosphere and mixed layer to this equilibrium. It is taken as 9.5 years (Oeschger, et al., 1975, Goudriaan and Ketner 1984, Fiddaman, 1997).

Buffer factor changes depending on atmospheric carbon dioxide concentration. Its normal value, which is represented as 'Ref buffer factor' in the model, is about 10. 'Buffer CO_2 coefficient' is the coefficient of atmospheric carbon concentration influence on buffer factor. It is taken as 4.05. 'Reference buffer carbon' is the carbon in atmosphere at normal buffer factor. Thus the buffer factor is defined with the following equation:

Buffer_factor =
Ref_buffer_factor+Buffer_CO_2_coefficient*LOGN(C_IN_ATM/Ref_buffer_Carbon) (4.16)

All other ten stocks representing deep ocean layers are designed with the same logic: Each layer receives an inflow, which is the outflow of its upper layer, and, discharges one

outflow, which is the inflow of its lower layer. The stock equation and the diffusion flow equations of one stock are given below as example:

Layer_02(t) = Layer_02(t - dt) + (Flux_to_02 - Flux_to_03) * dt (4.17)

Flux_to_02 = (Concentration[conc_L01]-Concentration[conc_L02])*Eddy_diff_coeff*2/ (Layer_thickness[Layer_01]+Layer_thickness[Layer_02]) (4.18)

Flux_to_03 = (Concentration[conc_L02]-Concentration[conc_L03])*Eddy_diff_coeff*2/ (Layer_thickness[Layer_02]+Layer_thickness[Layer_03]) (4.19)

The carbon concentration of layers is calculated by dividing the carbon content of the layer to its depth. Its unit is GtC/m.

Eddy diffusion coefficient is taken as 4000 m^2/year (Oeschger, et al., 1975, Fiddaman, 1997). For Eddy diffusion the flux from $layer_i$ to $layer_j$, F, is defined as:

$$F=-K(\partial c/\partial z) \quad (4.20)$$

where;

K Eddy diffusion coefficient

$\partial c/\partial z$ carbon concentration gradient with depth z.

The gradient $\partial c/\partial z$ can be approximated by $(c_i-c_j)/\Delta_{ij}$, where $\Delta_{ij}=(h_i+h_j)/2$ and h is the layer thickness. Thus,

$$F \cong -K\frac{ci-cj}{(hi+hj)/2} \quad \text{(Oeschger, et al., 1975)} \quad (4.21)$$

Complete set of equations of the sector can be found in Appendix A.

4.2.3. Atmospheric Carbon Sector

4.2.3.1. Background Information. The atmosphere is the third big component of the global carbon cycle after the terrestrial system and the ocean. It is a big reservoir of long-lived greenhouse gases (LLGHGs) the most important of which is carbon dioxide. Polar ice core records show that the atmospheric CO_2 concentration had increased by only 20 ppm over 8000 years before the beginning of industrial era while it increased more than 100 ppm after industrialization has begun (Solomon et. al., 2007). This is a clear evidence of the fact that this increase is caused by human activities, mainly by fossil fuel emissions. Carbon dioxide is emitted to the atmosphere mostly by anthropogenic sources and is removed from atmosphere by uptake of terrestrial biosphere and ocean. The rate of increase of atmospheric CO_2 concentration is the difference between these processes.

4.2.3.2. Description of the Atmospheric Carbon Sector. The sector consists of only one stock, the 'carbon in atmosphere'. All the inflows/outflows of the stock, except the 'anthropogenic emissions', are outflows/inflows of the reservoirs in terrestrial carbon, oceanic carbon and permafrost sectors. Anthropogenic emissions are exogenous inflow to the stock.

The simplified stock-flow structure of the sector can be seen below:

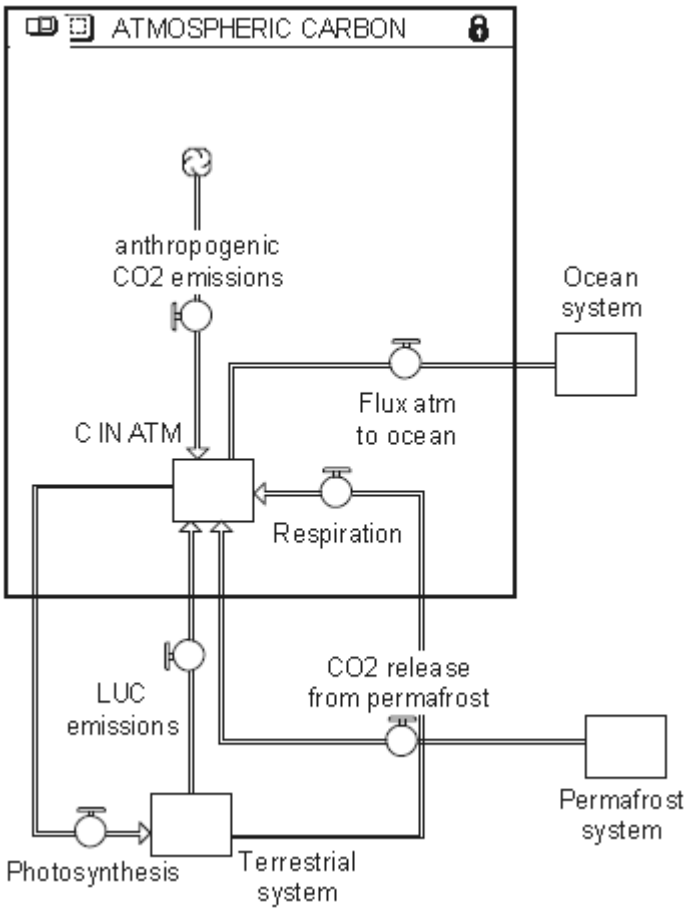

Figure 4.4 Simplified stock-flow structure of the atmospheric carbon sector

The stock equation of 'carbon in atmosphere' is:

C_IN_ATM(t) = C_IN_ATM(t - dt) + (Resp_of_NW_tree_parts + anthropogenic_CO_2_emissions_2 + LUC_W_to_atm + LUC_NW_to_atm + Resp_of_active_soil_carbon + Resp_of_woody_tree_parts + Resp_of_ground_veg + Resp_of_det_decomp + LUC_GW_to_atm + LUC_det_to_atm + LUC_ActSC_to_atm + C_release_from_permafrost_as_CO_2 - Photosynt_of_trees - Photosynt_of_ground_veg - flux_atmosphere_to_ocean) * dt (4.22)

Complete set of equations of the sector can be found in Appendix A.

4.2.4. Atmospheric Methane Sector

4.2.4.1. Background Information. Methane (CH_4), the main component of natural gas, is the most abundant greenhouse gas in the atmosphere after water vapor and carbon dioxide (CO_2) (Wuebbles and Hayhoe, 2002). Its Global Warming Potential is 21 times more than that of carbon dioxide for a time horizon of 100 years (Houghton[(1)] et. al., 1995). Atmospheric methane concentration has increased more than twofold since the beginning of industrial era (Rasmussen and Khalil, 1981). Both these rapid concentration increase and high global warming potential make methane, among other trace gases, a greenhouse gas deserving special importance and consideration in a climate change modeling study.

Methane is emitted to the atmosphere from several natural and anthropogenic sources and is mainly removed in the troposphere by reaction with the hydroxyl radical (OH). Natural sources are wetlands, termites, oceans and minor other sources. Main anthropogenic sources are waste decomposition, rice cultivation, domestic ruminants, biomass burning and fossil fuels (Wuebbles and Hayhoe, 2002).

4.2.4.2. Description of the Atmospheric Methane Sector. The sector comprises one stock, 'Atmospheric Methane'. The stock represents the amount of methane in atmosphere as gigatons (Gt). The stock is filled with eight inflows; five representing anthropogenic emissions, two representing natural emissions and one representing permafrost melting and, is drained with one outflow representing removal of methane by reaction with hydroxyl radical.

The simplified stock-flow structure of the sector can be seen below:

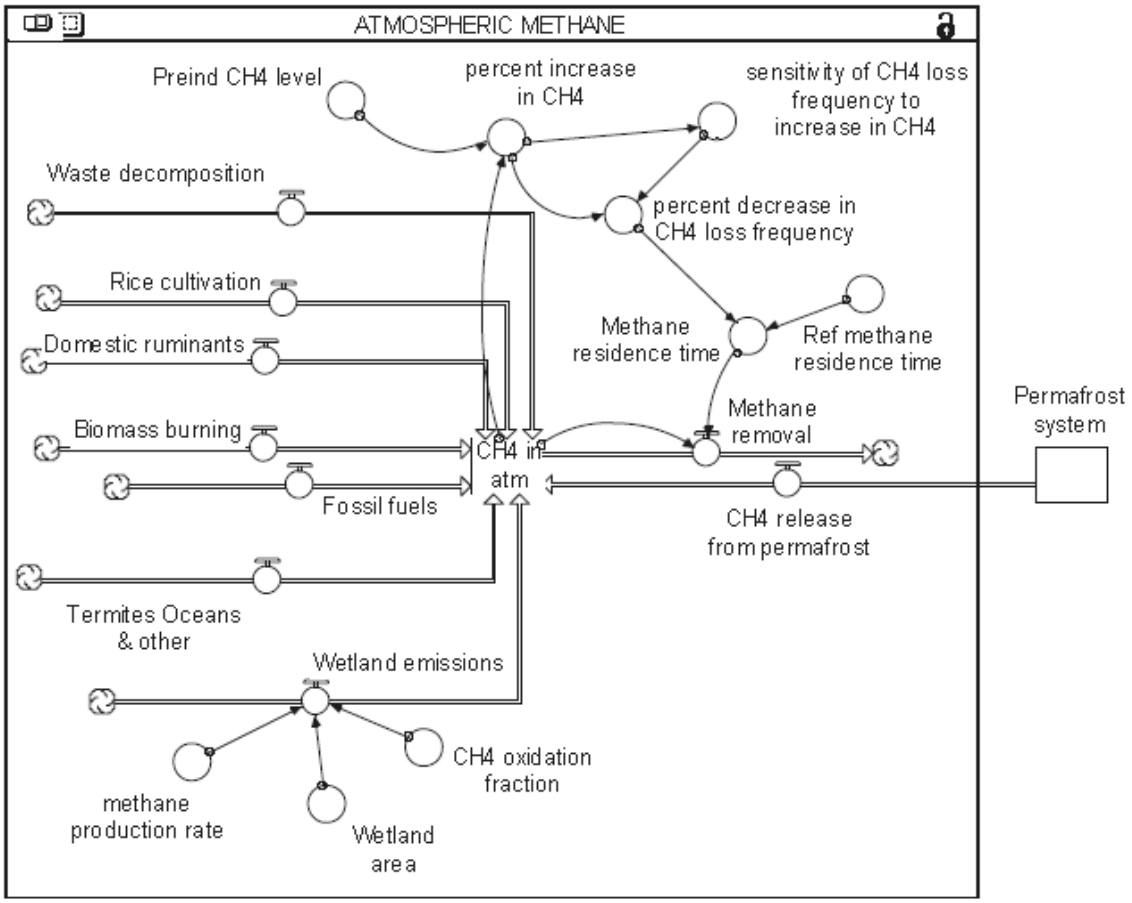

Figure 4.5 Simplified stock-flow structure of the atmospheric methane sector

The stock equation of the 'Atmospheric Methane' is:

Atmospheric_Methane(t) = Atmospheric_Methane(t - dt) + (Waste_decomposition + Rice_cultivation + Domestic_ruminants + Biomass_burning + Fossil_fuels + Wetland_emissions + Termites_Oceans_&_other + C_release_from_permafrost_as_CH_4 - Methane_removal) * dt (4.23)

Waste decomposition and Rice cultivation inflows represent methane emitted from anaerobic decomposition of organic matter by methanogenic bacteria in landfills and other waste disposal sites and, in rice fields respectively. Domestic ruminants inflow represents the emission of methane that is produced in the digestive tracks of domestic ruminants like cattle, sheep, etc. as a byproduct of incomplete digestion. Biomass burning inflow represents

methane produced by incomplete combustion of biomass. Fossil fuels inflow represents the methane leaked during natural gas processing, transmission and distribution and, emissions from coal mines (Wuebbles and Hayhoe, 2002). Although the emissions change depending on several environmental and anthropogenic conditions and human practices, their dynamics are not considered in this study. Instead, emissions estimates available in the literature are used as exogenous inflows. In the base run, the data used in these graphs are from Stern and Kaufmann for the 1860-1990 interval and, from the IS92a scenario of the IPCC for the 1995-2100 interval. These five emissions are the anthropogenic emissions.

Represented natural methane emissions are Termites, Oceans and other emissions and, Wetland emissions. Since termites, oceans and other emissions showed no significant change in time, they are assumed as constant in time as given in IS92a scenario of IPCC. However, wetland emissions constitute a vast majority of the natural methane emissions and they are dependent on several environmental parameters like soil characteristics, organic matter availability in soil, water table level and temperature. Among these factors of wetland emissions, only temperature and organic matter availability dependence of methane production are represented in the model. The change in methane production rate in wetlands creates a positive feedback in climate change. Methane is produced with anaerobic decomposition of organic matter under water table in wetlands. Increased temperature causes an increase in methane production rate of anaerobic bacteria. Also, increased amount of organic matter in soil, which is used as substrate by anaerobic bacteria, increases the methane production rate. The model adapts the factors considered in Walter and Heimann (2000) and Walter et al. (2001) to a global scale and to the problem of longer term temperature change. For the substrate availability for methane production, annual change in global NPP is calculated. For the temperature dependence of methane production, a Q_{10} formulation is used as suggested by Walter and Heimann (2000). Change in soil temperature is assumed equal to the change in atmosphere and mixed layer temperature. Q_{10} value is taken as 6 as proposed by Walter and Heimann (2000). However, due to the uncertainty associated with Q_{10} value, a sensitivity analysis is performed to test the effect of different Q_{10} values to wetland methane emissions. The reference methane production rate is taken as preindustrial wetland methane production rate (Houweling, 2000). Methane oxidation, which takes place in the oxic zone of the soil above the water table, is assumed to be 40% of the total methane production (Walter et al., 2001).

Thus the equations for methane production in wetlands and, wetland methane emissions are as follows:

$$\text{methane\_production\_rate}(t) = (\text{Ref\_CH}_4\text{\_production\_rate}) * (Q_{10\ CH4\ production})^{(\text{atm\_mixed\_layer\_temperature\_change}/10)} * (\text{NPP}(t)/(\text{NPP}(t-1)) \quad (4.24)$$

$$\text{Wetland\_emissions} = \text{methane\_production\_rate} * (1-\text{CH}_4\text{\_oxidation\_fraction}) * \text{Wetland\_area} \quad (4.25)$$

Methane is not conserved in the model like carbon. On the other hand, compared to carbon fluxes, carbon flows as methane are three orders of magnitude lower and therefore, it is not expected to create a significant change in carbon stocks. A comparison of the flow values is given in the below table:

Table 4.1 Comparison of carbon flows as carbon dioxide and as methane

	Years					
Carbon flows (GtC/year)	**1860**	**1900**	**1940**	**1980**	**2020**	**2060**
Waste decomposition	0.00	0.00	0.01	0.02	0.05	0.08
Wetland emissions	0.12	0.12	0.13	0.14	0.15	0.22
Rice cultivation	0.03	0.04	0.05	0.07	0.08	0.11
Termites, oceans and other	0.03	0.03	0.03	0.03	0.03	0.03
Fossil fuels	0.00	0.01	0.02	0.06	0.08	0.11
Domestic ruminants	0.02	0.02	0.04	0.07	0.13	0.17
Biomass burning	0.01	0.01	0.02	0.02	0.02	0.02
Photosynt of ground veg.ü	38.00	38.83	39.65	41.80	47.05	56.73
Resp of det decomp	48.06	46.15	46.91	48.74	53.20	60.00
Photosynt of trees	82.00	83.80	85.56	90.20	101.53	122.41
Resp of active soil carbon	14.05	12.62	11.91	11.65	12.10	13.61
Resp of woody tree parts	14.70	15.24	15.60	16.18	18.18	22.69
Resp of ground veg.	18.94	20.66	21.20	22.47	25.89	33.09
Resp of NW tree parts	25.74	29.32	30.14	32.12	37.40	48.98
Death of below ground of GW	5.57	6.05	6.14	6.39	6.98	7.80
Death of above ground of GW	11.14	12.10	12.28	12.79	13.96	15.61
Death of above ground of NW	19.38	21.99	22.37	23.40	25.83	29.59
Aging of NW trees	28.56	32.41	32.97	34.49	38.06	43.61
Death of above ground of WT	13.86	14.31	14.49	14.77	15.72	17.17
Death of below ground of WT	1.86	1.92	1.94	1.98	2.11	2.30
Transport of decomp matter to ASC	2.77	2.65	2.67	2.72	2.82	2.78

The last inflow of the stock is CH_4 release from permafrost, which is connected to the Permafrost sector. This is the carbon release from Permafrost sector which has been multiplied with a coefficient for conversion of the molecular weight of carbon to molecular weight of methane.

Although methane is emitted to the atmosphere through several sources, its main removal mechanism is its reaction with hydroxyl ion in the troposphere (Wuebbles and Hayhoe, 2002). Methane is oxidized in the troposphere in a series of reactions to form finally ozone (O_3). However, the hydroxyl ion is not only removed by methane but also by the products of its reaction with methane. Thus, increasing amount of methane in atmosphere decreases the amount of available hydroxyl ion thereby increasing the atmospheric lifetime of methane and creating a positive feedback in atmospheric methane (Lelieveld et al., 1998, Wuebbles and Hayhoe, 2002, Schimel et. al., 1995). On the other hand, OH is partly replaced as a by-product of CH_4 oxidation chain reactions and, formed by destruction of ozone by solar radiation (Lelieveld et al., 1998, Wuebbles and Hayhoe, 2002). The value, the rate and the pattern of change of the methane residence time is a subject including large uncertainties and needing further research. In this study, the following method is proposed for calculation of the residence time of methane:

The reference residence time of methane is taken as nine years, which is an intermediate value within the range of values used in the literature (Houghton[(1)] et. al., 1995, Lelieveld et al., 1998). The percent increase in the atmospheric methane concentration is calculated. Then, a sensitivity variable, which describes the percent change in CH_4 loss frequency (1/residence time) per 1% increase in CH_4 (Schimel et. al., 1995), is defined. Rather than assigning a constant value to this variable, a graphical function of percent increase in CH_4 is created. The starting value for the sensitivity variable is taken as the average of the values used in different models in Houghton[(1)] et. al. (1995). The function is assumed to be an asymptotically decreasing one to support the fact that the effect of increasing atmospheric methane concentration on methane residence time becomes less significant as methane concentration increases (Lelieveld et al., 1998). Then the percent decrease in CH_4 loss frequency is calculated by multiplying the percent increase in CH_4 by the sensitivity. Finally the remainder fraction of CH_4 loss frequency is calculated and the reference residence time is divided to that value to

calculate new residence time of methane. The relevant formulas and meanings of variables are stated below:

$$\Delta CH_4 = \frac{CH_{4(t)} - CH_{4(t_0)}}{CH_{4(t_0)}} * 100 \quad (4.26)$$

$$\Delta CH_4 LF = \Delta CH_4 * \text{sensitivity} \quad (4.27)$$

$$RT_{(t)} = \frac{RT_{(t_0)}}{(100 - \Delta CH_4 LF)/100} \quad (4.28)$$

where;

ΔCH_4 is percent increase in atmospheric methane concentration

$CH_{4(t)}$ is atmospheric methane concentration at time 't'

$CH_{4(t_0)}$ is atmospheric methane concentration at preindustrial times

$\Delta CH_4 LF$ is percent decrease in CH_4 loss frequency

$RT_{(t)}$ is residence time of methane at time 't'

$RT_{(t_0)}$ is residence time of methane at preindustrial times =reference methane residence time = 9 years,

$CH_4 LF$ is the loss frequency of methane = $\frac{1}{RT}$

Sensitivity is the sensitivity of the CH_4 loss frequency to the increase in atmospheric CH_4 concentration (Schimel et. al., 1995).

Finally, the unit of the methane accumulated in the stock is converted to ppbv and the radiative forcing of methane is calculated according to the formula given in Houghton et. al. (1990) (see Appendix C). Historical atmospheric methane records are taken from Carbon Dioxide Information Analysis Center (CDIAC). Projections for the future are taken from IS92a scenario of IPCC for the base run.

Complete set of equations of the sector can be found in Appendix A.

4.2.5. Permafrost Sector

4.2.5.1. Background Information. Permafrost (permanently frozen ground) is defined as the soil that remains at or below the 0°C for at least two years. It extends across about 25% of land in the northern hemisphere, mostly at the arctic zone (Zhang et al., 2000). Its thickness changes from a few centimeters to more than 1000 meters. Permafrost is a large carbon reservoir. Yet, this carbon stock was not incorporated into global carbon budget studies and was not a matter of concern for global warming until recently because, all organic matter was trapped into a frozen environment that keeps it inactive. However there is strong evidence that permafrost is permanently thawing due to global temperature increase; forming new wetlands, causing methane flux and thus creating a strong positive feedback contributing to temperature increase. Though the existence of considerable uncertainty and an ongoing debate among the scientists about the potential effects of thawing permafrost to climate warming, simulation of thawing permafrost efforts are being performed lately. There exist some modeling studies projecting the area of permafrost shrinking to 1 million square kilometers by 2100 (Lawrence and Slater, 2005). In case that happens, it is quite evident that a serious increase in global temperature will occur.

The total carbon content of permafrost and its releasing mechanisms to the atmosphere are not well known currently. However, it is obvious that increasing global temperature may increase the depth of seasonally thawing soil and cause the carbon that was previously inactive to be released to the atmosphere (Zimov et al., 2006).

4.2.5.2. Description of the Permafrost Sector: There are two stocks in this sector: ‘Permafrost Area’ and ‘Carbon in Permafrost’.

The simplified stock-flow structure of the sector can be seen below:

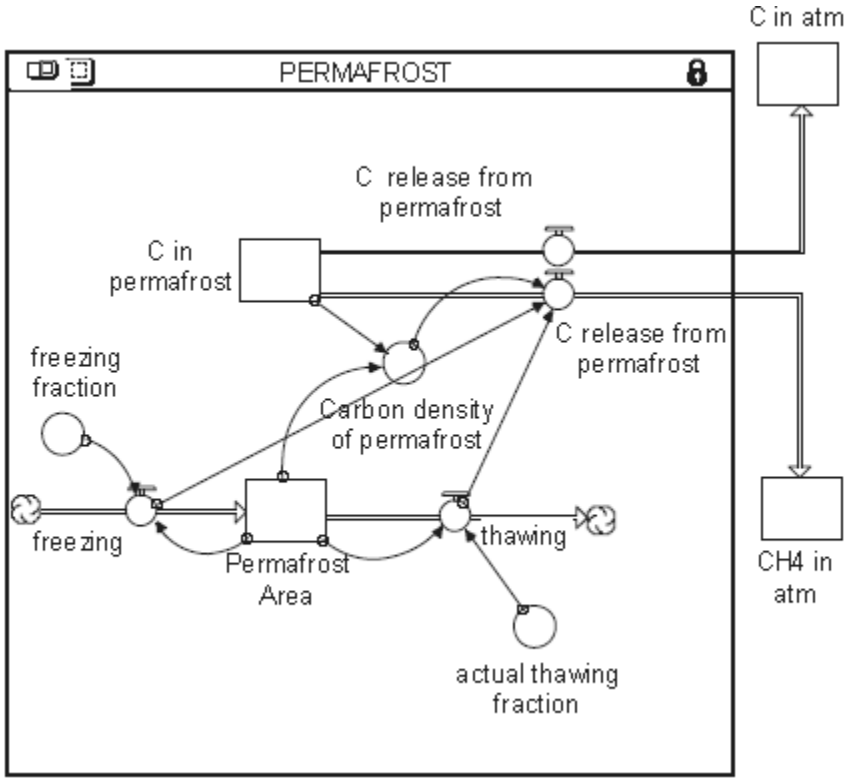

Figure 4.6 Simplified stock-flow structure of the permafrost sector

Permafrost Area represents the area of permafrost in square kilometers. The stock has one inflow, freezing, and one outflow, thawing, representing the seasonal increase and decrease in the area of permafrost respectively. When undisturbed, these flows are in dynamic equilibrium. When temperature increases, thawing begins to exceed freezing and carbon release to the atmosphere begins. The stock equation of the 'Permafrost Area' is:

$$Permafrost\_Area(t) = Permafrost\_Area(t - dt) + (freezing - thawing) * dt \quad (4.29)$$

The equations describing the linear relationships between the stock and the flows are:

$$freezing = freezing\_fraction*Permafrost\_Area \quad (4.30)$$

$$thawing = actual\_thawing\_fraction*Permafrost\_Area \quad (4.31)$$

The seasonal freezing fraction is assumed to be constant. However, actual thawing fraction is assumed to change indirectly with temperature and, a hypothesis is suggested to represent this change.

The hypothesis and underlying assumptions are as follows:

Preindustrial thawing fraction is taken to be equal to the freezing fraction.

Although it is not practically possible to calculate the average temperature of permafrost, for modeling purposes, the first one meter depth of it is assumed to be laid homogenously and to have an initial average temperature of -1°C.

Heat capacity of permafrost is taken as equal to the heat capacity of atmosphere and mixed layer by assuming that all atmosphere, mixed layer and soil behave as a one dimensional homogeneous column.

Since the melting temperature of ice is 0°C, the temperature change to start the devastating melting is calculated as $\Delta T=T_{final}-T_{initial}=0-(-1)=1°C$.

The heat required to start the severe melting process, which is called as 'the critical heat for devastating melting', is calculated with the heat exchange formula of basic physics, ΔQ=heat capacity*ΔT.

The 'ratio of heat difference to critical heat' is calculated by dividing the 'Atmosphere and mixed layer heat difference', a stock value which was calculated in temperature change sector, to the 'critical heat for devastating melting'.

A variable called 'thawing fraction multiplier' is defined as an exponentially growing function of the ratio of heat difference to critical heat. Two different thawing fraction multipliers are created to test different permafrost melting scenarios (see section 7.2.).

Then actual thawing fraction is calculated by multiplying preindustrial thawing fraction with thawing fraction multiplier.

The ‘time conversion parameter’ used in all below formulations is simply a multiplier to convert year to seconds in order to keep unit consistency.

The relevant equations of the model are:

critical_heat_for_devastating_melting = heat_capacity_of_permafrost*
(0-initial_average_temperature_of_permafrost)*time_conversion_parameter (4.32)

ratio_of_heat_difference_to_critical_heat = control_8*
(Atm_mixed_layer_heat_difference/critical_heat_for_devastating_melting) (4.33)

actual_thawing_fraction =
preindustrial_thawing_fraction*thawing_fraction_multiplier (4.34)

The other stock of the sector, Carbon in permafrost, represents the carbon stored in upper one meter of permafrost as Gigatons Carbon (GtC). Its initial value is assigned as 375 GtC (Khvorostyanov et al., 2008). However, since this value has a large uncertainty, a sensitivity analysis with different values is performed in section 7.2. The stock has two outflows representing carbon release as CH_4 and carbon release as CO_2 from permafrost. The equations of the stock and its outflows are:

C_in_permafrost(t) = C_in__permafrost(t - dt) + (- C_release_from_permafrost_as_CH_4-
C_release_from_permafrost_as_CO_2) * dt (4.35)

C_release_from_permafrost_as_CH_4 = Carbon_density_of_permafrost*(thawing-freezing)*
CH_4_release_fraction*(16/12) (4.36)

C_release_from_permafrost_as_CO_2 = Carbon_density_of_permafrost*(thawing-freezing)*
CO_2_release_fraction*(44/12) (4.37)

Carbon density of permafrost is calculated by dividing the initial value of the ‘Carbon in permafrost’ to the initial value of the ‘Permafrost area’ stock.

Finally, the carbon release outflows are connected to ‘C in atm’ and ‘atmospheric methane’ stocks.

Complete set of equations of the sector can be found in Appendix A.

4.2.6. Atmospheric Nitrous Oxide Sector

4.2.6.1. Background Information. Nitrous oxide (N_2O), also known as laughing gas, is a colorless, non-flammable gas with a sweet odor. It is used as anesthetic in medicine. Among all trace gases in the atmosphere, Nitrous oxide is the second important greenhouse gas after methane because of its long lifetime and its big global warming potential (GWP). Its atmospheric lifetime is 120 years (Houghton[(1)] et. al., 1995). Its GWP is 310 times more than that of carbon dioxide for a time horizon of 100 years (Houghton[(1)] et. al., 1995). Atmospheric N_2O concentration has increased from about 276 ppbv in preindustrial times to about 322 ppbv in 2008 (GISS).

Nitrous oxide has both natural and human-related sources. Main human-related sources are agriculture, fossil fuels combustion, adipic acid production in nylon industry and, nitric acid production. The main removal mechanism of N_2O from the atmosphere is photolysis (breakdown by sunlight) in the stratosphere.

4.2.6.2. Description of the Atmospheric Nitrous Oxide Sector. The dynamics of atmospheric nitrous oxide are very simply represented in the model. There is one stock in the sector representing the quantity of nitrous oxide in the atmosphere in units of teragram ($Tg=10^{12}$ g).

The simplified stock-flow structure of the sector can be seen below:

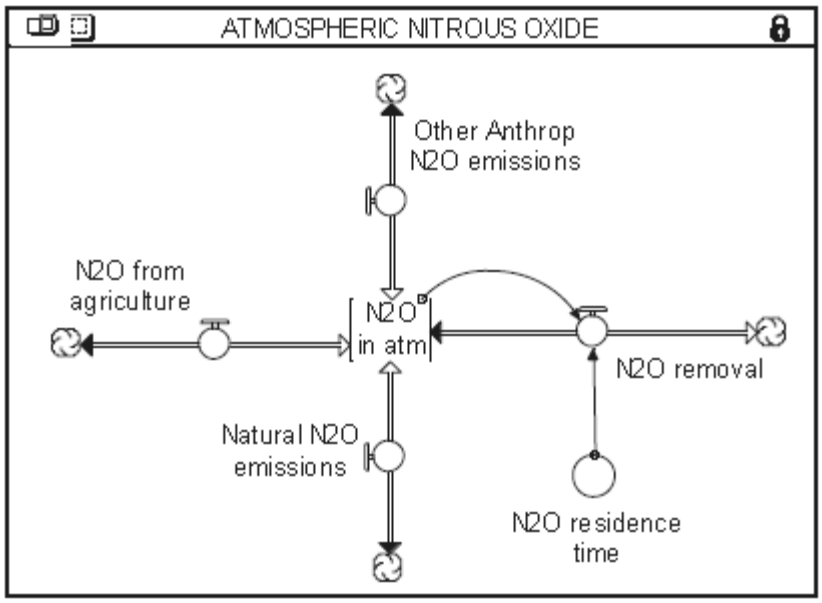

Figure 4.7 Simplified stock-flow structure of the atmospheric nitrous oxide sector

The stock has two inflows representing anthropogenic emissions and, one inflow representing natural emissions. Anthropogenic emissions are given as graphical functions of time. The IPCC IS92a scenario values are used for years after 1985. These values are extended back to 1860 by keeping the same trend. The emissions from nitric acid and fertilizers are considered as N_2O emissions from agriculture. The emissions arising from fossil fuel combustion, biomass burning, land clearing and adipic acid production are grouped as other anthropogenic N_2O emissions. N_2O emissions from oceans, temperate soils and tropical soils are grouped as natural N_2O emissions and, are assumed constant throughout the time as supposed by IS92a scenario. The only outflow of the stock is N_2O removal which is represented with a linear relationship. The equations of the stock and the outflow are:

$$N_2O\_in\_atm(t) = N_2O\_in\_atm(t - dt) + (Other\_Anthrop\_N_2O\_emissions + Natural\_N_2O\_emissions + N_2O\_from\_agriculture - N_2O\_removal) * dt \quad (4.38)$$

$$N_2O\_removal = N_2O\_in\_atm/N_2O\_residence\_time \quad (4.39)$$

The nitrous oxide accumulated in the atmosphere, which was calculated as Tg, is then converted to ppbv and the radiative forcing of N_2O is calculated according to the formula given in Houghton et.al. (1990) (see Appendix C). Historical atmospheric nitrous oxide

records are taken from the webpage of Goddard Institute for Space Studies (GISS). Projections for the future are taken from IS92a scenario of IPCC for the base run.

Complete set of equations of the sector can be found in Appendix A.

4.2.7. Radiative Forcing and Temperature Change Sector

4.2.7.1. Background Information. Radiative forcing, hereinafter referred as RF, is a concept commonly used in climate science. It is a measure of the influence of anthropogenic and natural factors causing climate change to the energy balance of the Earth-atmosphere system and is usually quantified as the 'rate of energy change per unit area of the globe as measured at the top of the atmosphere' (Forster et. al., 2007). The exact definition of radiative forcing is given in Third Assessment Report (TAR) of IPCC by Ramaswamy et al (2001) as 'the change in net (down minus up) irradiance (solar plus longwave; in W/m^2) at the tropopause (the boundary between troposphere and stratosphere) after allowing for stratospheric temperatures to readjust to radiative equilibrium, but with surface and tropospheric temperatures and state held fixed at the unperturbed values'.

When unperturbed, the earth-atmosphere system is in an energy balance. About 30% of the incoming solar energy is reflected back to space due to the albedo of earth-atmosphere system while the rest is absorbed. The absorbed energy is then re-emitted as infrared radiation. Some part of this infrared radiation is trapped by greenhouse gases and re-radiated to the earth. This phenomenon, which is called natural greenhouse effect, makes it possible for earth-atmosphere system to keep its mean temperature at +15°C and, makes earth home for thousands of species for millennia. However, increasing concentration of emitted greenhouse gases since the beginning of industrial era has disturbed and, is still continuing to disturb this energy balance. Higher amount of greenhouse gases in the atmosphere causes more infrared radiation to be absorbed, more heat storage and consequently a heat surplus in the balance of the system. Thus, this extra heat causes an increase in global average temperature while the system is striving to reach a new equilibrium state.

The change in the heat budget of the earth-atmosphere system can be expressed as:

$$dH/dt = RF-\alpha T \quad (4.40)$$

where;

dH/dt is the rate of heat storage in the system

RF is the radiative forcing

αT is the net effect of processes acting to balance the changes in mean global temperature (Cubasch et. al., 2001).

Since the heat content and the thermal inertia of the ocean are very big compared to that of the earth-atmosphere system, the rate of heat storage is dominated by the ocean and it can be approximated that $dH/dt=dH_0/dt=F_0$ where H_0 is the heat content of ocean and F_0 is the heat flux into the ocean. Thus the equation (4.40) becomes:

$$RF = F_0+\alpha T \quad (4.41)$$

which means that when the equilibrium conditions are disturbed by RF in the heat balance of the system, both the heat flux into ocean and other feedback mechanisms act together to balance the effect of RF and, the temperature of the system increases until the new equilibrium state is reached.

4.2.7.2. Description of the Radiative Forcing and Temperature Change Sector. The sector contains two distinct parts: the first part where the RF effect of greenhouse gases are calculated and, the second part where the global temperature change is calculated. The RF value calculated in the first part is used as an input in the second part.

The simplified stock-flow structure of the sector can be seen below:

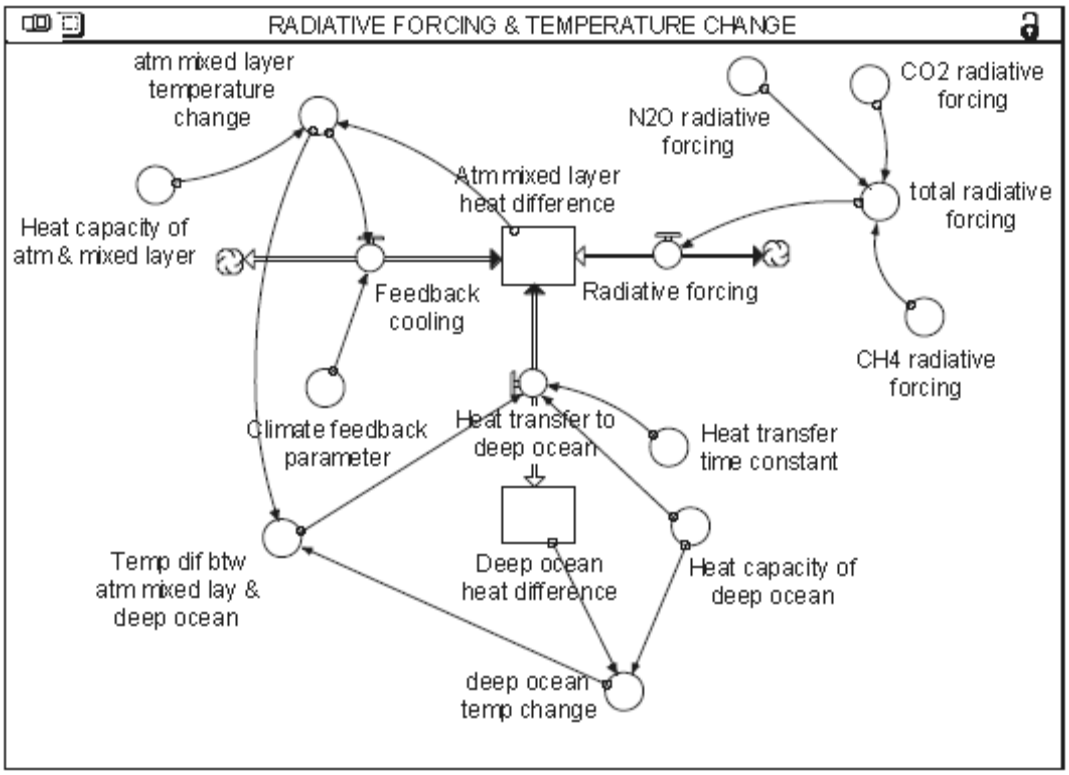

Figure 4.8 Simplified stock-flow structure of the radiative forcing and temperature change sector

There is no stocks in the first part. The total RF disturbing the system is calculated by adding up the RFs of CO_2, CH_4 and N_2O. The RF values of CH_4 and N_2O are taken from related sectors where they were already defined and calculated (see Appendix C). The radiative forcing of CO_2 is a logarithmic function of the CO_2 concentration in atmosphere implying that increasing atmospheric CO_2 concentration has a gradually diminishing forcing effect on the radiative balance. The RF of CO_2 is calculated with the following formula:

$$RF = \alpha \ln(C/C_0) \qquad (4.42)$$

where;

α is the radiative forcing coefficient

C_0 is the preindustrial atmospheric CO_2 concentrations in ppm

C is the actual atmospheric CO_2 concentrations in ppm.

The last revised α value is 5.35.

The structure of the second part of the sector is built on the DICE model (Nordhaus, 1992). However, the temperature stocks used by Nordhaus and Fiddaman (1997) are converted to heat stocks and, temperature changes are calculated separately. This part of the sector has two stocks; 'atmosphere and mixed layer heat difference' and, 'deep ocean heat difference'. All the stock variables and the temperature change variables represent the deviations from preindustrial conditions. For this reason, their initial values are zero.

'Atmosphere and mixed layer heat difference' stock represents the heat accumulation per unit area in the system with disturbance of equilibrium conditions. For this stock variable the troposphere, the earth surface and the upper 75 m depth of the ocean are treated as a well mixed box and, are assumed to have the same thermal properties, which is a common practice in coupled atmosphere-ocean climate modeling literature. The stock has one inflow, 'Radiative forcing' and, two outflows, 'Feedback cooling' and 'Heat transfer to deep ocean', which represent the mechanisms counteracting the RF, i.e. αT in equations (4.39) and (4.40).

'Deep ocean heat difference' stock represents the heat accumulation per unit area in the deep ocean since preindustrial times. The only inflow of this stock is 'heat transfer to deep ocean', which is the outflow of the 'Atmosphere and mixed layer heat difference' stock. The stock equations are:

Atm_mixed_layer_heat_difference(t) = Atm_mixed_layer_heat_difference(t - dt) +
(Radiative_forcing - Feedback_cooling - Heat_transfer_to_deep_ocean) * dt (4.43)

Deep_ocean_heat_difference(t) = Deep_ocean_heat_difference(t - dt) +
(Heat_transfer_to_deep_ocean) * dt (4.44)

Heat transfer to deep ocean is a very slow process because of the large heat capacity of the ocean. The model equation for this flux is:

Heat_transfer_to_deep_ocean =
Heat_capacity_of_deep_ocean*Temp_dif_btw_atm_mixed_lay_&_deep_ocean/
Heat_transfer_time_constant*time_conversion_parameter (4.45)

The ‘Heat capacity of deep ocean’ represents the heat capacity of the ocean per unit area. It is taken as 220 W*year/m^2/degreesC. This value is computed by multiplying the ‘Heat transfer time constant’, 500 years, with the heat capacity ratio, 0.44 W/m^2/degreesC, both given in DICE (Nordhaus, 1992).

The ‘Heat transfer time constant’ represents the time required for heat transfer between the atmosphere and upper ocean and the deep ocean. It may be interpreted as a mixing time constant (Fiddaman, 1997).

The ‘deep ocean temp change’ represents the change in the temperature of deep ocean since the beginning of preindustrial age. It is calculated by dividing the ‘deep ocean heat difference’ to its heat capacity and to unit conversion parameter.

Feedback cooling, the other outflow of the ‘atm-mixed layer heat difference’ stock that counteracts RF, is given with the following formula:

Feedback_cooling = Climate_feedback_parameter*atm_mixed_layer_temperature_change* time_conversion_parameter (4.46)

‘atm-mixed layer temp change’ represents the change in the temperature of atmosphere, ground surface and upper 75 m of ocean. It is also calculated the same way ‘deep ocean temp change’ was, i.e. by dividing the ‘atm-mixed layer heat difference’ to the heat capacity of atmosphere and mixed layer and to unit conversion parameter. The heat capacity of atmosphere and mixed layer is also taken from Nordhaus (1992) and (Fiddaman (1997) as 44.248 W*year/m^2/degreesC/.

‘climate sensitivity’(Houghton et. al., 1990) is defined as the change in global mean temperature that results when the climate system, or a climate model, attains a new equilibrium with the forcing change resulting from a doubling of the atmospheric CO_2 concentration. It is taken as 2.908°C from Fiddaman (1997). ‘climate feedback parameter’ is defined as the feedback effect that occurred from temperature increase, $\Delta RF/\Delta T$ where ΔRF is the change in RF and ΔT is the change in temperature. Since by definition, climate sensitivity is the change in temperature with a doubling of atmospheric CO_2,

$\Delta T = 2.908°C$ (4.47)

$\Delta RF = RF_{actual} - RF_0$ (4.48)

$$\Delta RF = \text{rad. forc. coeff. } CO_2 * \ln\left[\frac{2*C_0}{C_0}\right] - \text{rad. forc. coeff. } CO_2 * \ln\left[\frac{C_0}{C_0}\right] \quad (4.49)$$

which is equal to:

$\Delta RF = \text{rad. forc. coeff. } CO_2 * \ln(2)$ (4.50)

then,

Climate feedback parameter= rad. forc. coeff. CO_2*ln(2)/2.908°C (4.51)

Then a ‘global temperature anomaly’ variable is calculated by subtracting the average temperature change between years 1951 and 1980, from the ‘atmosphere and mixed layer temperature change’.

Complete set of equations of the sector can be found in Appendix A.

5. MODEL REFERENCE BEHAVIOR

The model is run from 1860 to 2100. Historical GHG emissions, either measured or estimated, are obtained from several data sources (CDIAC). The IS92a scenario of IPCC is used for future emissions. The IS92a scenario, which is well known as "Business as Usual" (BAU) scenario in climate change policy studies, represents a global energy use pattern that does not take into account global warming concerns. This scenario predicts an increase in anthropogenic CO_2 emissions of 8.2 GtC/year in 2006 to 20.4 GtC/year in 2100, also an atmospheric CO_2 concentration of about 700 ppmv with a global population of 11.3 billion in year 2100. The estimates of IS92a are based on global carbon cycle models that include solely the CO_2 fertilization feedback (Rotmans and de Vries, 1997).

All GHG emissions, LUC emissions, temperature-photosynthesis, temperature-respiration and temperature-wetland emissions feedbacks are present in the reference run. Only the permafrost feedback is inactive.

The atmospheric CO_2 concentration and the temperature show a similar increasing pattern. The simulated atmospheric CO_2 concentration attains the value of 746 ppm in year 2100 while it is 677 ppm in the IS92a scenario which does not consider the temperature feedback. However, both data have good fit until about 2010's (see Figure 5.1). The simulated temperature increase is 3.21°C compared to preindustrial times in year 2100. The $2xCO_2$ value, which means twice preindustrial atmospheric CO_2 concentration and which is an important milestone in global warming policy debates, is attained in year 2064. The climate sensitivity parameter is 2.908 in the reference run. The behaviors of atmospheric CO_2 and the temperature are depicted below:

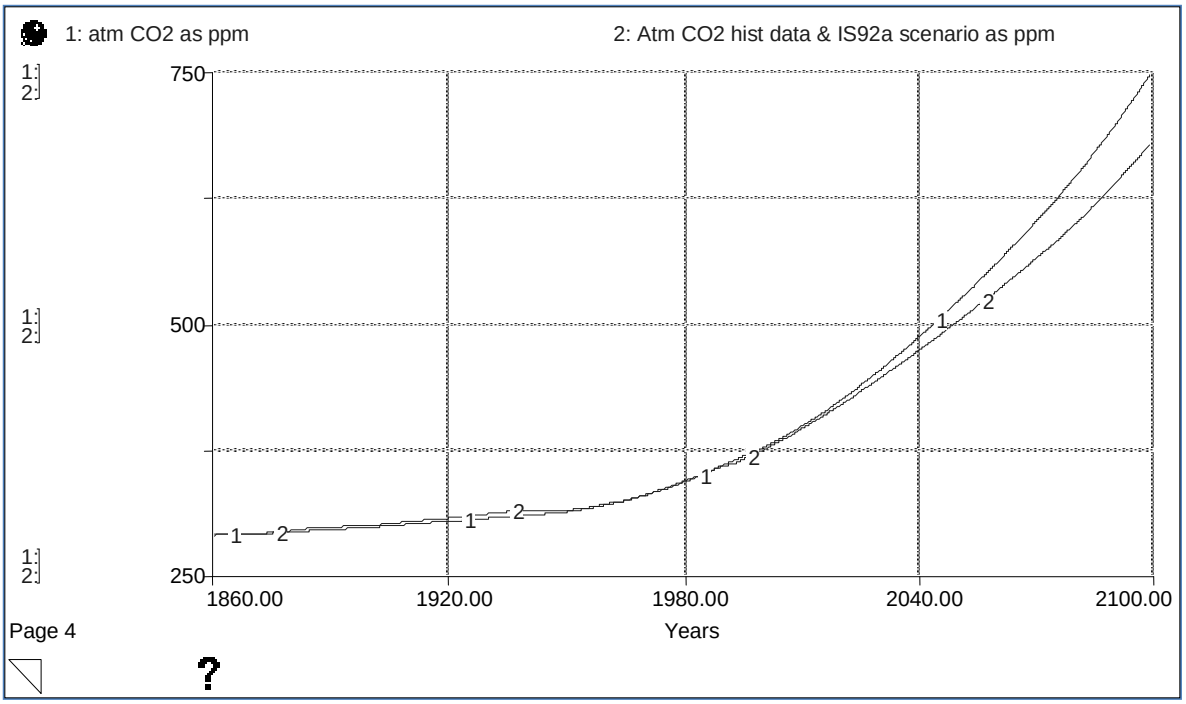

Figure 5.1 Atmospheric CO_2 as ppm (1: reference behavior, 2: historical data and IS92a scenario)

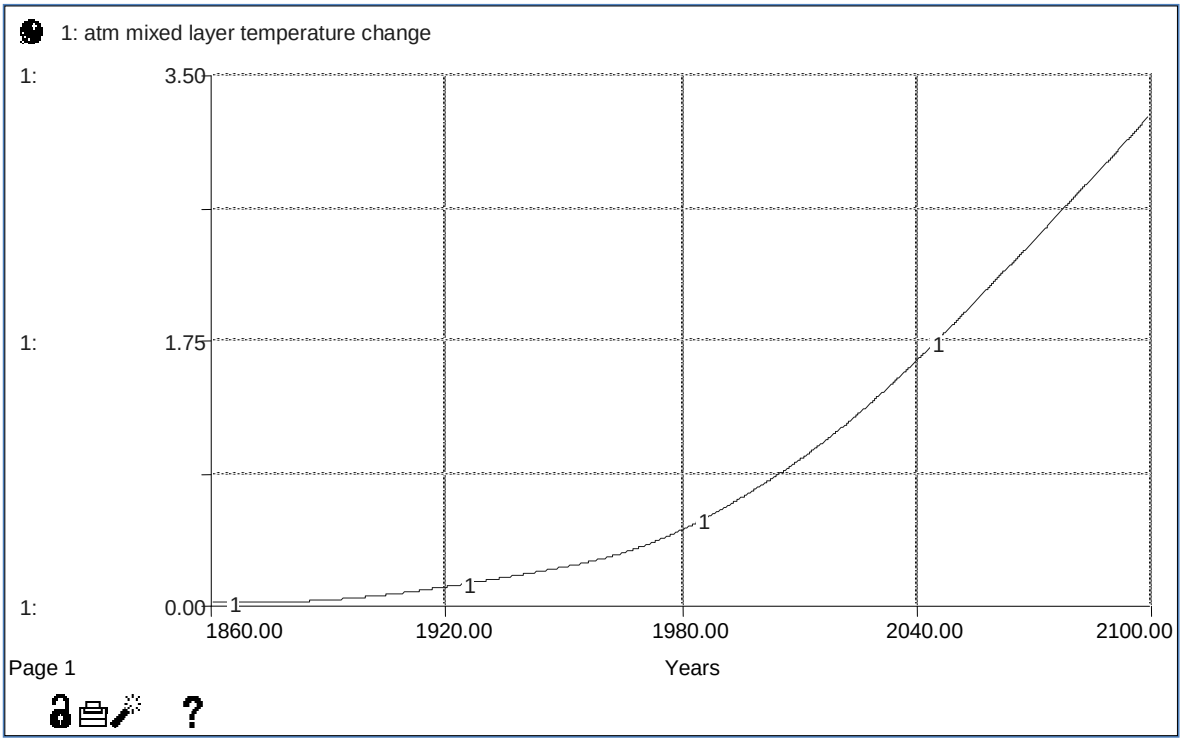

Figure 5.2 Reference behavior of the atmosphere-mixed layer temperature

The Gross primary production (GPP) and net primary production (NPP) have an increasing trend due to both increasing carbon content of the stocks and the increasing temperature. The NPP/GPP ratio that was estimated as about 0.5 in Watson et. al. (2000) decreases from 0.48 to 0.41 till the end of simulation (Figure 5.3). The value of biostimulation coefficient, β, is 0.5 in the reference run.

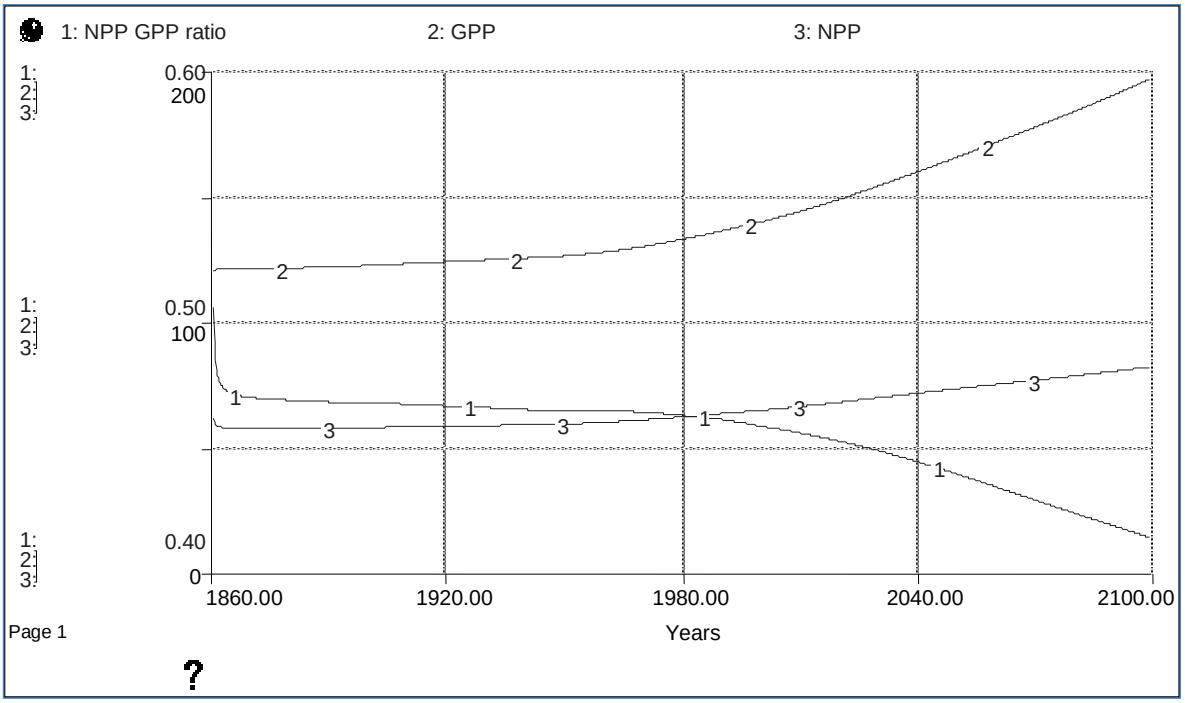

Figure 5.3 Reference behavior of GPP and NPP in GtC and, of NPP/GPP ratio

The terrestrial stocks have different behaviors. Active soil carbon decreases while carbon in woody tree parts increases. Their behavior in the reference run is illustrated in Figure 5.4.

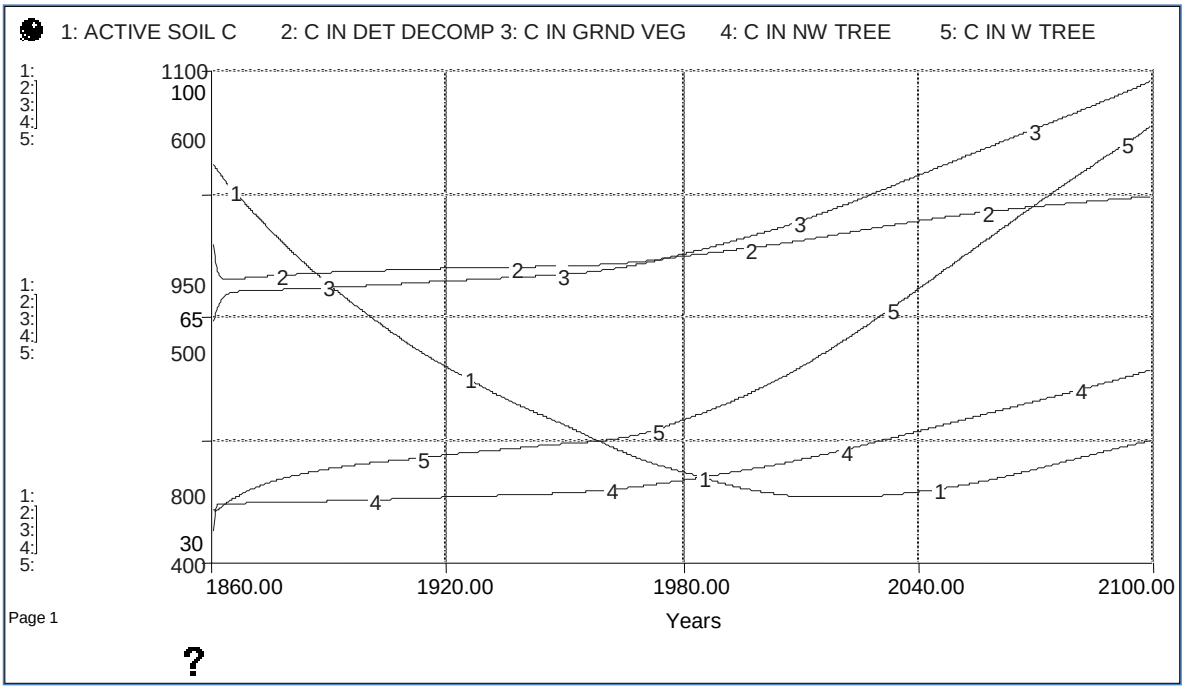

Figure 5.4 Reference behavior of the terrestrial stocks in GtC

The three main stocks of the carbon cycle; the atmosphere, the ocean and the land behave as in Figure 5.5 in the reference run. The terrestrial sum first decreases, then increases while the atmospheric and oceanic stocks grow continuously.

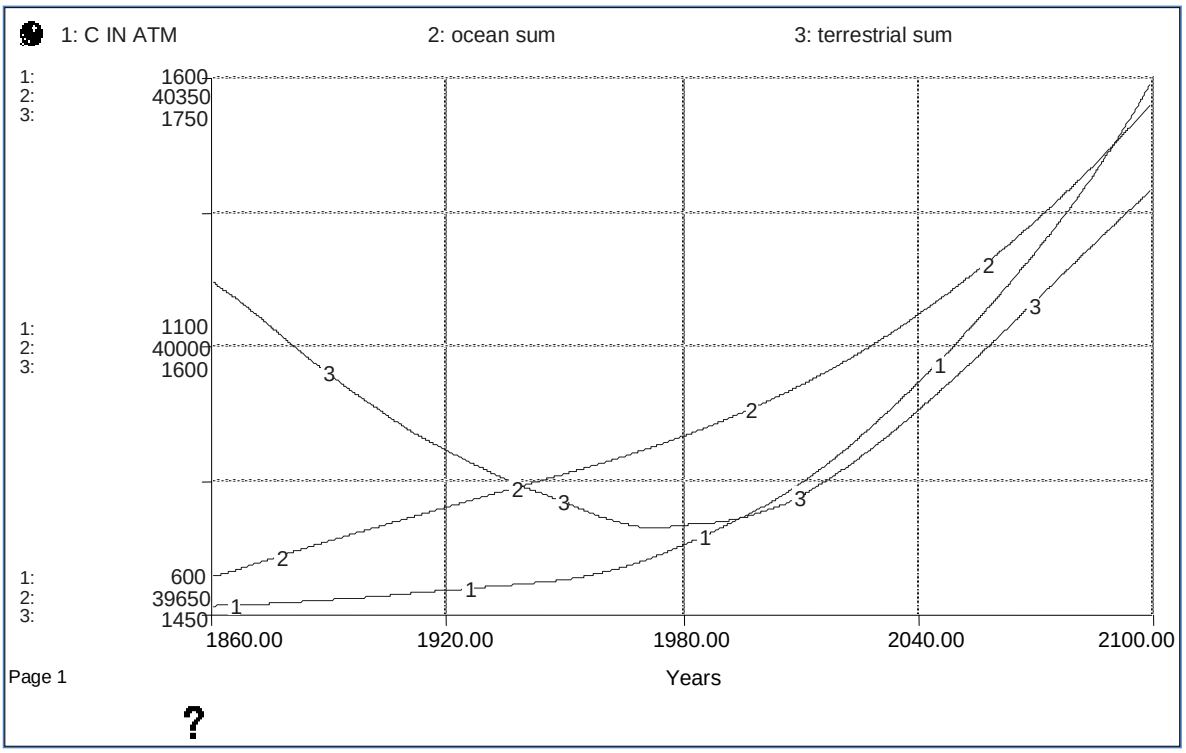

Figure 5.5 Reference behavior of the aggregated main stocks of the carbon cycle in GtC

The temperature coefficients for photosynthesis, respiration and wetland methane emissions are assigned as 1.37, 2 and, 6 respectively in the reference run. The GPP, total respiration and wetland emission patterns corresponding to those values are shown below:

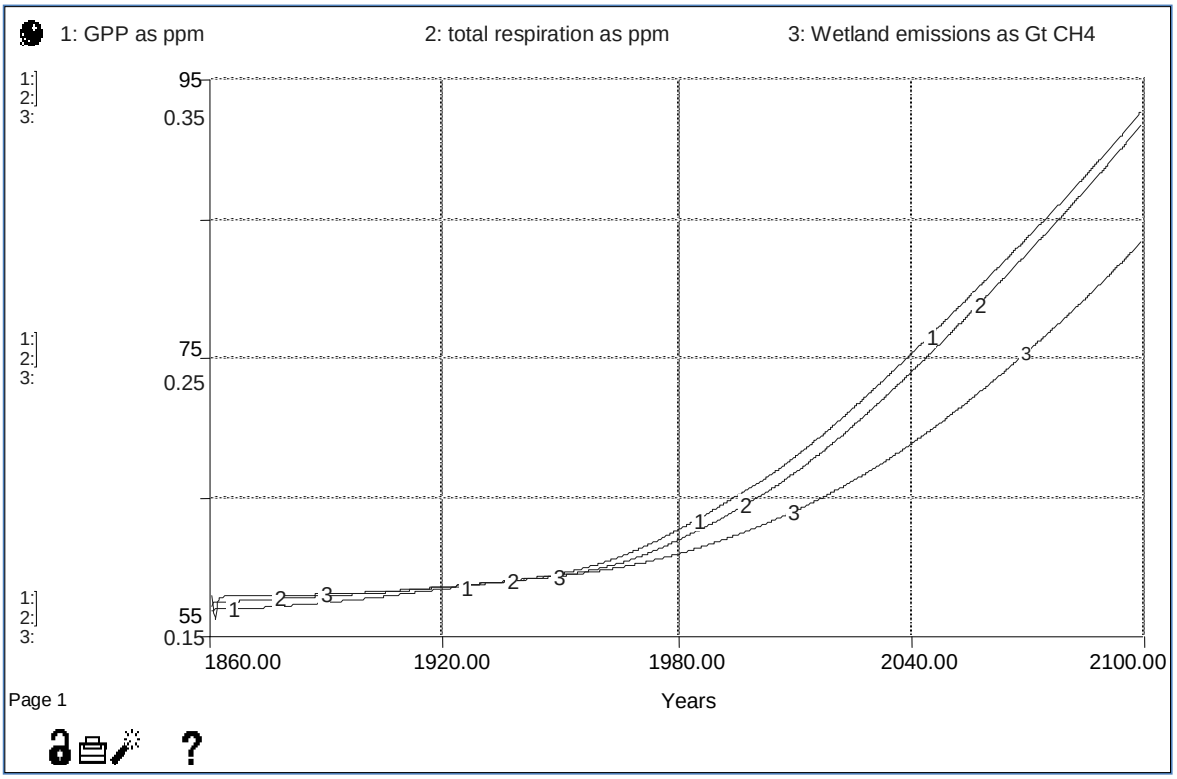

Figure 5.6 Reference behavior of the GPP, respiration and wetland methane emissions

The behavior of the atmospheric methane and nitrous oxide stocks in the reference run and, their historical and IS92a scenario values are also presented in Figures 5.7 and 5.8 respectively.

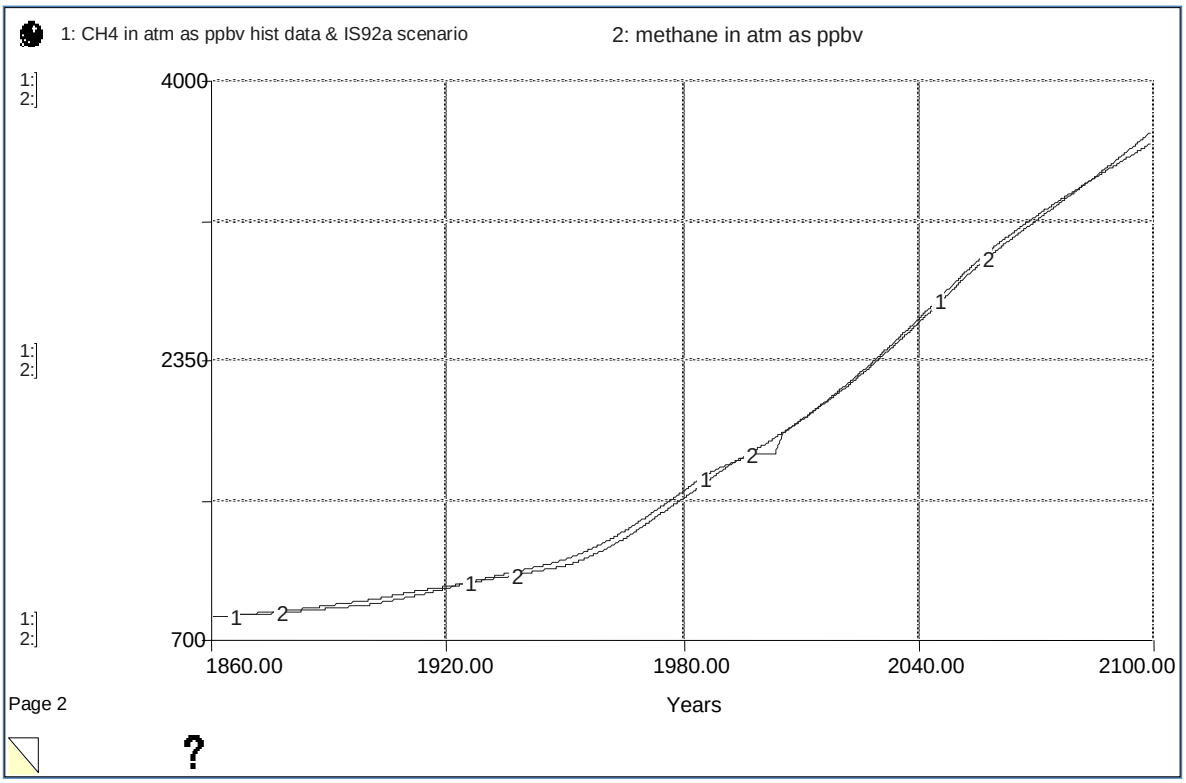

Figure 5.7 Reference behavior of the atmospheric methane (curve 2) and, historical data and IS92a scenario (curve 1) as ppbv

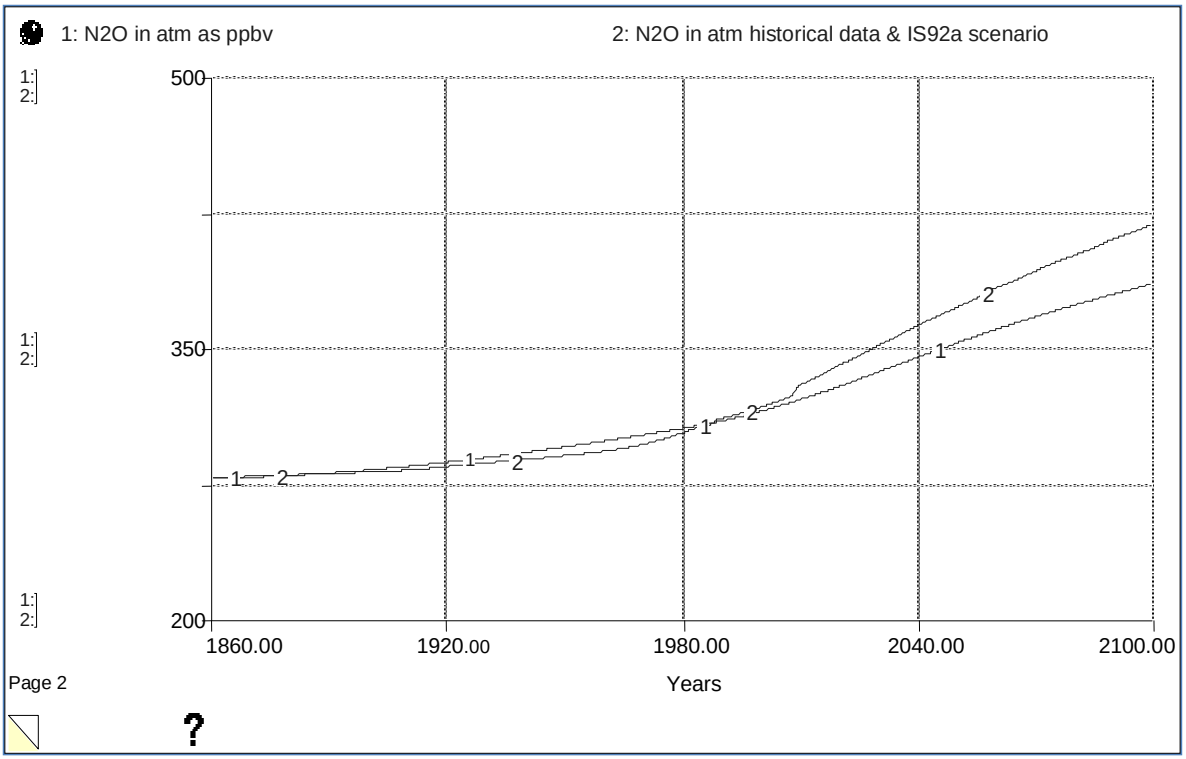

Figure 5.8 Reference behavior of the atmospheric nitrous oxide (curve 1) and, historical data and IS92a scenario (curve 2) as ppbv

6. MODEL VALIDATION

6.1. Validation Procedure

Model validation is one of the most important stages of a model-based study. In causal descriptive models, such as the equation based dynamic system models, since model behavior is created by the structure of the model, first the model structure validity must be tested. After building sufficient confidence in model structure, observations on behavior pattern validation becomes relevant, because, even significantly flawed model structures can produce spurious fits (Barlas, 1996). Therefore, model validation procedure comprises two main parts in sequence: 1) assessing the structural validity of the model and 2) assessing the behavioral validity of the model.

The structural validity of the model is assessed with direct structure tests and with indirect structure tests, also called as structure-oriented behavior tests. Direct structure tests compare the model structure with the real system by taking each relationship individually and, do not involve any simulation (Barlas, 1996). They include tests like parameter confirmation tests, direct extreme condition tests, and dimensional consistency tests. The information necessary in the nature for direct structure tests is generally based on empirical observations and can hardly be expressed with mathematical equations. Nevertheless some mathematical relationships in the model structure are only theoretical and can hardly be verified by observation. For this reason, it is hard to implement a formal direct structure tests procedure. However, some of those tests are performed in this study during model construction, wherever the information is available. Direct extreme-condition tests are performed on the model equations. Suitability of the parameters to the real system and, dimensional consistency of the model equations are checked throughout the study.

6.2. Structural Validation with Indirect Structure Tests

6.2.1. Extreme Condition Tests

Test 01: No Anthropogenic CO_2 Emissions

For this test, all anthropogenic CO_2 emissions and LUC emissions are set to zero. Since there is no anthropogenic disturbance to carbon cycle, the atmospheric CO_2 level fluctuates between 279 and 287 ppm during the simulation period. This fluctuation is due to natural processes between terrestrial stocks, atmosphere and the ocean (Figure 6.1).

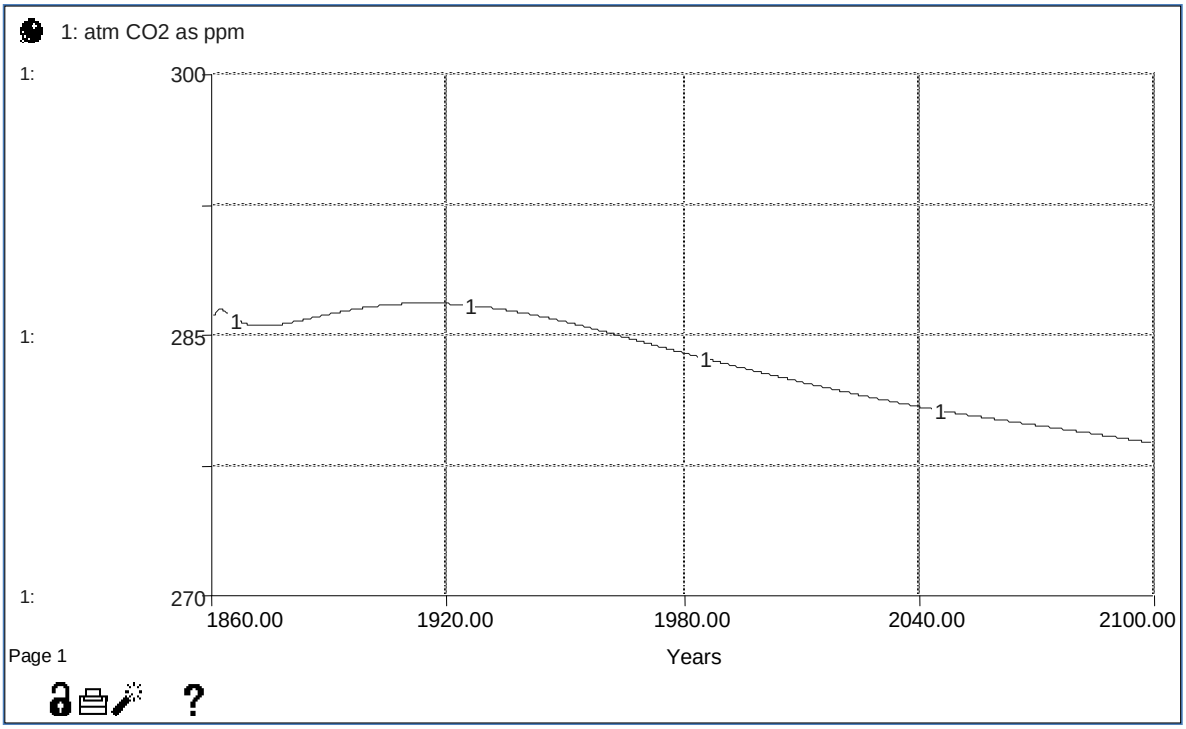

Figure 6.1 No anthropogenic CO_2 emissions

Test 02: No Radiative Forcing

For this test, all three GHG radiative forcings are set to zero and the simulation is run. Since there is no disturbing effect of radiative forcing to the global heat balance, heat stocks do not change, no heat transfer occurs between them and thus no temperature change is observed (Figure 6.2).

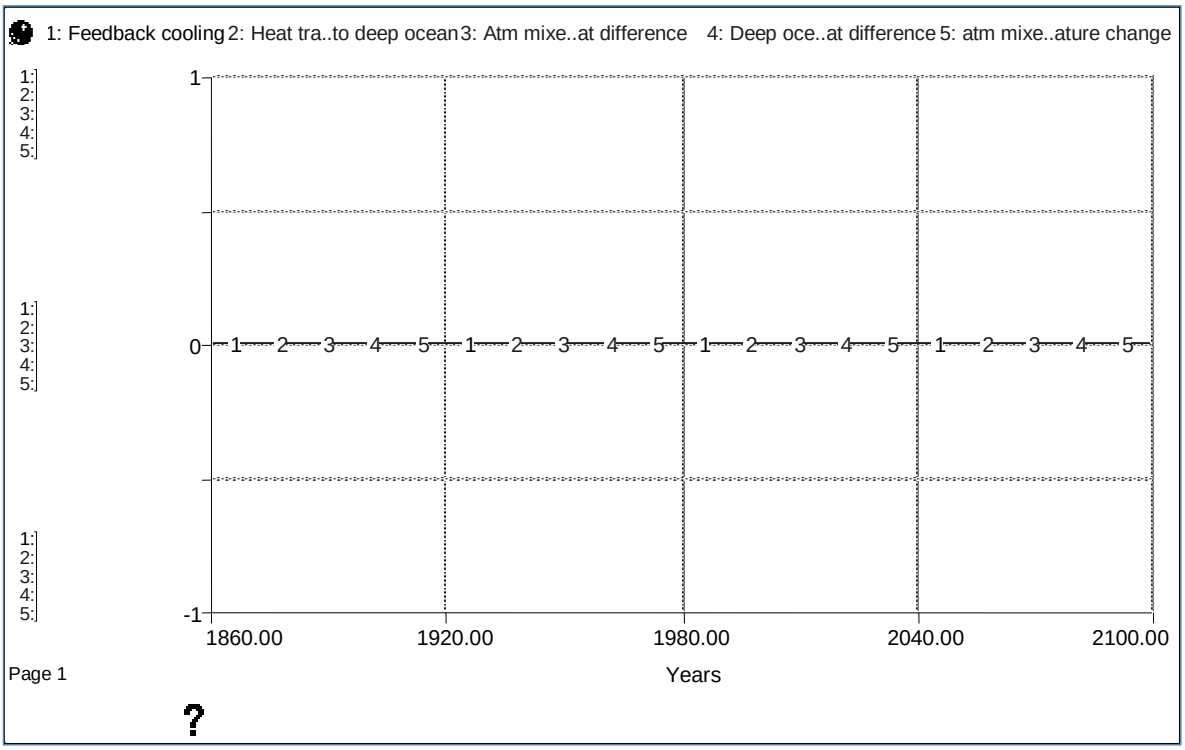

Figure 6.2 No radiative forcing

Test 03: No Photosynthesis

For this test, the two photosynthesis flows, the anthropogenic CO_2 emissions and the LUC emissions are set to zero and, the simulation is run. Since there is no photosynthesis, the carbon stocks of all the terrestrial reservoirs are used up due to respiration. The photosynthetic stocks, i.e. ground vegetation and non-woody tree parts, are discharged much faster than the others (Figure 6.3).

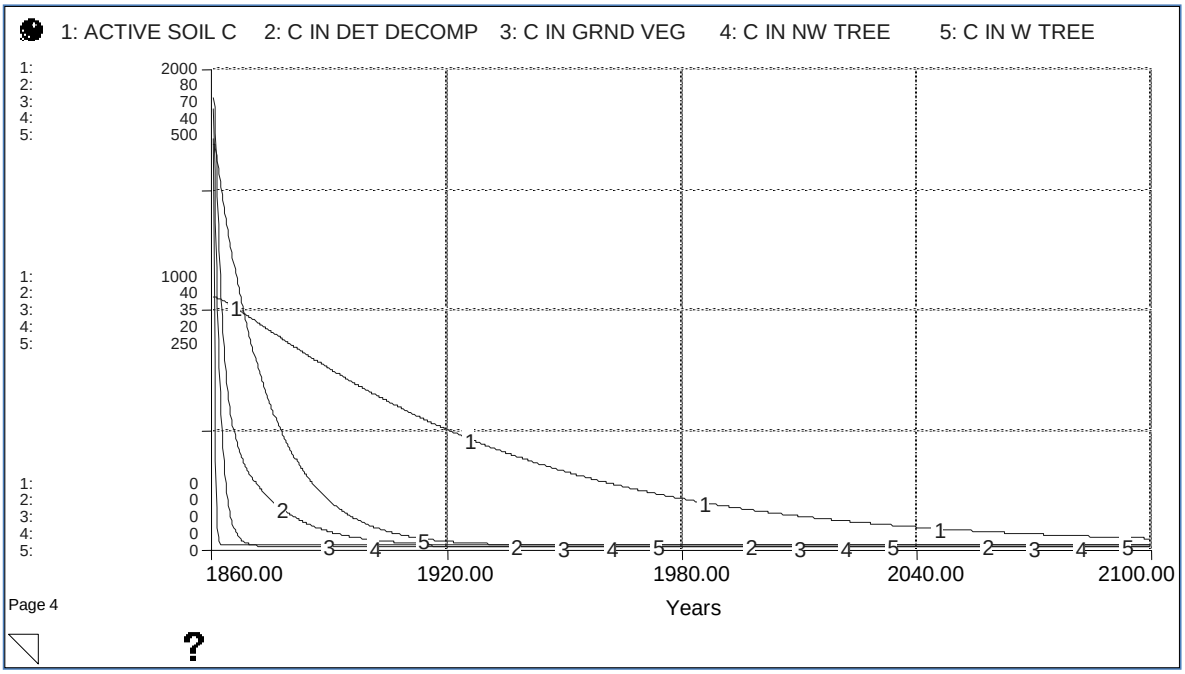

Figure 6.3 No photosynthesis test
(behavior of terrestrial carbon stocks in GtC when no photosynthesis exist)

The atmospheric CO_2 concentration first increases significantly due to fast transfer of the terrestrial carbon to the atmosphere through respiration. Then, its increase slows down and it begins to decrease due to carbon flux to the ocean. Carbon flux to ocean increases to compensate the fast accumulation in the atmosphere. The carbon released from terrestrial stocks with respiration is shared between the atmosphere and ocean reservoirs. The behavior of the system with and without photosynthesis is shown in Figures 6.4 through 6.6.

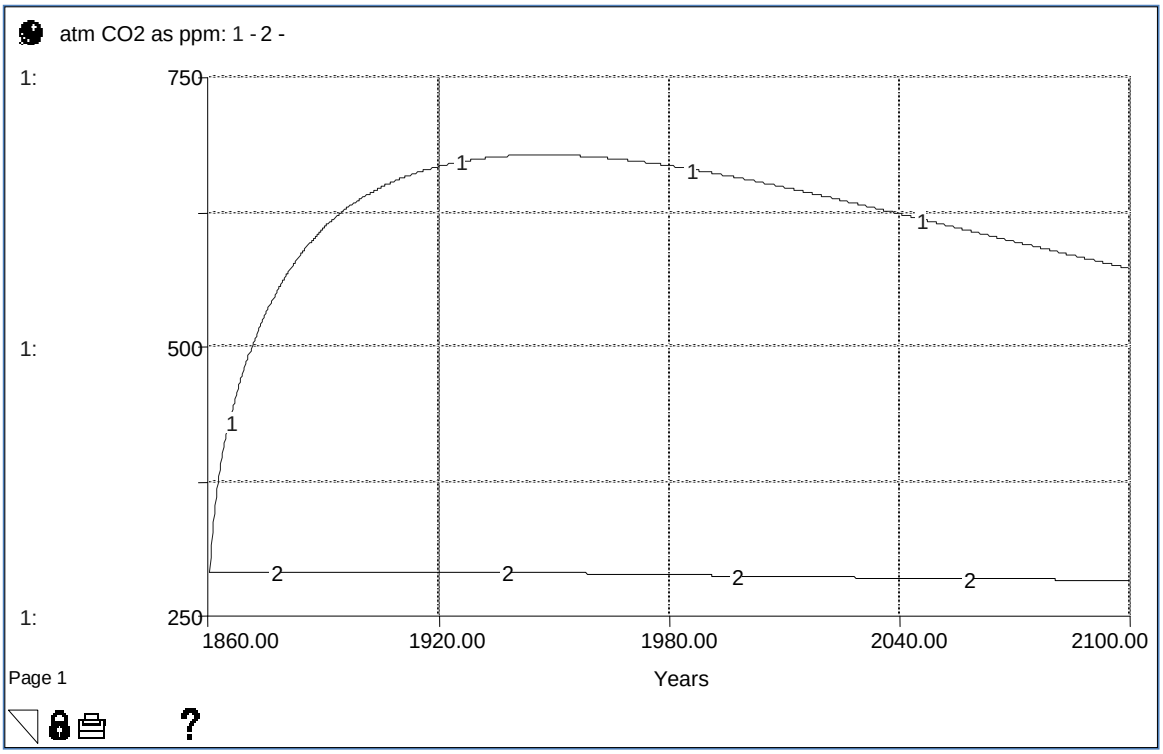

Figure 6.4 No photosynthesis test
(atmospheric CO_2 in ppm, 1: without photosynthesis, 2: with photosynthesis)

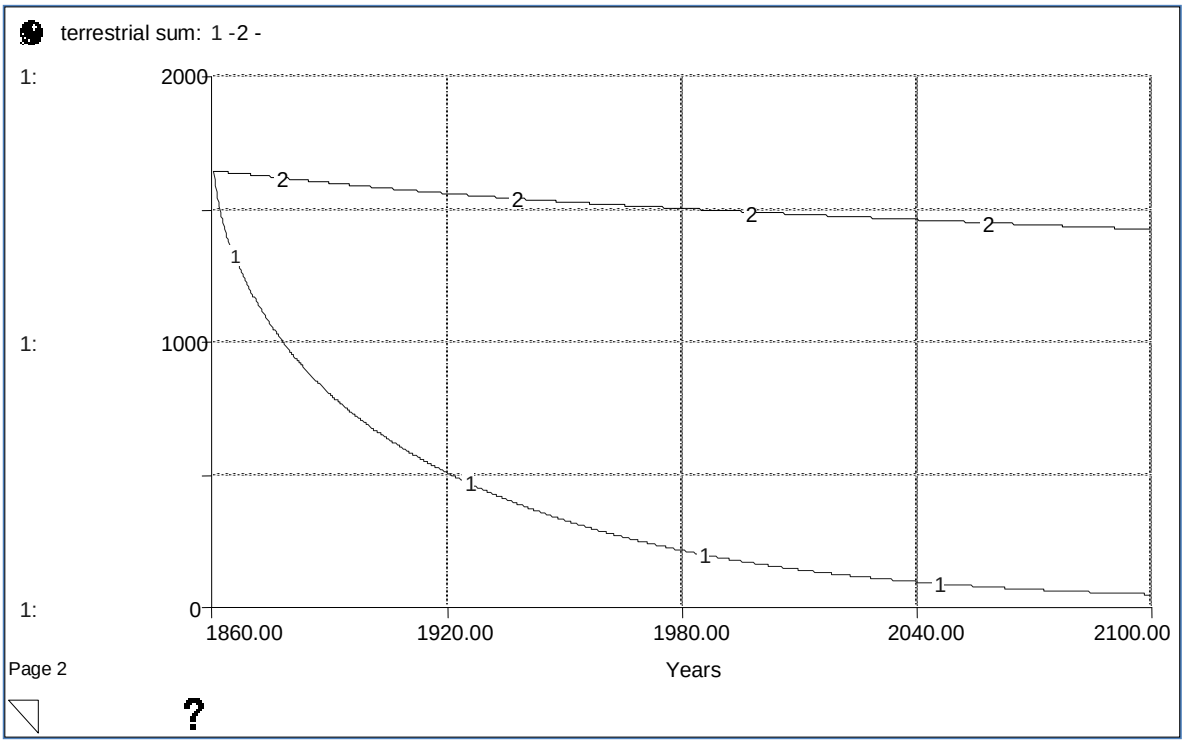

Figure 6.5 No photosynthesis test
(terrestrial carbon in GtC, 1: without photosynthesis, 2: with photosynthesis)

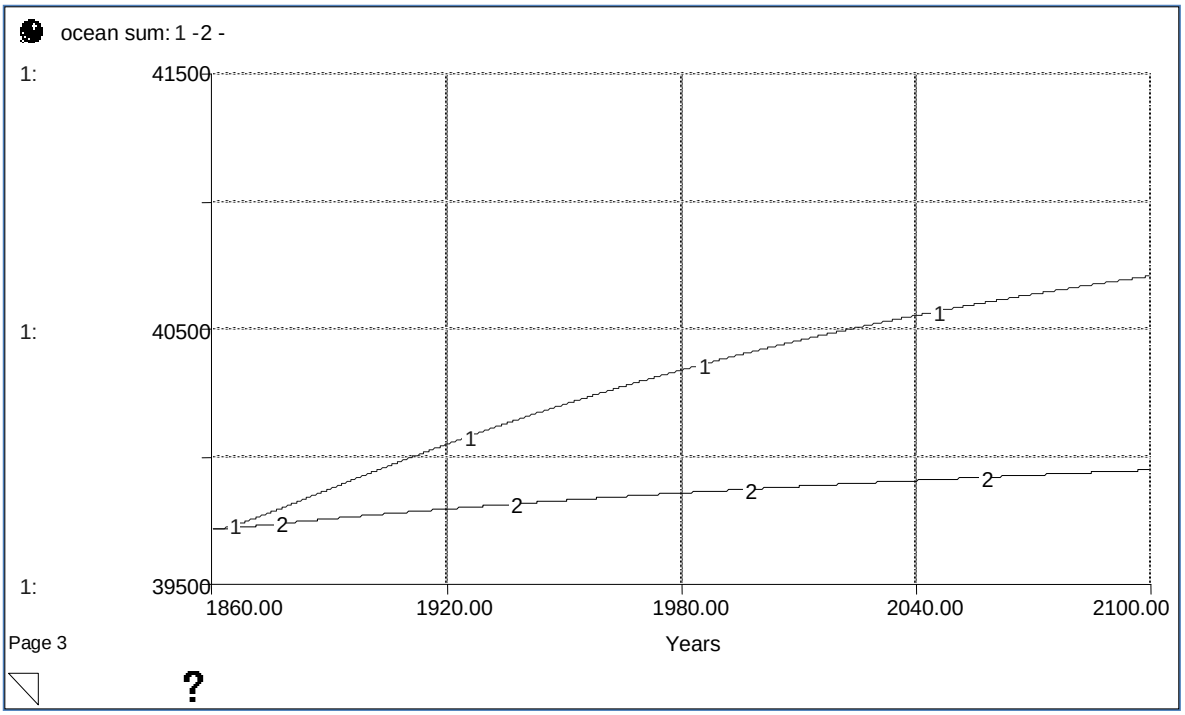

Figure 6.6 No photosynthesis test

(ocean sum in GtC, 1: without photosynthesis, 2: with photosynthesis)

Test 04: No Buffer Factor

As explained previously, buffer factor limits the carbon uptake capacity of the ocean. In this test, the effect of buffer factor on equilibrium carbon in mixed layer is cancelled and the behavior is observed. When there is no buffering effect, the uptake capacity of the ocean increases, thus the ocean absorbs more carbon from the atmosphere and, a smaller increase in temperature is observed. The temperature increase at the end of simulation without the buffering capacity of the ocean is observed to be 1.61°C while it is 3.21°C with buffer factor. The results are depicted in figures 6.7 to 6.9.

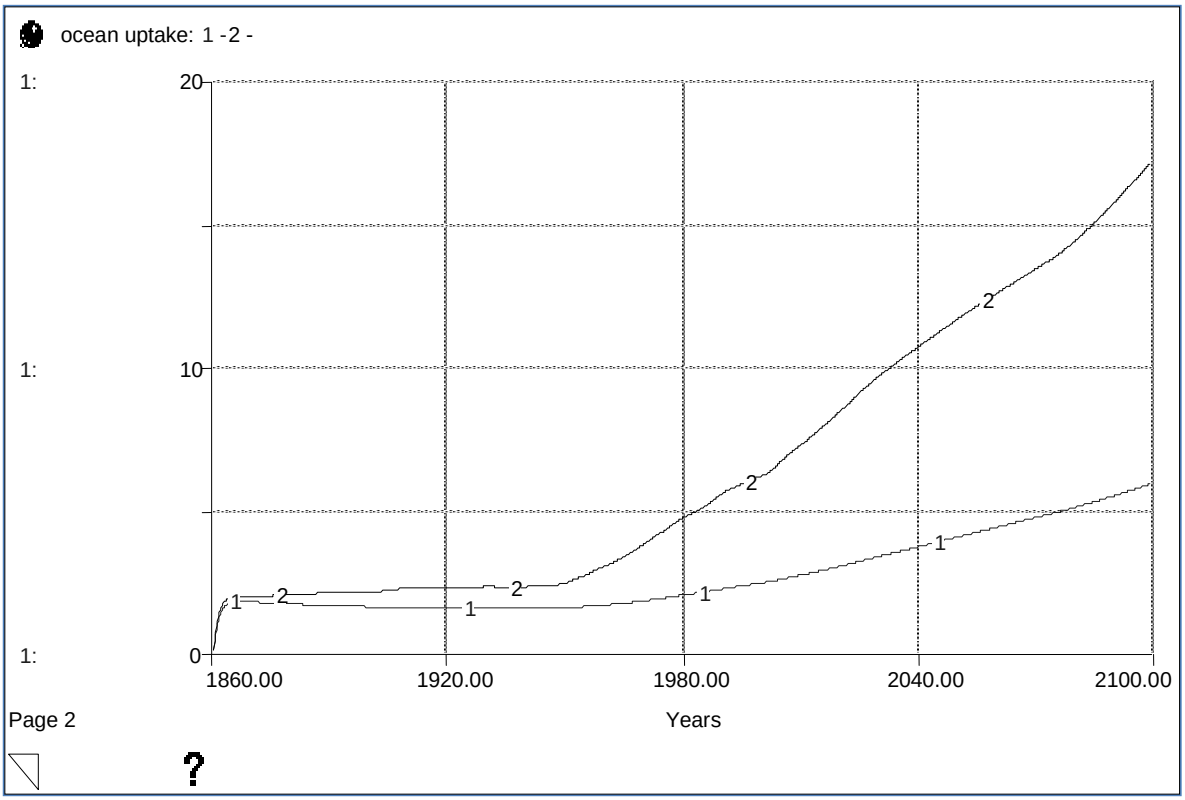

Figure 6.7 No buffer factor test
(ocean uptake in GtC, 1: with buffer factor, 2: without buffer factor)

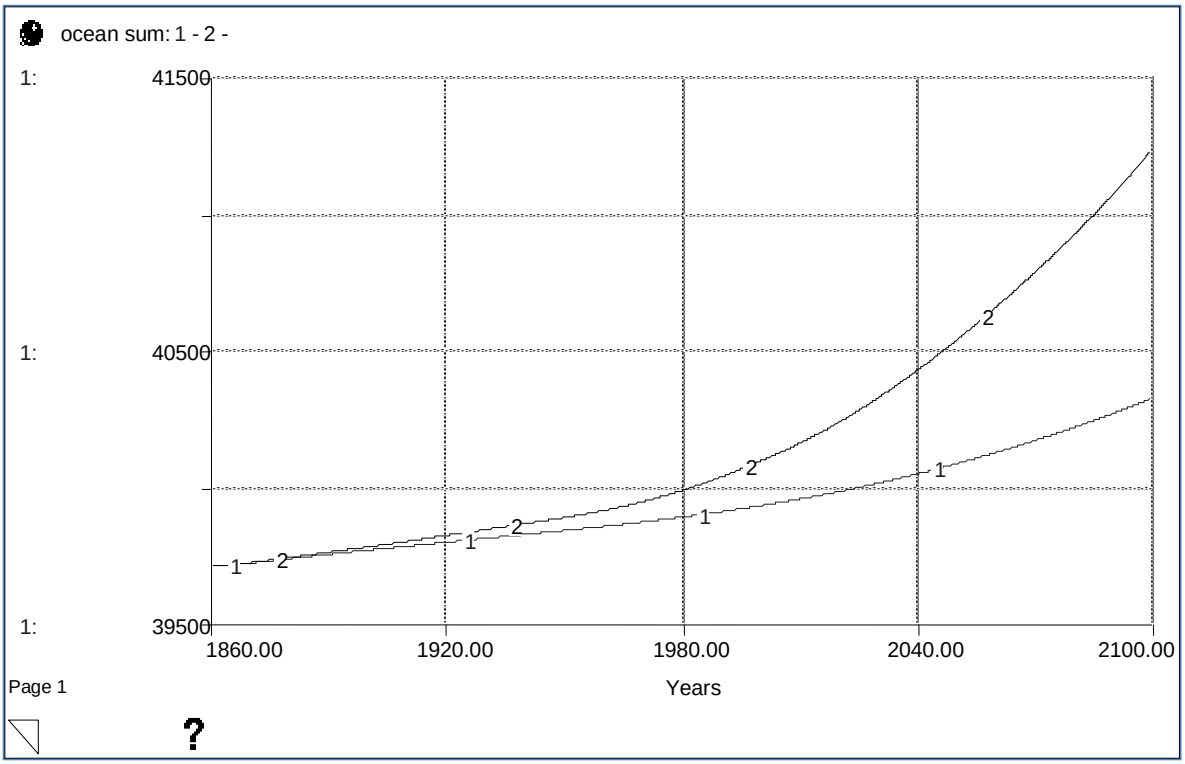

Figure 6.8 No buffer factor test
(ocean sum in GtC, 1: with buffer factor, 2: without buffer factor)

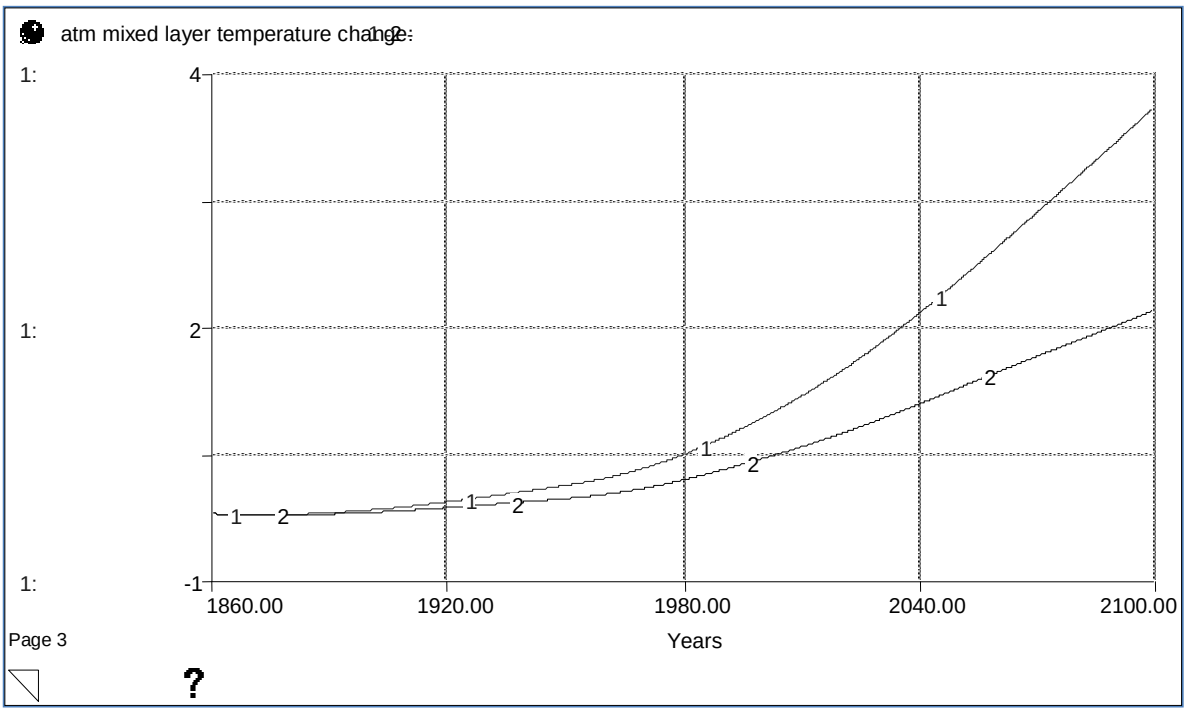

Figure 6.9 No buffer factor test
(temperature change, 1: with buffer factor, 2: without buffer factor)

6.2.2. Parameter Sensitivity Tests

Test 05: Sensitivity of the Atmospheric Carbon, the GPP and the Atmospheric Temperature to the Biostimulation Coefficient

The biostimulation coefficient β, which is the coefficient determining the response of GPP to increasing atmospheric CO_2, is the major uncertain parameter of the photosynthesis formulation. The uncertainty range is given as 0 to 0.7 in Goudriaan and Ketner (1984).

A sensitivity analysis is performed with the values 0, 0.2, 0.4, 0.6 and 0.8 of β. The results are depicted in below graphs with curves 1 to 5, each representing the behavior of the relevant variable for β values of 0, 0.2, 0.4, 0.6 and 0.8 respectively.

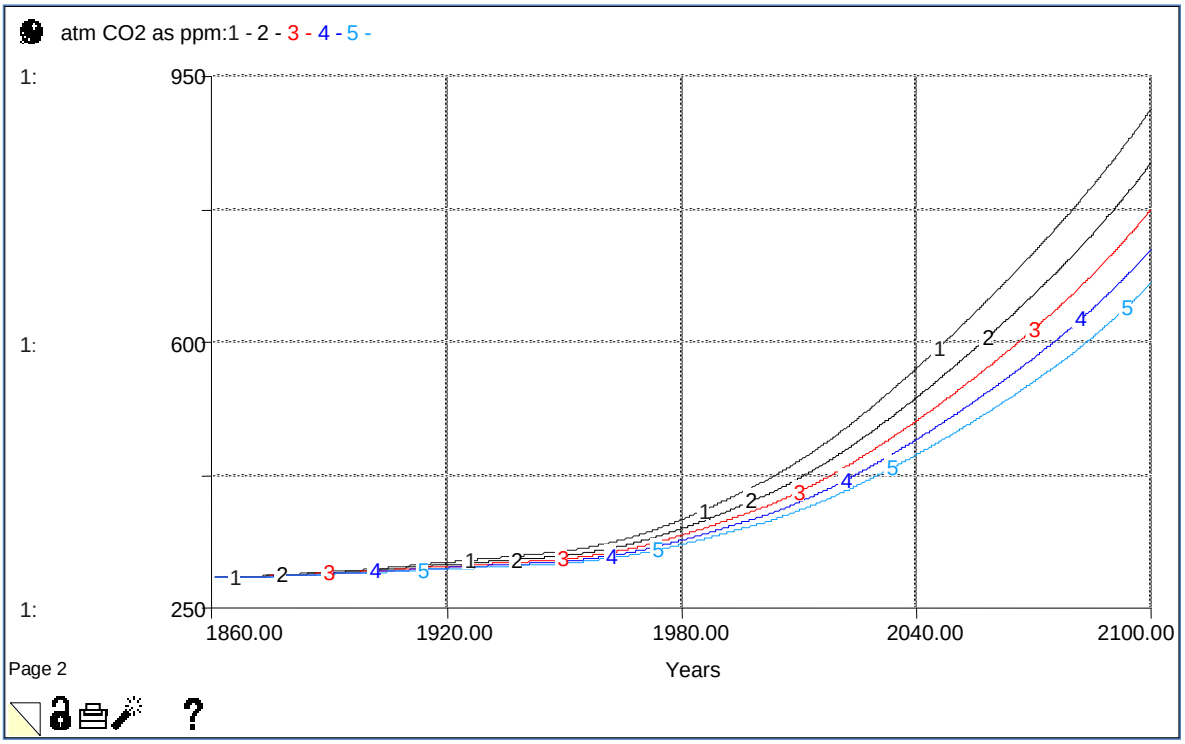

Figure 6.10 Sensitivity analysis for β (change of atmospheric carbon level)

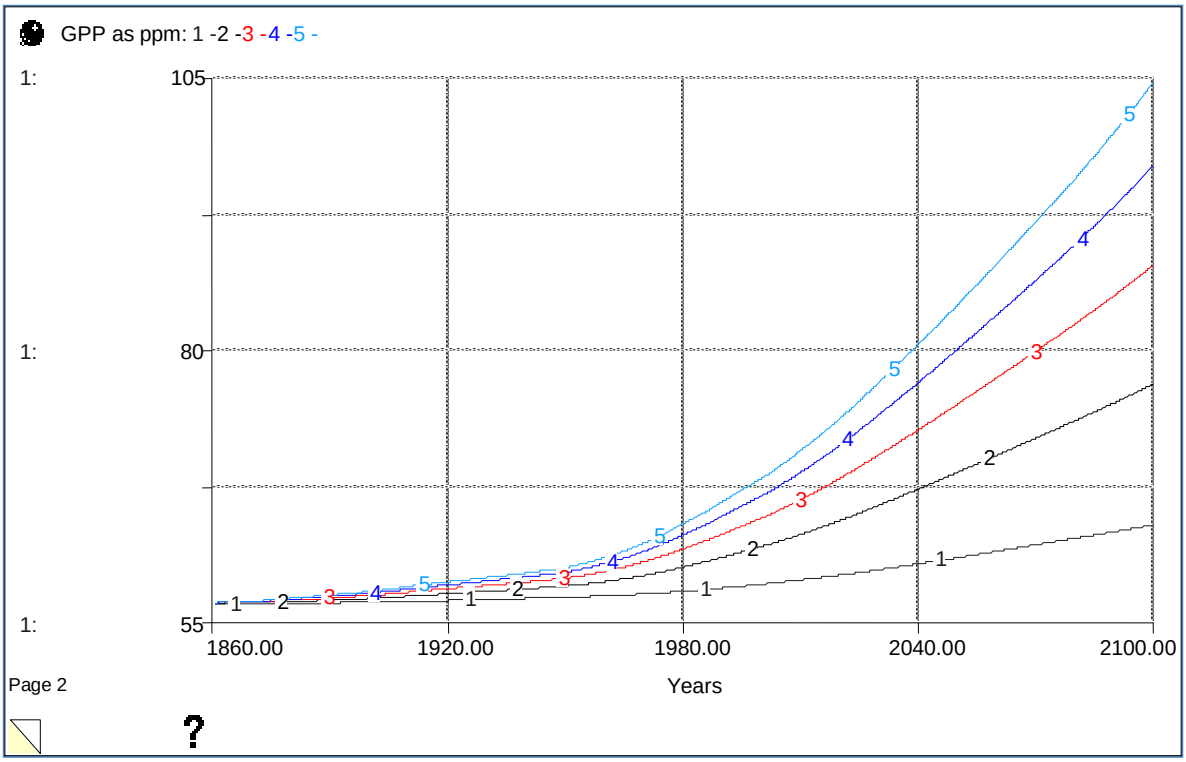

Figure 6.11 Sensitivity analysis for β (change of GPP)

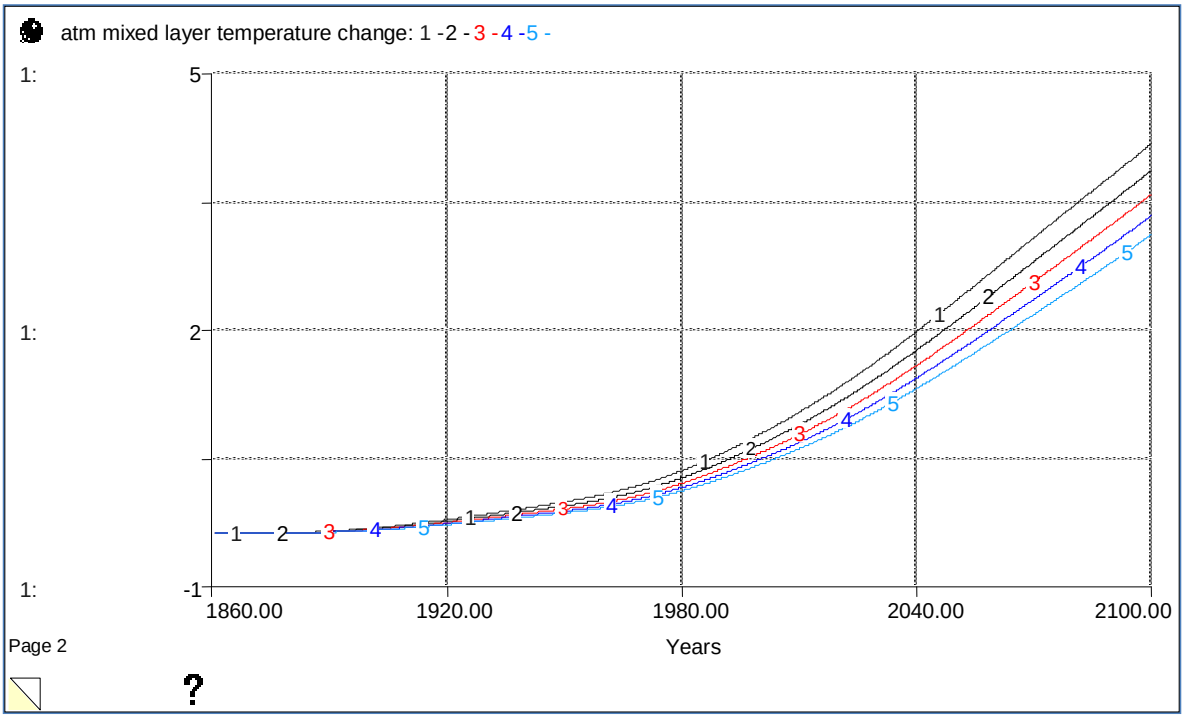

Figure 6.12 Sensitivity analysis for β (change of atmospheric temperature)

As can be seen from the generic equation for photosynthesis (equation 4.8.), when β=0, the GPP becomes independent of atmospheric CO_2 concentration and only dependent on temperature effect on the initial value of GPP. When β increases, GPP increases, which means the terrestrial system absorbs more carbon, causing the atmospheric carbon level and the temperature to increase less. However, since the relationship is logarithmic, as β increases, its effect to the inspected variables decreases. For instance, in year 2040, increase of β from 0.2 to 0.4 causes an increase of 31 ppm in atmospheric carbon level while its increase from 0.6 to 0.8 causes an increase of 20 ppm.

Test 06: Sensitivity of Photosynthesis to Temperature Coefficient, $Q_{10photsynth}$

The Q_{10} formulation that was described previously, indicates the temperature dependence of biochemical reaction rates. The Q_{10} temperature coefficient is a measure of the rate of change of a biological or chemical process by an increase of 10°C in temperature. The temperature coefficient of photosynthesis, $Q_{10photsynth}$, determines the response of photosynthesis to changing temperature. A sensitivity analysis is performed by assigning the values 0.5, 1, 1.5 and 2 to this parameter. The response of GPP to different values is shown below with curves 1 to 4 respectively:

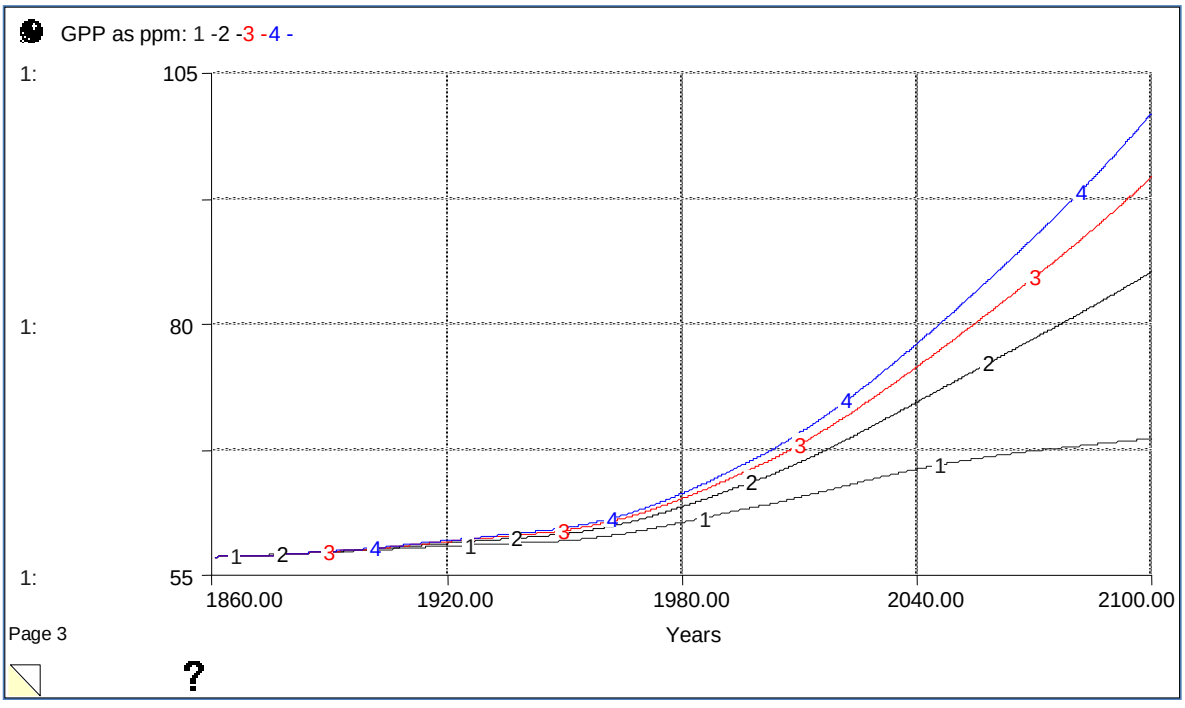

Figure 6.13 Sensitivity analysis for $Q_{10photsynth}$ (change of GPP)

Increase of $Q_{10photsynth}$ stimulates the photosynthesis and increases the GPP. However, increasing $Q_{10photsynth}$ levels have a decreasing effect on GPP.

Test 07: Sensitivity of Respiration to Temperature Coefficient, Q_{10resp}

The temperature coefficient of respiration determines the response of respiration of the terrestrial system stocks to changing temperature. A sensitivity analysis is performed by assigning the values 0.5, 1, 1.5, 2 and 2.5 to this parameter. The response of terrestrial respiration to different values is shown below with curves 1 to 4 respectively:

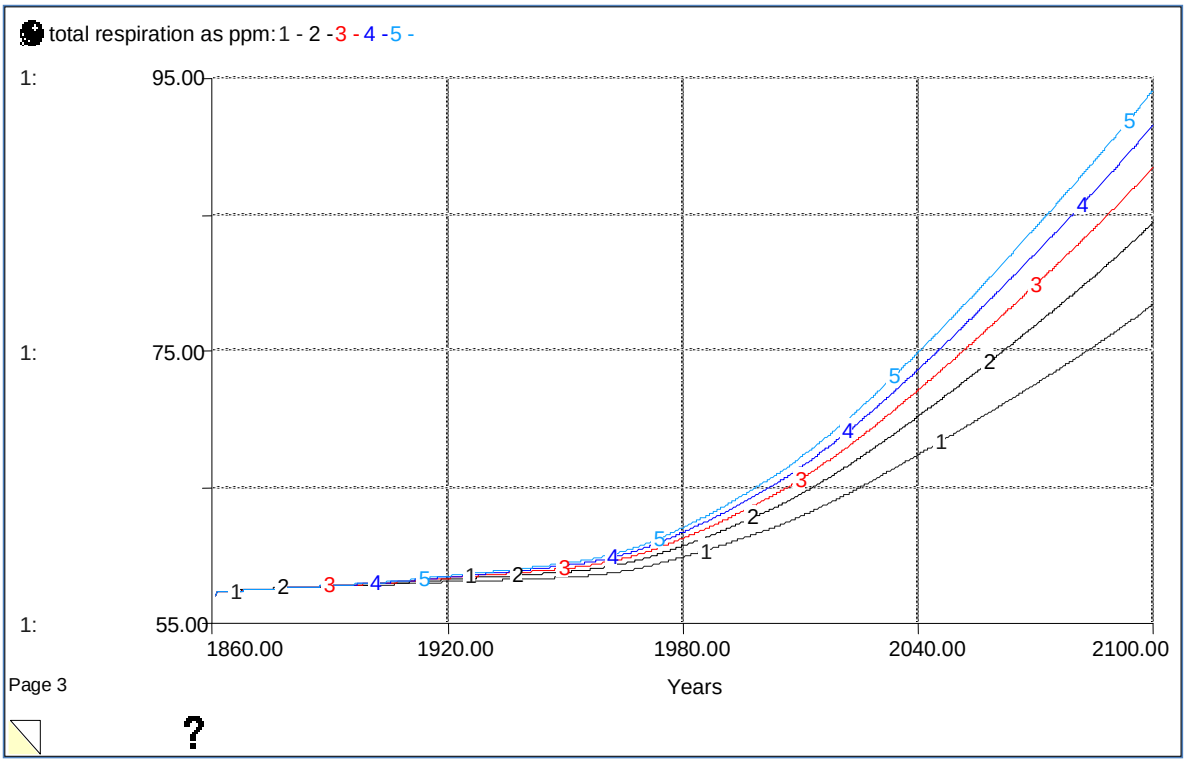

Figure 6.14 Sensitivity analysis for Q_{10resp} (change of total respiration)

Increase of Q_{10resp} stimulates the respiration of all the terrestrial biomes and increases the total respiration of terrestrial system. Nevertheless, increasing Q_{10resp} levels have a decreasing effect on respiration.

Test 08: Sensitivity of Wetland Methane Emissions to Temperature Coefficient of Methane Production Rate, $Q_{10\ CH4\ production}$

The temperature coefficient of methane production in wetlands also has a large range of uncertainty. A sensitivity analysis is performed to observe the effect of changing values of this parameter to global methane production from wetlands. The model is run with five different values of $Q_{10\ CH4\ production}$, 1.5, 3, 4.5, 6 and 7.5 respectively. The results are depicted in below graph with curves 1 to 5:

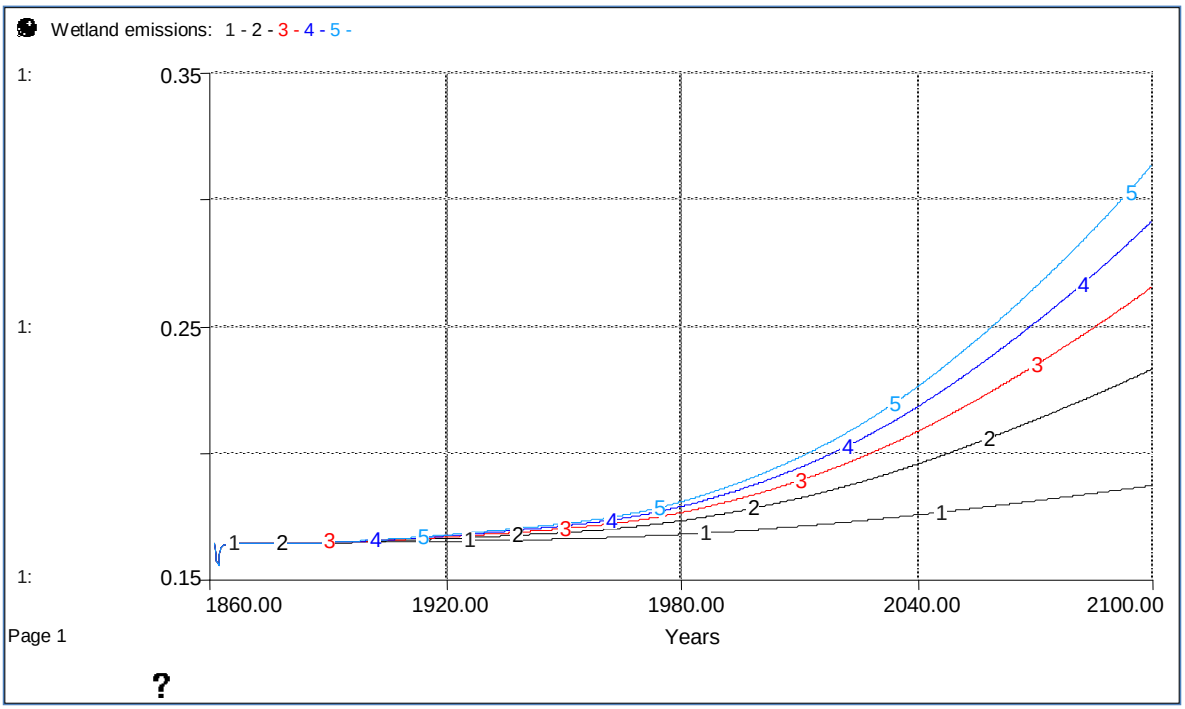

Figure 6.15 Sensitivity analysis for $Q_{10\ CH4\ production}$
(change of wetland methane emissions in $GtCH_4/y$)

As observed with other temperature coefficients, increasing Q_{10} values increases wetland methane emissions but at a decreasing rate.

Test 09: Sensitivity of the Temperature to Climate Sensitivity Parameter

The climate sensitivity parameter, which is defined as the 'Equilibrium temperature change in response to a $2xCO_2$ equivalent change in radiative forcing', is an important, yet highly uncertain parameter in temperature change calculations. A sensitivity analysis is performed with changing values of this parameter and the resulting change in atmospheric temperature is observed (Figure 6.16). The curves 1 to 5 represent the behavior with climate sensitivity parameter value of 2, 2.5, 3, 3.5 and 4 respectively.

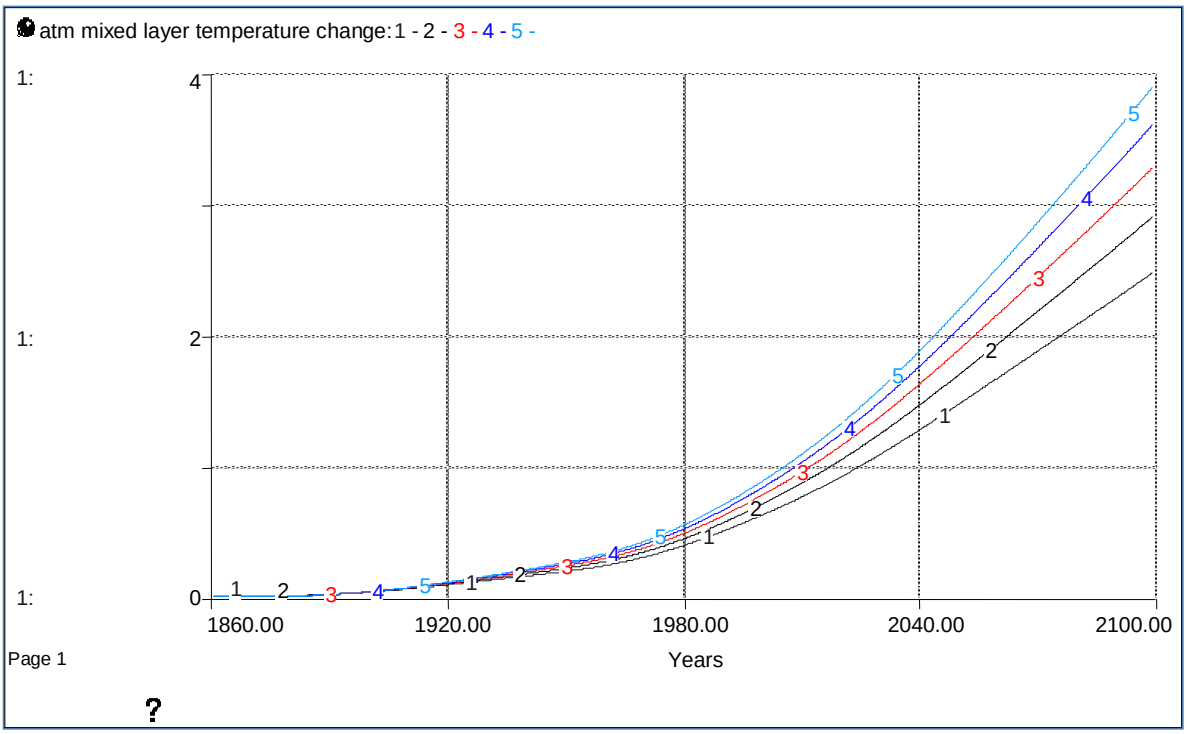

Figure 6.16 Sensitivity analysis for climate sensitivity parameter
(change of atmosphere and mixed layer temperature)

A climate sensitivity parameter value of 2 results in a warming of 2.49°C in year 2100 while a value of 4 results in a warming of 3.92°C in the same year.

6.2.3. Phase Relationship Test

Test 10: Comparison of NBP with Terrestrial Uptake

All carbon emissions exogenously added into the system are distributed among the three main reservoirs, the land, ocean and, the atmosphere. Therefore, the terrestrial uptake, which means the carbon assimilation of the terrestrial system, can be calculated by summing all anthropogenic CO_2 emissions and LUC emissions that were exogenously added into the system and, by subtracting the ocean uptake and the amount retained in the atmosphere from this sum. In other words;

$$\text{Terrestrial uptake} = \sum \text{emissions} - \text{ocean uptake} - \text{atmospheric retention} \quad (6.1)$$

The net biome production (NBP) is the difference between gross primary production and the respiration of the terrestrial system. It represents the net carbon assimilation of the terrestrial system. In other words;

$$\text{NBP} = \sum \text{photosynthesis} - \sum \text{autotrophic respiration} - \sum \text{heterotrophic respiration} \quad (6.2)$$

Therefore, these two variables are expected to exhibit the same quantitative and qualitative behavior. In this test, the NBP and terrestrial uptake are calculated and compared (Figure 6.17).

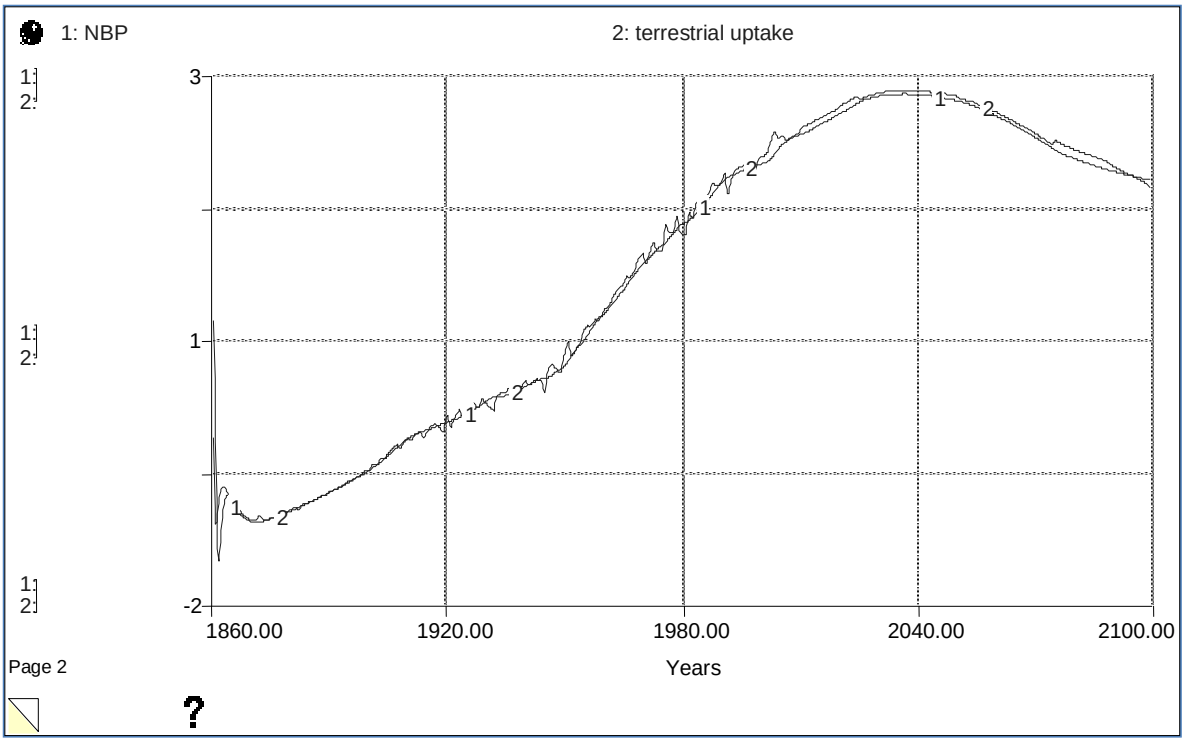

Figure 6.17 Comparative graph of NBP with terrestrial uptake in GtC/year

The two curves fit well confirming indirectly the structure of the model.

6.2. Behavioral Validation with Behavior Pattern Tests

The model outputs are also compared with available information about the real system and, with historical data. Below are the comparative graphs and their interpretation:

Test 11: Comparison of Model Produced Atmospheric Carbon Levels with Historical Data

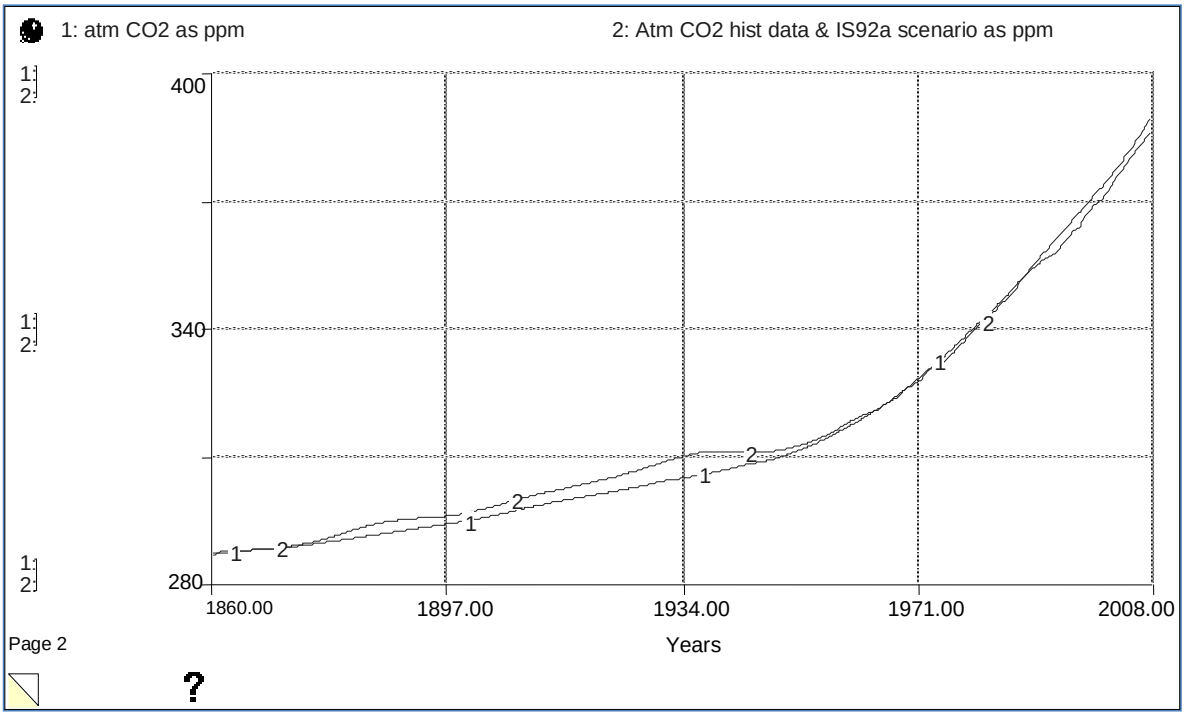

Figure 6.18 Carbon in atmosphere (simulation: curve 1, historical data: curve 2)

In Figure 6.18, the data for historical CO_2 records are taken from CDIAC. For the 1860-1958 period, the data obtained from Vostok ice core and, for the period 1959-2008 the data obtained from Mauna Loa observation station are used. These values are shown with curve no:2. Then the data for anthropogenic CO_2 emissions and for LUC emissions are taken from CDIAC and, the model is run with those emission values. The produced behavior is shown with the curve no:1. As can be seen from the graph, the model produced behavioral pattern is in good agreement with historical data. The quantitative difference between two curves from 1860 to until about 1950s can be due to the uncertainties contained in the ice core records. However, the biggest difference between two curves within this period is in the range of 1.7% of the historical concentrations,

occurring in year 1936. The simulation curve exhibits a much better fit with the more accurate Mauna Loa data.

Test 12: Comparison of Model Produced Terrestrial Carbon Uptake with Historical Data

The carbon content of the terrestrial system is not a directly measurable quantity like atmospheric carbon concentration. For this reason, the terrestrial carbon uptake cannot be computed, but only estimated. The estimations for the period 1957-2007 are taken from Le Quéré (2008). The error range of estimation is stated around +/-0.7 Gt/y. The calculation method used by Le Quéré for estimating the terrestrial uptake is the same with the method used in the model (See equation 6.1.). The plot of estimated data has a highly fluctuating pattern because of uncertainties included in variables that are used in calculation. However, the curve produced by the model has a smoother pattern, fitting well in trend to the estimation of Le Quéré (Figure 6.19).

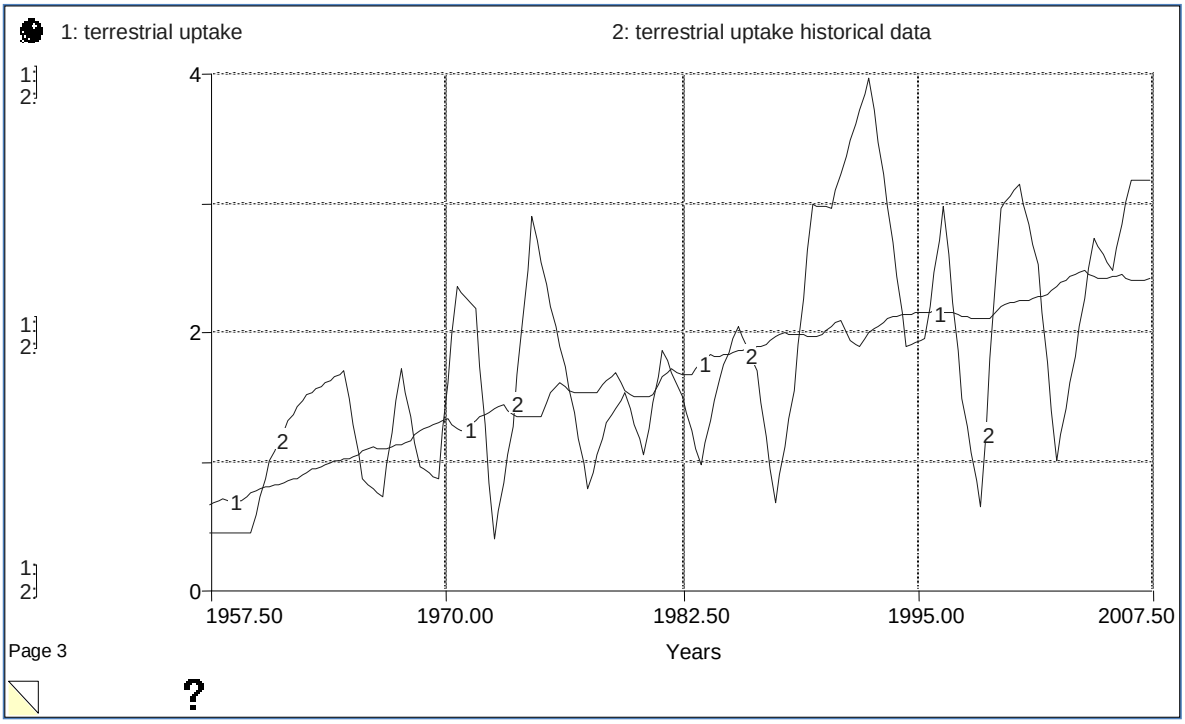

Figure 6.19 Terrestrial uptake as GtC (simulation: curve 1, historical data: curve 2)

Test 13: Comparison of Model Produced Atmospheric Methane with Historical Data and IPCC Scenario

In the atmospheric methane sector of the model, methane emission estimates in literature are used for historical anthropogenic emissions (Stern and Kaufmann, 1995). However, wetland emissions and methane removal processes are represented with formulations that include feedbacks. The behavior of the 'atmospheric methane' reservoir shows good correlation with historical records (CDIAC) and IPCC IS92a scenario. The results are depicted in Figure 5.7 of the 'Model Reference Behavior' chapter.

Test 14: Comparison of Model Produced Temperature Change with Historical Data:

For historical temperature record, the data from Hansen et al. (2006) are used. The 1951-1980 interval is taken as base period and the temperature deviations from the average of this period are calculated. Since the year-by-year data have a very fluctuating pattern, a 5 year mean graph is also plotted to smooth the trend. Then the temperature deviations from the base period are calculated by the model in the same manner and are plotted. For 1930-1950 interval, the values calculated by the model are a little below of the data of Hansen. However, the curves exhibit a relatively better fit after 1950s (Figure 6.20).

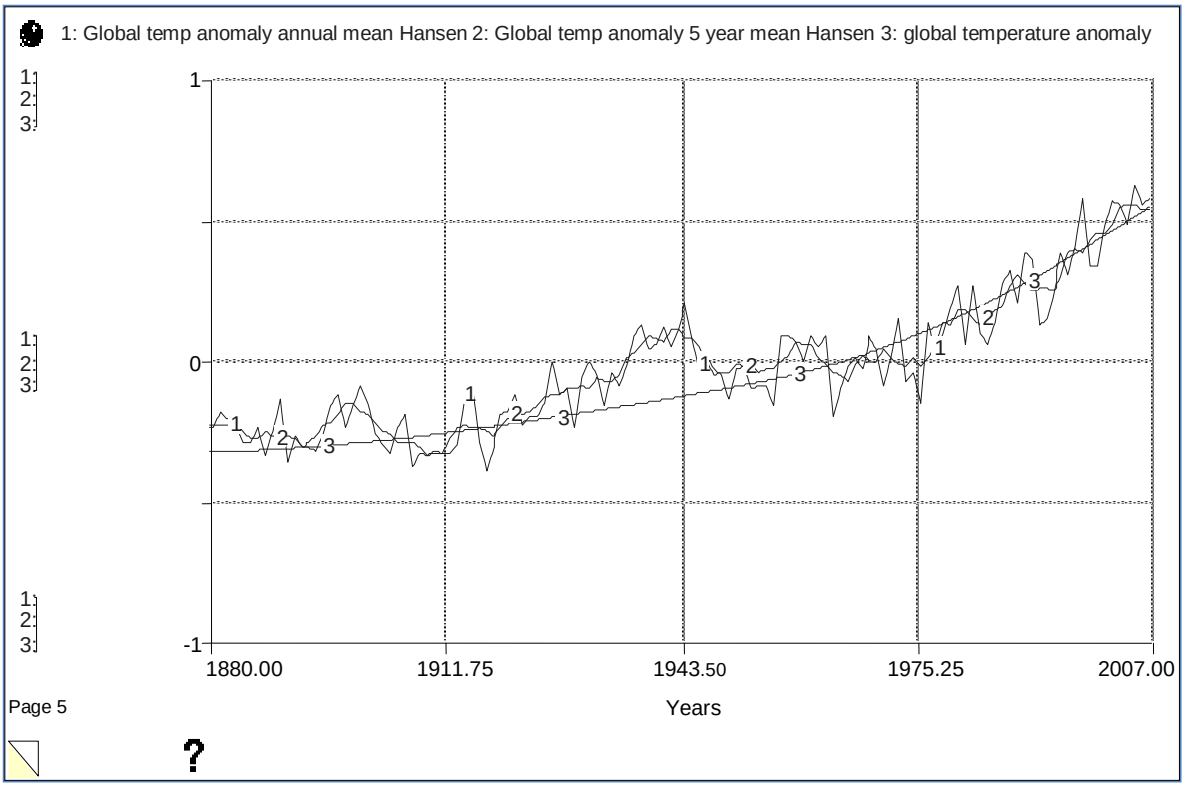

Figure 6.20 Temperature deviations from 1951-1980 base period
(simulation: curve3, historical data and scenario: curve 1 and curve 2)

7. MODEL BEHAVIOR SENSITIVITY AND SCENARIO ANALYSIS

7.1. Analysis of Temperature-Photosynthesis, Temperature-Respiration and Temperature-Wetland Emissions Feedbacks

Increasing temperature affects both photosynthesis and respiration of land biota and, wetland methane emissions. It creates three feedback loops shown in Figure 7.1. The reinforcing respiration and methane emissions loops increase the temperature while the counteracting photosynthesis loop decreases. The systemic effects of the feedback loops are analyzed below.

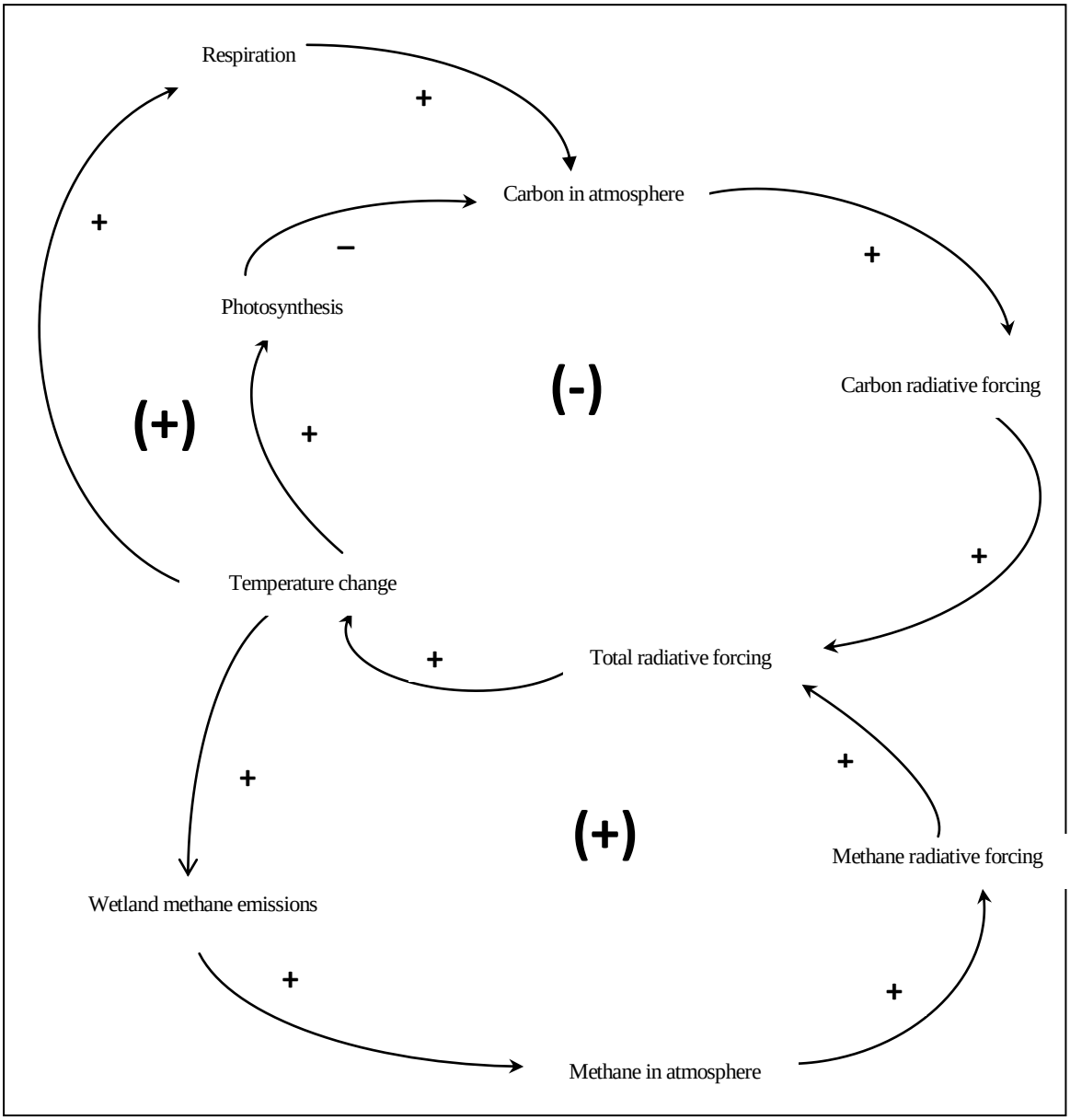

Figure 7.1 Photosynthesis, respiration and wetland emissions feedback loops

Temperature increase stimulates the photosynthesis, hence the atmospheric carbon level and radiative forcing decreases causing less temperature increase (Figure 7.2).

When only the temperature-photosynthesis feedback is evaluated, a temperature difference of +0.14°C is observed in the end of simulation, between the cases the feedback is active and inactive.

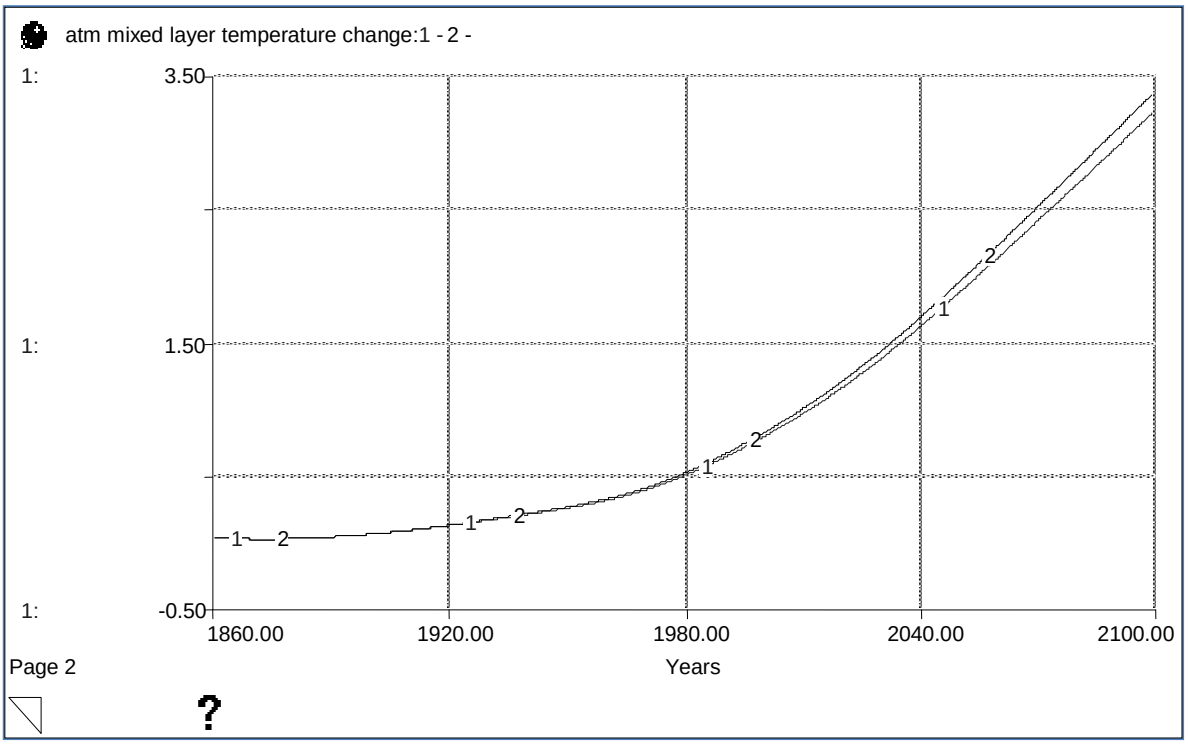

Figure 7.2 Global temperature change with
(curve 1) and without (curve 2) the temperature-photosynthesis feedback

When the respiration is not stimulated by temperature increase, less respiration occurs; less carbon is released to the atmosphere hence, temperature increases less (Figure7.3).

When only the temperature-respiration feedback is evaluated, a temperature difference of -0.37°C, which is almost 2.5 times the difference in photosynthesis, is observed in the end of simulation, between the cases the feedback is active and inactive.

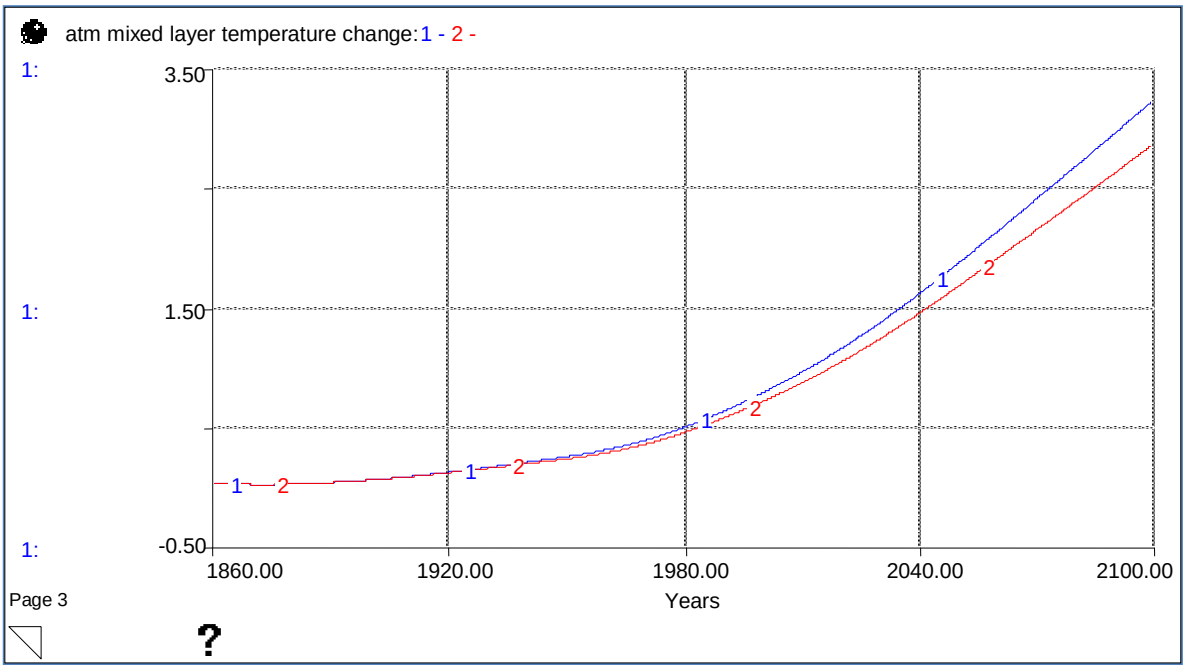

Figure 7.3 Global temperature change with
(curve 1) and without (curve 2) the temperature-respiration feedback

When methane release from wetlands is not stimulated by temperature increase, less methane is released to the atmosphere causing less radiative forcing, hence, the temperature increase is slightly lower (Figure 7.4). When only the temperature-wetland methane emissions feedback is evaluated, a temperature difference of only -0.07°C is observed in the end of simulation; between the cases the feedback is active and inactive.

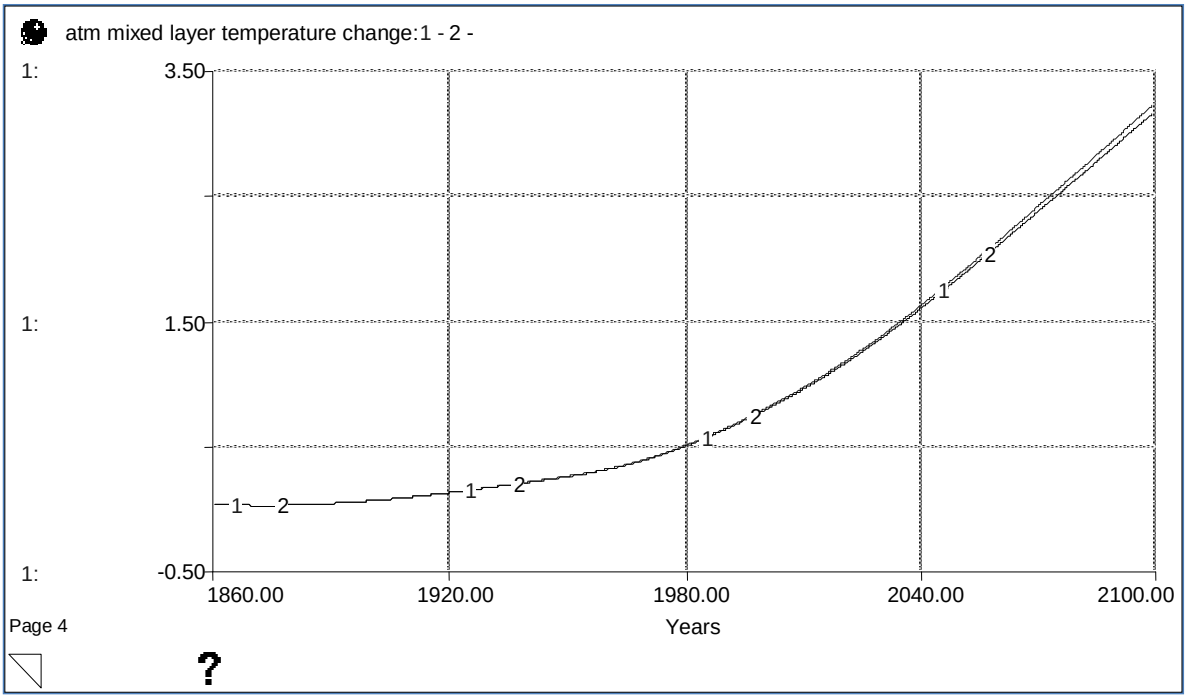

Figure 7.4 Global temperature change with (curve 1) and without (curve 2) the temperature-wetland methane emissions feedback

When all three feedbacks shown in Figure 7.1 are active, the cumulative temperature increase is 3.21°C in year 2100 while it is 2.92°C in the same year when all three are inactive. It can be concluded from this analysis that although the temperature increases photosynthetic activity, it also stimulates respiration and wetland emissions. However, the increase in the latter two dominates the effect of photosynthesis. Thus a temperature difference of 0.29°C occurs in the end of two simulations (Figure 7.5).

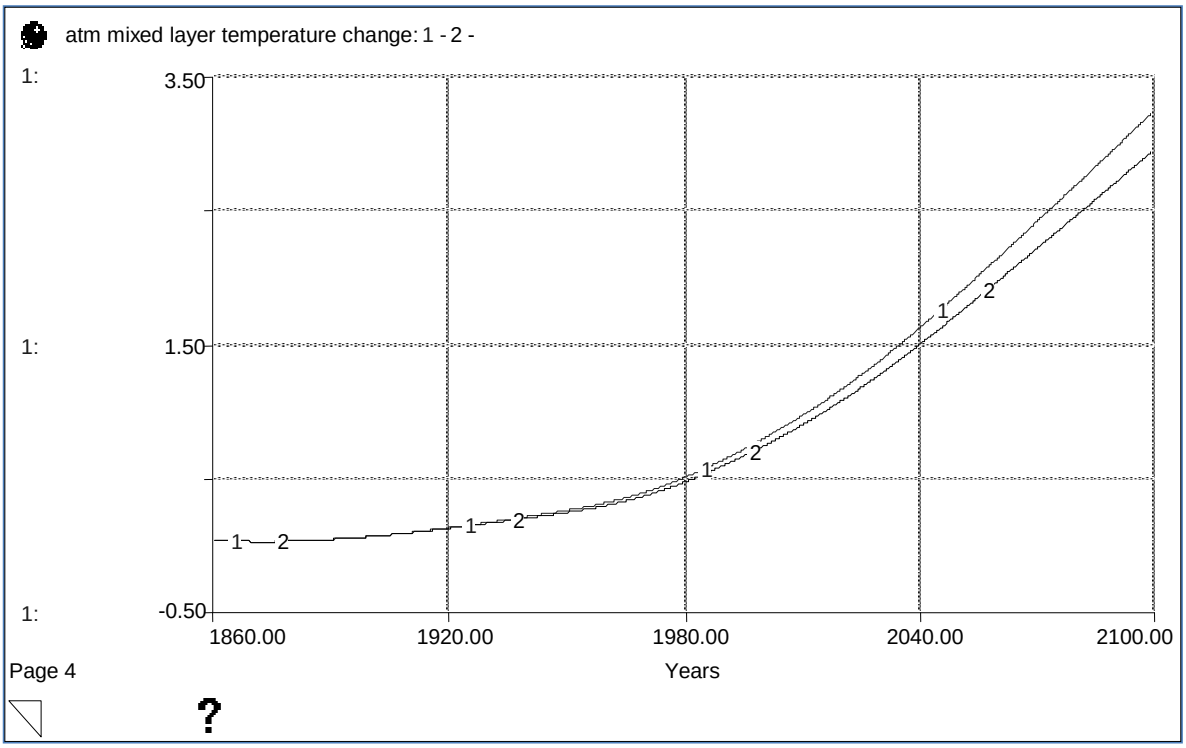

Figure 7.5 Global temperature change with (curve 1) and without (curve 2) the effect of temperature on terrestrial processes

When the simulated atmospheric CO_2 levels are plotted together with historical data and IS92a scenario estimates which does not consider the temperature feedbacks, it is observed that the simulated behavior fits well with the feedback free data produced by IPCC, when the temperature feedbacks are inactive (Figure 7.6). However, when the temperature feedbacks are active, the simulation graph begins to deviate from scenario estimations starting from 2010's on, when the temperature increase is at about 1°C (See Figure 5.1).

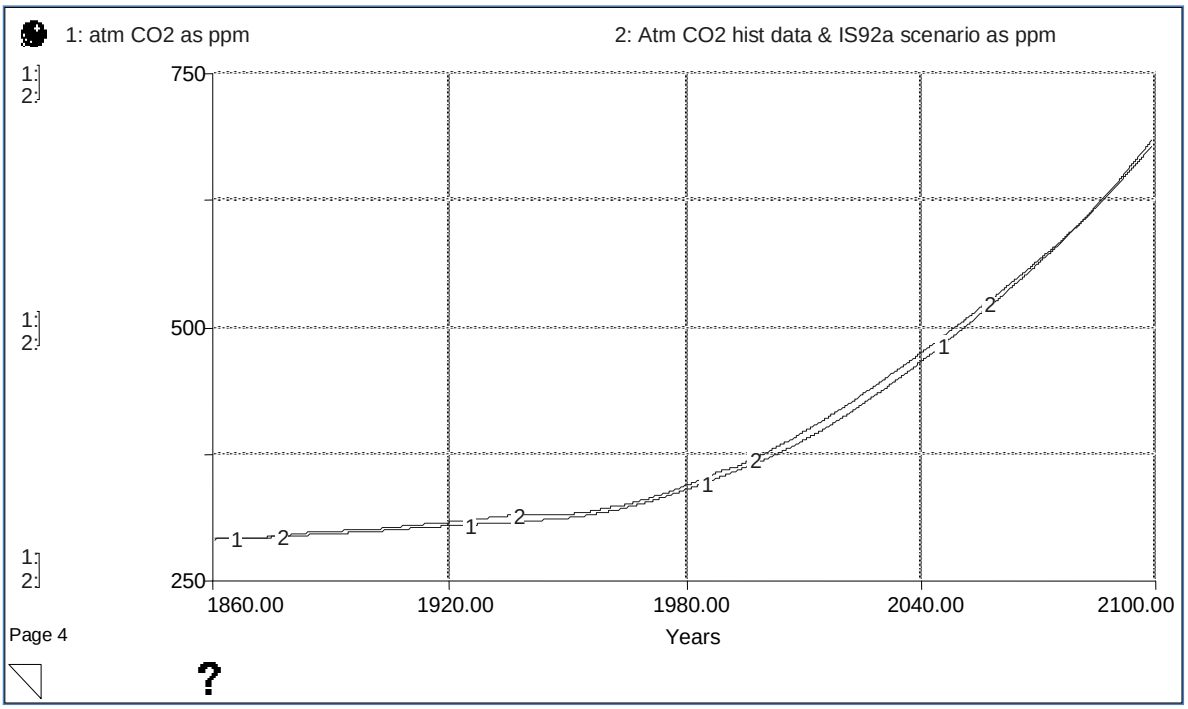

Figure 7.6 Atmospheric CO_2 (curve 1: simulation without temperature feedbacks, curve 2: historical data and IS92a scenario)

Figure 5.1 and Figure 7.6 show that the difference between IPCC IS92a scenario and the model behavior after 2010's is caused by the effect of temperature on photosynthesis, respiration and methane emissions feedbacks.

Another experiment to observe the effect of temperature on terrestrial processes is to compare the NPP/GPP ratio. In IPCC reports, the global total GPP is estimated about 120GtC/year and, the global NPP is estimated about half of the GPP, i.e. about 60GtC/year (Watson et. al., 2000). This estimation is checked in the model. The behaviors of the GPP, the NPP and, the NPP/GPP ratio in the existence of temperature-

photosynthesis and temperature-respiration feedbacks can be seen in Figure 5.3 of the ‘Model Reference Behavior’ chapter.

The NPP is equal to GPP minus the autotrophic respiration. As can be seen from the graph, both GPP and NPP have increasing trends. This is because of the temperature effect included in the model structure. The increasing temperature stimulates both photosynthesis and respiration. However, since the change in the photosynthesis is defined with a logarithmic function, but the respiration functions are linear, the GPP increases faster than the respiration and the gap between GPP and NPP increases. The NPP/GPP ratio remains constant at about 0.47 until 1990s. Then it decreases to 0.41 until the end of simulation. This behavior has certainly a large degree of uncertainty due to the uncertain biostimulation coefficient and temperature coefficients. The sensitivity analysis for these parameters was performed in previous sections.

However, when the temperature feedback is deactivated, the GPP and NPP values increase according to the carbon content of related stocks but their ratio displays very small changes around the value 0.47 during the entire simulation (Figure 7.7). In other words, the NPP/GPP ratio keeps closer to 0.5 in the absence of temperature effect.

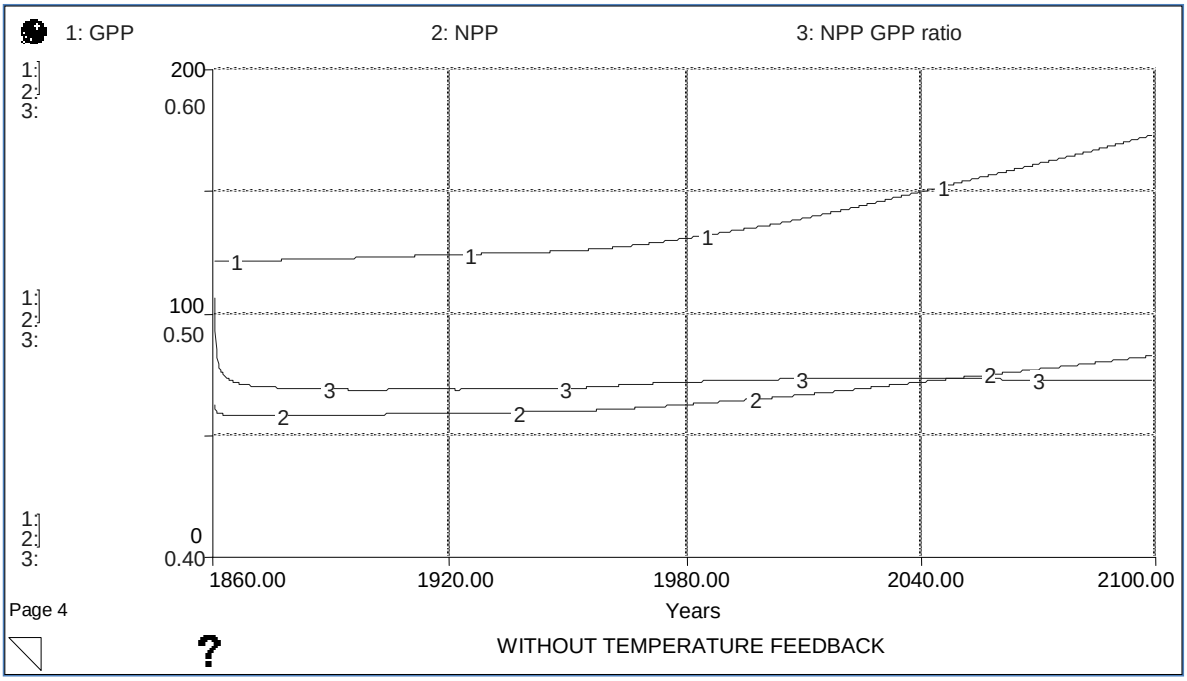

Figure 7.7 Global GPP and NPP as GtC and,
NPP/GPP ratio in the absence of temperature feedbacks

7.2. Analysis of Permafrost Feedback

Methane release from permanently thawing permafrost, which is not represented much in simple climate models, is a subject of big concern recently for its potential effect to global warming. The permafrost module constructed in this study aims to represents the permafrost feedback depicted in Figure 7.8 and, to allow to observe its effect on global temperature increase. Note that this feedback loop is not included in the reference behavior.

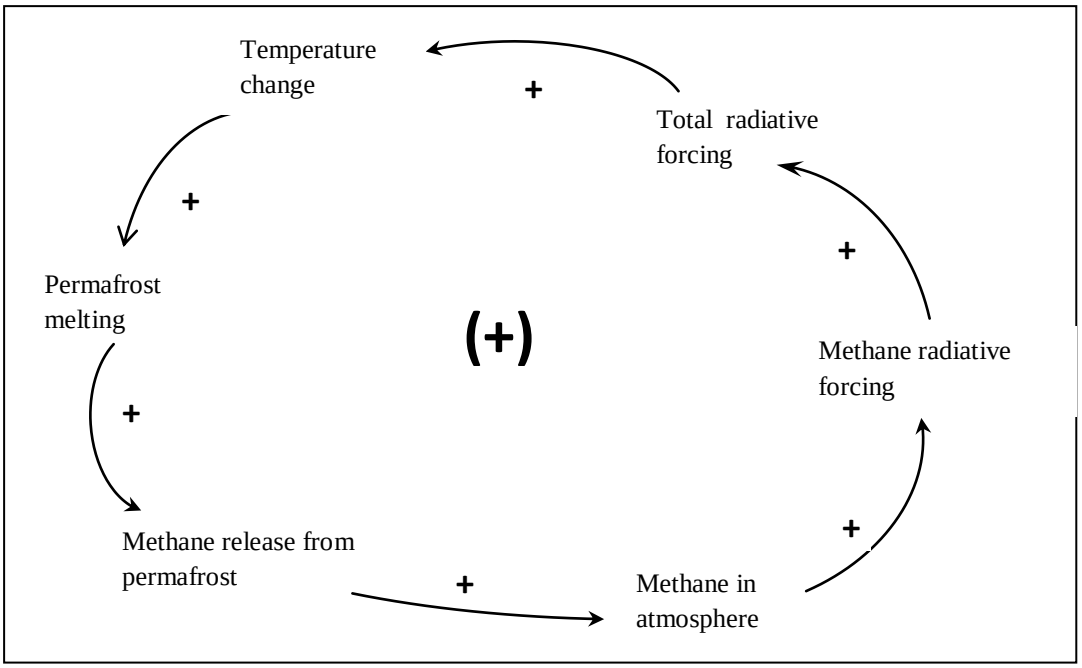

Figure 7.8 Permafrost feedback

The permafrost feedback has three main uncertainties:

- thawing pattern of permafrost,
- carbon content of permafrost,
- percentages of CO_2 and CH_4 released from permafrost depending on whether the post-melting organic activity is aerobic or anaerobic.

Two different thawing patterns are described in the model. Sensitivity analyses are performed for each of these patterns with different carbon content and, CO_2 and CH_4 release percentages.

When the permafrost melting process is off, the thawing rate is equal to the freezing rate. The area of permafrost does not change, thus no GHG is released from permafrost to the atmosphere (Figure 7.9).

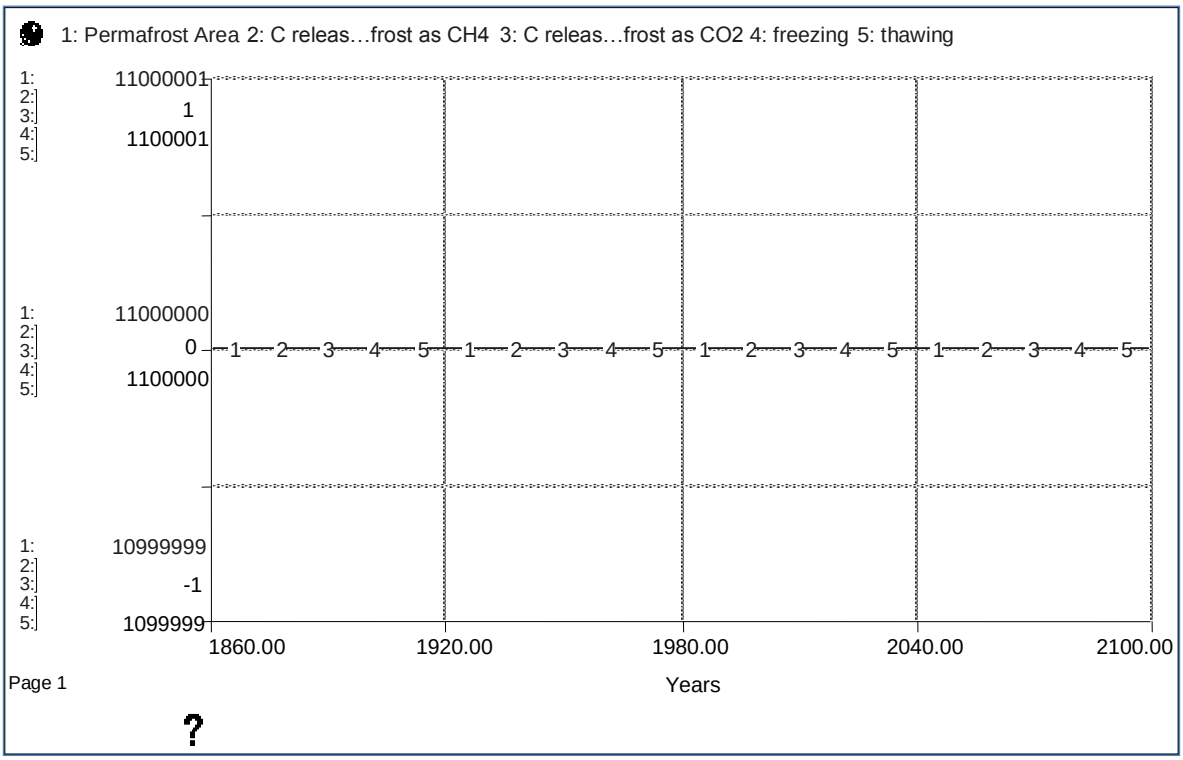

Figure 7.9 Permafrost feedback is inactive

When the permafrost feedback is activated, a fast decrease in permafrost area is observed. As the temperature increases, thawing begins to exceed freezing and the permafrost area begins to collapse. Two different thawing fraction multipliers are defined in the model: one aiming at representing the extreme estimation of Lawrence and Slater (2005), about one million square kilometers of permafrost area remaining in 2100, and, the other one aiming at the milder statement of IPCC (Hansen et al., 2007), about 20 to 35% of permafrost area decreasing until mid 21st century. The behavior of permafrost area for two different thawing fraction multipliers is depicted in Figure 7.10.

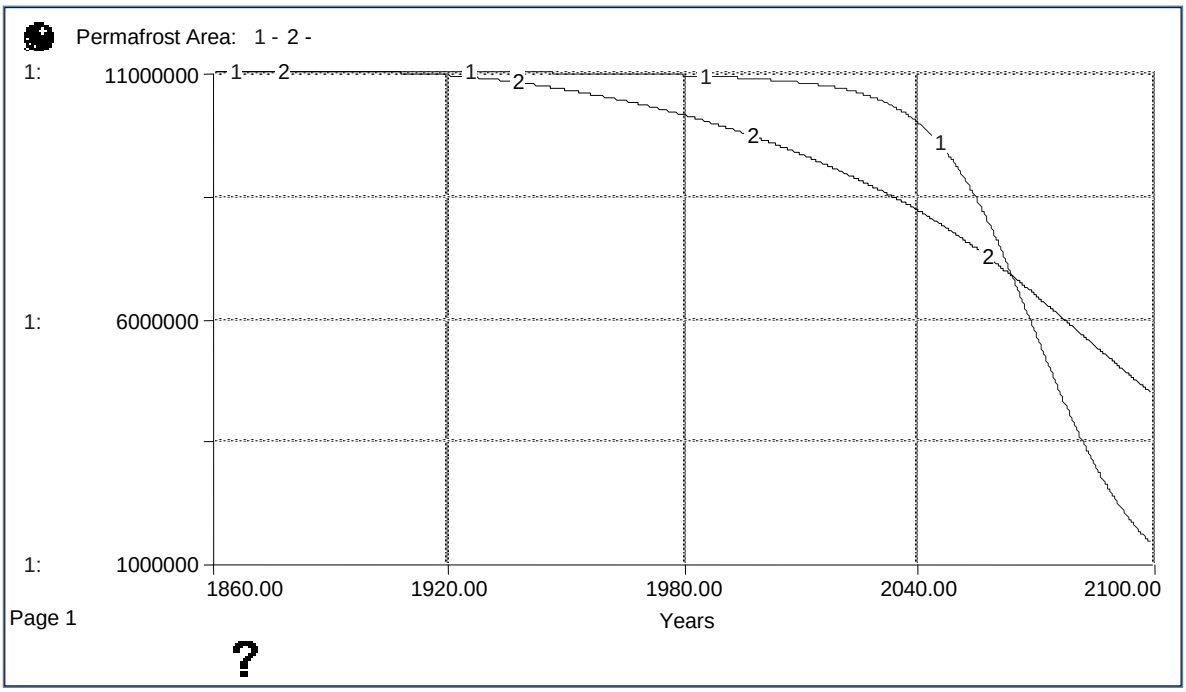

Figure 7.10 Permafrost feedback is active.
Decrease of permafrost area in km^2 for two different thawing fraction multipliers
(curve 1: extreme scenario, curve 2: milder scenario)

Permafrost melting leads to a fast GHG release from previously frozen soils and to a big increase in their atmospheric concentrations. The nature and quantity of the GHG released depend on how much of the microbial activity occurs in aerobic conditions and how much occurs in anaerobic conditions. Since methane has a much stronger radiative forcing effect than CO_2, the increase in methane release causes a serious increase in total radiative forcing and thus in global temperature.

Sensitivity analyses are performed with both thawing fraction multipliers. The analyses comprise 100 runs for each melting scenario. The changes of two variables are analyzed: 'Carbon in permafrost' and 'CH_4 release fraction'. A normal distribution pattern is chosen. For 'carbon in permafrost' the mean value is 375 GtC and the standard deviation is 150. For 'CH_4 release fraction' the mean value is 0.5 and the standard deviation is 0.2. The simulation is run 100 times with randomly changing values of these two variables. The results are illustrated below:

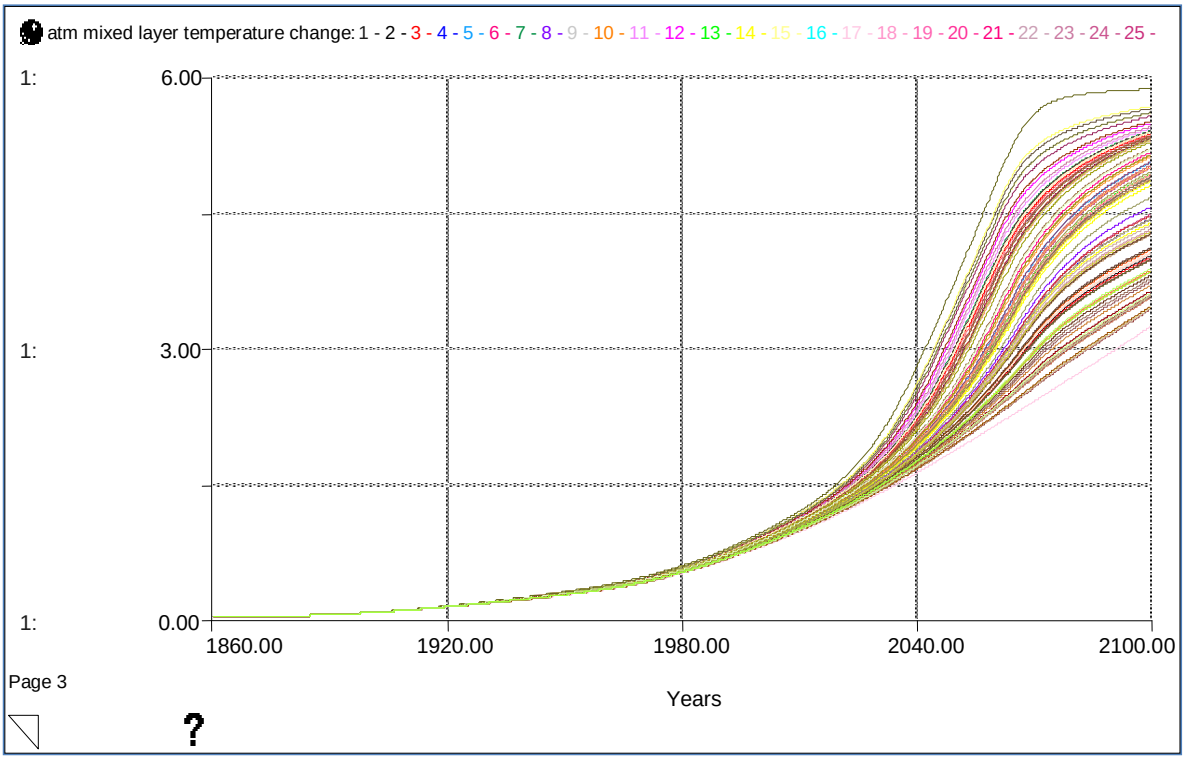

Figure 7.11 Permafrost feedback is active. Sensitivity of the temperature to 'carbon in permafrost' and to 'CH_4 release fraction' with extreme melting scenario

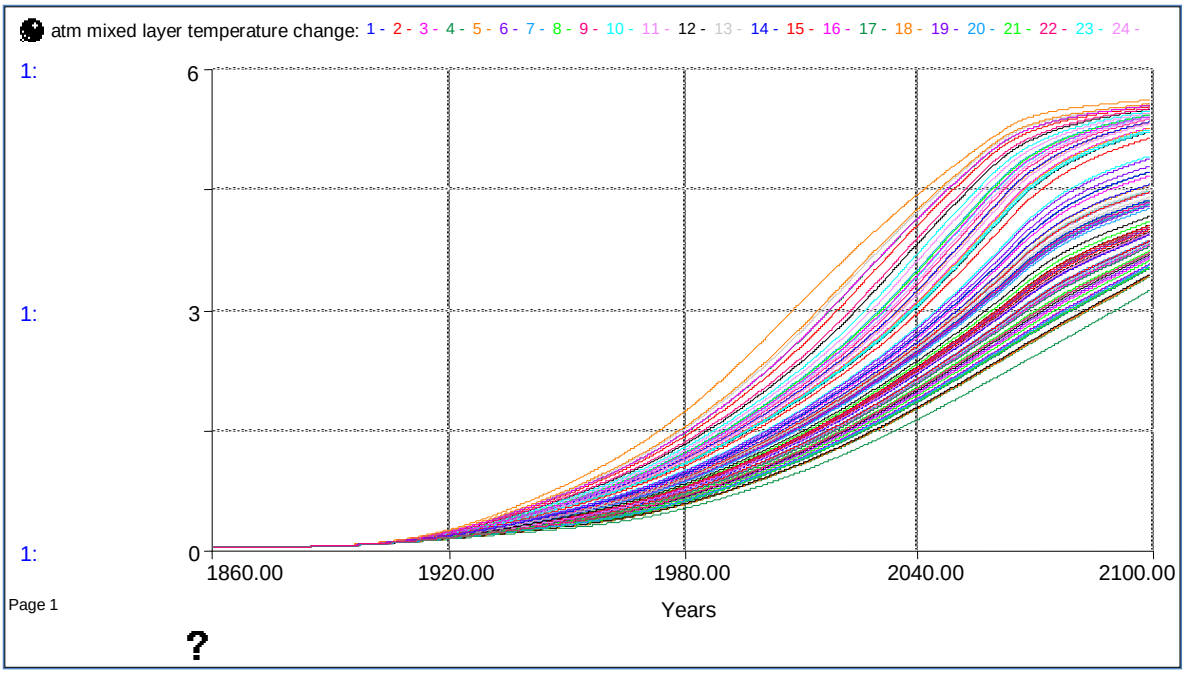

Figure 7.12 Permafrost feedback is active. Sensitivity of the temperature to 'carbon in permafrost' and to 'CH_4 release fraction' with milder melting scenario

The minimum temperature increase is observed with initial carbon content of permafrost of 106 Gt and CH_4 release fraction of 0.141 while the maximum temperature increase is observed with initial carbon content of permafrost of 682 Gt and CH_4 release fraction of 0.910. The sensitivity analyses' results are depicted below:

Table 7.1 Extreme values of the sensitivity analyses

	min. temp. increase (°C)	max. temp. increase (°C)
extreme scenario	3.40	5.86
mild scenario	3.38	5.59
C in permafrost (Gt)	106	682
CH_4 release fraction	0.141	0.910

The analysis of permafrost feedback reveals that when the GHG release from permafrost is considered, even modest estimations for system variables result in higher temperature increases than the permafrost feedback-free behavior. The temperature increase reaches disastrous values with higher permafrost carbon stock and higher anaerobic activity rate estimations. Therefore, the permafrost feedback should seriously be considered as a subject of further research.

7.3. Scenario Analysis

The response of the climate system to the change in emissions is delayed due to several fast and slow feedbacks and the thermal inertia of the ocean. According to Hansen et al. (2008), one-third of the response of the ocean occurs in the first few years, in part because of rapid response over land, one-half in nearly 25 years, three-quarters in 250 years, and nearly full response in a millennium.

Furthermore, recent studies reveal that it may currently exist some delayed warming 'in the pipeline' due to slow climate feedback processes, implying the urgency of determining mitigation policies and the need for even more conservative approach in establishing dangerous GHG concentration limits (Hansen et al., 2005, 2007, 2008).

In this section, several emission scenarios are applied to the model and the resulting behavior is observed. The scenarios are based on solely CO_2 emissions, because:

- the emissions which are the most manageable by humans are CO_2 emissions
- the increase rate of non-CO_2 GHG emissions already tend to fall below the estimations of IPCC scenarios
- there is a large uncertainty in calculation of the radiative forcings of non-CO_2 GHGs, and, the radiative forcing of non-CO_2 GHGs tend to offset the negative aerosol forcing, which is not accounted in this study.

Therefore, the net human disturbance to the natural radiative balance can be measured by anthropogenic CO_2 emissions and it is logical to determine target CO_2 levels in policy analyses to alleviate the global warming (Hansen et al., 2008).

Scenario 01: Abrupt Anthropogenic CO_2 Emissions Cut in 2010

For this hypothetical extreme scenario, all anthropogenic CO_2 and LUC emissions are cut to zero in year 2010. The permafrost feedback is deactivated and, the radiative forcings of CH_4 and N_2O are turned off in order to observe the sole effect of CO_2 on temperature. When the simulation is run, it is observed that the atmospheric CO_2 concentration begins to decrease from year 2010 on. However, the temperature continues to increase until year 2033.5, then begins to decrease. But its rate of decrease after 2033.5 is smaller than its rate of increase until 2033.5. The temperature increase comes down to its 2010 level in year 2080 (Figure 7.13).

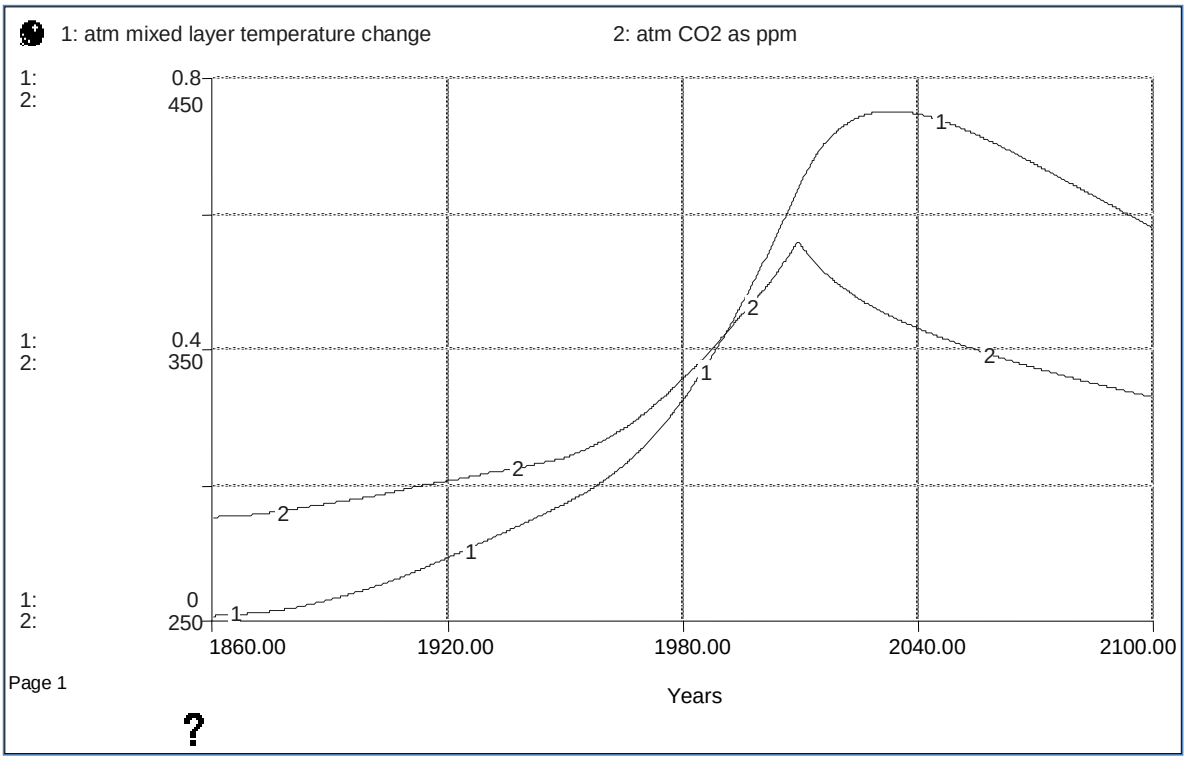

Figure 7.13 CO_2 and LUC emissions cut to zero in 2010.
Behavior of the temperature and the atmospheric CO_2 concentration

Scenario 02: Anthropogenic CO_2 Emissions Halved in 2010

For this scenario, anthropogenic CO_2 and LUC emissions are halved in year 2010 and kept constant at those values till the end of simulation. The permafrost feedback is deactivated and, the radiative forcings of CH_4 and N_2O are turned off in order to observe the sole effect of CO_2 on temperature. When the simulation is run, it is observed that the atmospheric CO_2 concentration and the temperature continued to increase albeit at a slower

rate. The increase in atmospheric CO_2 concentration is 1.6 ppm/year for the 40 years period from 1970 to 2010 while it is 0.5 ppm/year for the following 40 years period. It is obvious from this experiment that even cutting the anthropogenic emissions to half, which is already a far difficult target in climate change mitigation debates, does not stop the increase in atmospheric CO_2 concentration and related global temperature increase but only slows their paces (Figure 7.14).

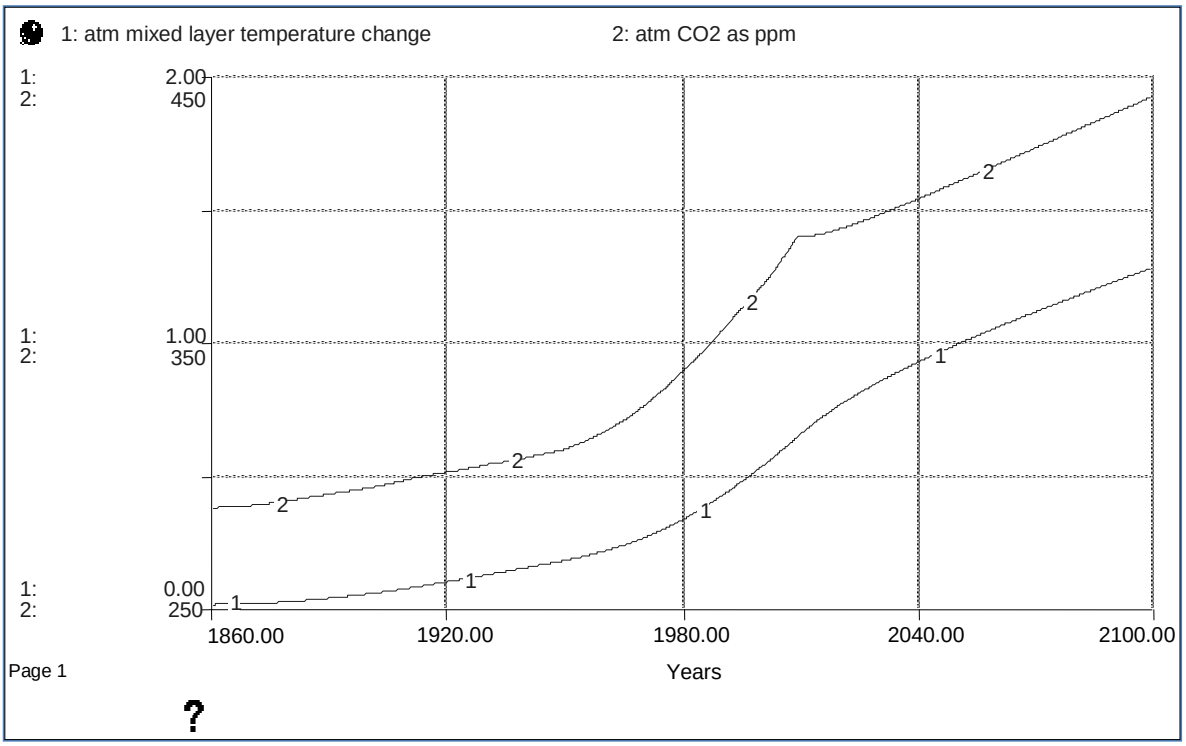

Figure 7.14 CO_2 and LUC emissions cut to half in 2010.
Behavior of the temperature and the atmospheric CO_2 concentration

Scenario 03: Attempts for Target CO_2 Levels

There is an ongoing debate in the scientific community about the target levels of atmospheric CO_2 concentration in order to stop the global warming. Although the impossibility of determining a definite upper limit for GHG concentrations and related warming due to the uncertainties contained in the system, the general consensus is that a global warming of more than 2-3°C would be very dangerous (Mastrandrea and Schneider, 2004). The target temperature increase adopted by European Union (European Council, 2005) to limit anthropogenically caused warming is 2°C while Hansen et al. (2007) point to an even lower limit, 1.7°C increase compared to preindustrial times, in order to prevent

the irreversible ice melting processes, implying an atmospheric CO_2 concentration of 450 ppm maximum. Besides, it is asserted in a more recent study by Hansen et al. (2008) that even the current ~390 ppm level is dangerous for humanity due to slow feedbacks that are not taken into account in most climate models, and, 350 ppm level should be put as the target to be reached in a time horizon of not longer than decades in order the earth continues to be a comfortable home for humankind.

The critical 350 ppm atmospheric CO_2 level proposed by Hansen et al. (2008) is targeted for this scenario. The permafrost feedback is deactivated. The radiative forcings of CH_4 and N_2O are turned on this time to observe the full response of the climate system to decrease in CO_2 emissions. The fossil fuel CO_2 emission scenario of Hansen et al. (2008) that assumes phasing out of coal emissions by 2030 and that depends on IPCC estimates of oil and gas reserves is applied to the model (see Figure 7.15). The LUC emissions are kept the same as base run estimates. The CH_4 and N_2O emissions are kept constant at their estimated 2010 levels. The model is run until year 2250 to observe longtime behavior of atmospheric CO_2.

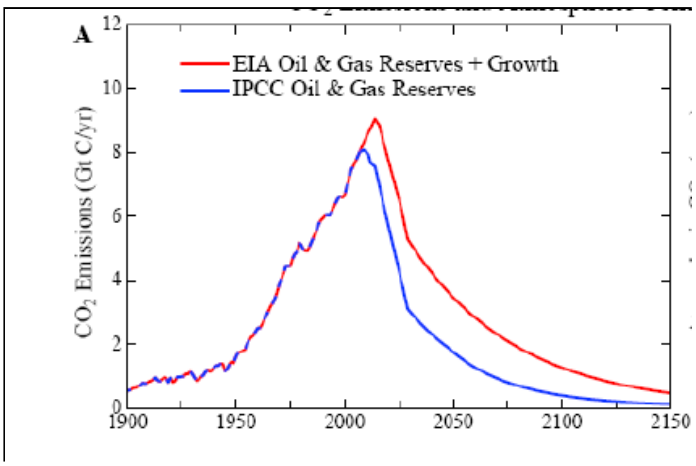

Figure 7.15 Fossil fuel CO_2 emissions with coal phase-out based on IPCC and EIA estimated fossil fuel reserves (Hansen et al., 2008)

The resulting behavior of the model is illustrated below:

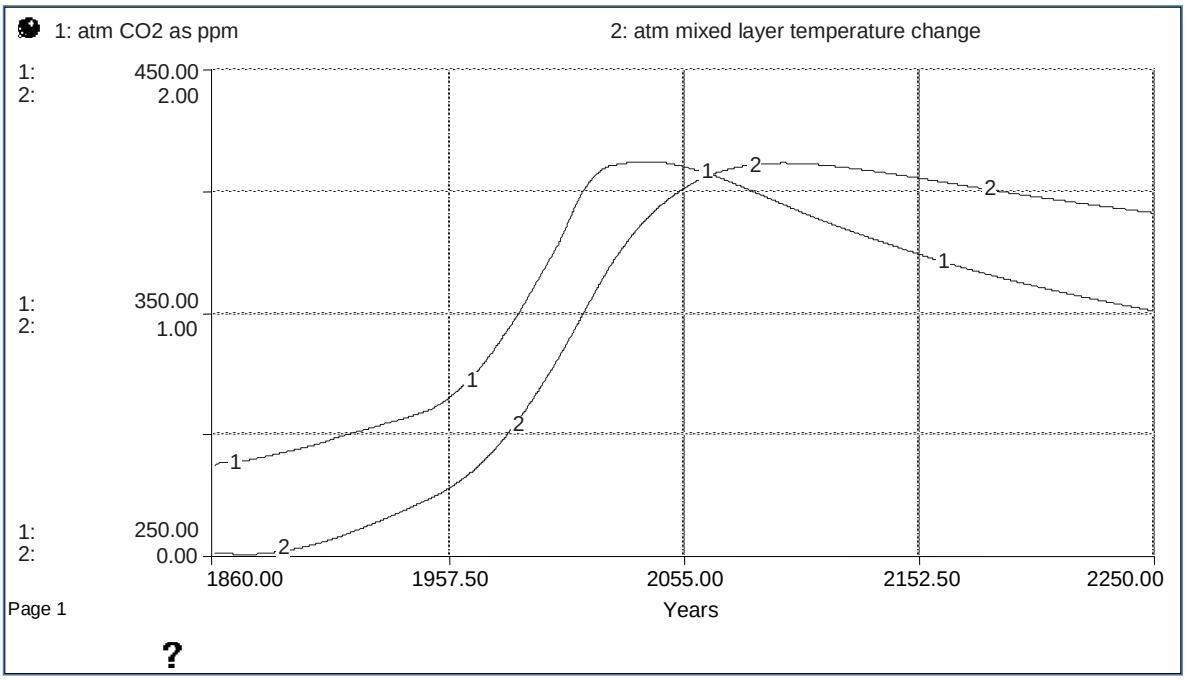

Figure 7.16 '350 ppm target' scenario.
Behavior of the temperature and atmospheric CO_2 concentration

As can be seen from above graphs, although the fossil fuel emissions begin to decrease sharply in 2010, atmospheric CO_2 concentration keeps increasing until year 2041, takes the maximum value of 411 ppm, and then, begins to decrease slowly. It attains the target 350 ppm level in year 2249. In other words, it takes more than two centuries for atmospheric CO_2 level to reach the critical 350 ppm level. This result is in well agreement with Hansen et al. (2008). The corresponding temperature to this emission scenario barely stops increasing after attaining its maximum level of 1.61°C in year 2100, then begins to decrease very slowly down to 1.41°C in 2250. Even the application of this harsh scenario proves the inertia of the climate system and, the seriousness of the global warming problem and the urgency of action.

8. CONCLUSION

Global warming currently is and will continue to be in the future the most serious problem for humankind due to its impairing effect on the sensitive ecological balances of the planet by causing arctic ice melting, sea-level rise, droughts, extreme meteorological events, etc. Because of the severity of its potential harms and the needed urgency of mitigation efforts, this problem must be well understood and conceptualized by ordinary people.

This modeling study was intended to reveal the nonlinear feedback dynamics of the climate system and to enable the user to observe and assess the results of various emission scenarios. First the importance of the problem and the necessity of mitigation efforts are emphasized. Then the nonlinear, dynamic nature of the climate system is described and the convenience of the system dynamics approach for studying this systemic problem is assessed. In this study, the system dynamics is chosen as the methodology to construct a model of anthropogenic global climate change because, it is a powerful procedure to understand, model and analyze complex systems, to create and test hypotheses and to constitute policies. The feedback structure of the system dynamics approach enables the modeler to build the model on circular causalities instead of direct causalities between the system variables.

A box model coupling the atmospheric, terrestrial and oceanic carbon is constructed. The stocks of the model represent the main carbon reservoirs that exist in nature. Carbon in terrestrial system is distributed among five stocks and, the flows between these stocks and between the stocks and the atmosphere are defined. Carbon in ocean is distributed among one mixed layer and ten deep ocean layers. Transfer of carbon between ocean layers is described with an Eddy diffusion model. In addition, the atmospheric methane, nitrous oxide, and the heat stored in the system are represented with stock variables.

The model parameters are identified from the relevant literature and adjusted when needed for model calibration purposes. The most uncertain parameters of the model structure are the biostimulation coefficient of photosynthesis, β, the temperature

coefficients, Q_{10}s, and the climate sensitivity parameter. Changing values of those parameters strongly affect the simulation results.

The structure of the model is validated with structure oriented behavior tests like extreme condition tests, parameter sensitivity tests and phase relationship test. The model behavior is also validated with behavior pattern tests. For behavioral validation, the model behavior is compared with available information about the real system and, with historical data. The model behavior exhibits good agreement with historical data.

The stimulative effect of temperature on photosynthesis, respiration and, wetland methane emissions are studied in detail within the context of temperature related feedbacks of terrestrial system. It is found that the model results are more compatible with IS92a scenario estimates when the temperature-photosynthesis, temperature-respiration, and temperature-wetland emissions feedbacks are omitted.

In this study, the photosynthesis is defined as a logarithmic function of the atmospheric carbon level. It is dependent on the initial GPP, the biostimulation coefficient, and, is stimulated by increasing temperature. No saturation point is defined for photosynthesis rate. However, the hypothesis stating that the increase in carbon assimilation rate is limited by some factors like nutrient availability or moisture and has some asymptotic upper limits also deserves further research.

Several sensitivity analyses are performed and it is observed that the model structure is sensitive to the biostimulation coefficient, β, to the temperature coefficients, Q_{10}s, and, to the climate sensitivity parameter.

Some emission scenarios are applied to the model and the behavior is analyzed. It is observed that there exists a large time gap between emission decrease and the response of the system to this decrease due to the inertia of the system components like ocean. The target 350 ppm atmospheric CO_2 assertion of Hansen et al. (2008) is analyzed and it is found that, even in case of abandoning coal consumption in next 20~30 years, it takes more than two centuries for atmospheric CO_2 to go below the 350 ppm level.

The permafrost melting process and its probable serious effects to the climate system, which is an important subject in current climate change debates, is also analyzed and, a hypothesis is proposed to represent related feedback. Since the variables used to describe the process has large uncertainties, sensitivity analyses are performed to observe the range of different results. Two different melting scenarios are created and, relevant GHG outflows are defined.

The permafrost sector was inactive in the base run and in other analyses. When it is activated, the global temperature increase that is 3.21°C for the base run, reached a minimum value of 3.38°C with the mild melting scenario, low carbon content of permafrost and low CH_4 release fraction while it reached a maximum value of 5.96°C with the extreme melting scenario, high carbon content of permafrost and high CH_4 release fraction.

The model can be used to apply different emission decrease scenarios and to observe resulting behavior. It can also be used to observe effects of the parameters with high degree of uncertainty on model behavior by assigning them different values. The effects of the feedbacks included in the structure, and, of the emissions and/or radiative forcings of different GHGs to the global temperature increase can be analyzed by turning on and off relevant control switches.

As endeavors to improve the model structure, the ‘carbon saturation of the vegetation’ hypothesis can be included in the photosynthesis formulations, and/or the LUC emissions can be represented endogenously in model structure. Also, the mixed layer of ocean can be divided into warm ocean and cold ocean mixed layers and, their carbon exchange with the atmosphere can be analyzed separately. Different feedbacks like ice-albedo feedback or water vapor feedback and, radiative forcings of other GHGs and aerosols can be included into the model structure.

As an even further study subject, the model can be transformed to an interactive learning environment. A user friendly interface not necessitating the user to fully understand the logic and formulations underlying the model structure but letting him to enter different emission scenarios and observe the results, and then, giving instructions

about the dynamics causing those results can be developed. The model with such an interface can be used as a tool to improve the understanding of ordinary people about dynamics of climate change and to increase the awareness.

REFERENCES

Baede, A.P.M., Ahlonsou, E., Ding Y., Schimel, D., 2001. The climate system: An overview. In Watson, R.T. (Ed.), Climate Change 2001: The Scientific Basis, 87-98, Cambridge University Press, Cambridge, UK.

Barlas, Y., 1996. Formal Aspects of Model Validity and Validation in System Dynamics. System Dynamics Review, 12/3, 183-210.

Barlas, Y., 2002. "System Dynamics: Systemic feedback modeling for policy analysis", http://www.ie.boun.edu.tr/~barlas/EOLSS-BarlasReprint.pdf.

Carbon Dioxide Information Analysis Center home page. http://cdiac.ornl.gov/trends/atm_meth/lawdome_meth.html. (accessed February 2009).

Climate Interactive Organization home page. http://www.climateinteractive.org.(accessed December 2009).

Claussen, M., 2000. Earth System Models. In Ehlers E., Krafft T. (Eds.), Understanding the Earth System: compartments, processes and interactions, 147-163, Springer-Verlag, NY.

Claussen, M., Mysak, L.A., Weaver, A.J., Crucifix, M., Fichefet, T., Loutre, M., Weber, L., Alcamo, J., Alexeev, V.A., Berger, A., Calov, R., Ganopolski, A., Goosse, H., Lohmann, G., Lunkeit, F., Mokhov, I.I., Petoukhov, V., Stone, P., Wang, Z., 2002. Earth system models of intermediate complexity: closing the gap in the spectrum of climate system models. Climate Dynamics, 18, 579-586.

Corinne Le Quéré web page. http://lgmacweb.env.uea.ac.uk/lequere/co2/carbon_budget.htm. (accessed October 2009).

Cubasch, U., Meehl, G.A., Boer, G.J., Stouffer, R.J., Dix, M., Noda, A., Senior, C.A., Raper, S., Yap, K.S., 2001. Projections of future climate change. In Watson, R.T. (Ed.), Climate Change 2001: The Scientific Basis, 527-582, Cambridge University Press, Cambridge, UK.

Denman K.L., Brasseur G., Chidthaisong A., Ciais P., Cox P.M., Dickinson R.E., Hauglustaine D., Heinze C., Holland E., Jacob D., Lohmann U., Ramachandran S., da Silva Dias P.L., Wofsy S.C., Zhang X., 2007. Couplings between changes in the climate system and biogeochemistry. In Solomon, S., Qin, D., Manning, M., Chen, Z., Marquis, M., Averyt, K.B., Tignor, M., Miller, H.L. (Eds.), Climate Change 2007: The Physical Science Basis, 501-587, Cambridge University Press, Cambridge, UK.

Dessler, E., Parson, E.A., 2007. The Science and Politics of Global Climate Change: A guide to the debate, Cambridge University Press, NY.

den Elzen, M.G.J., Beusen, A.H.W., Rotmans, J., van Asselt, M.B.A., 1997. Human disturbance of the global biogeochemical cycles. In Rotmans, J., de Vries, B., (Eds.), Perspectives on global change: The TARGETS approach, 345-370, Cambridge University Press, Cambridge, UK.

Emanuel, W.R., Killough, G.G., Olson, J.S., 1981. Modelling the circulation of carbon in the world's terrestrial ecosystems. In Bolin, B. (Ed.), Scope 16: Carbon cycle modelling, 335-353, John Wiley & Sons, NY.

European Council web page.
http://register.consilium.europa.eu/pdf/en/05/st07/st07242.en05.pdf (accessed November 2009).

Fiddaman, T.S., 1997. Feedback complexity in integrated climate-economy models, Ph.D. Thesis, Massachusetts Institute of Technology.

Foley, J.A., 1995. An equilibrium model of the terrestrial carbon budget. Tellus, 47B, 310-319.

Foley, J.A., Ramankutty, N., 2003. A primer on the terrestrial carbon cycle: What we don't know but should. In Field, C.B., Raupach, M.R. (Eds.), Scope 62: The global carbon cycle, 279-294, Island Press, USA.

Ford, A., 2007. Global Warming and System Dynamics, Proceedings of the 25th International Conference and 50th Anniversary Celebration: International Conference of the System Dynamics Society, Boston, Massachusetts, July 29-August 02/2007, 25.

Forster, P., Ramaswamy, V., Artaxo, P., Berntsen, T., Betts, R., Fahey, D.W., Haywood, J., Lean, J., Lowe, D.C., Myhre, G., Nganga, J., Prinn, R., Raga, G., Schulz, M., van Dorland, R., 2007. Changes in atmospheric constituents and in radiative forcing. In Solomon, S., Qin, D., Manning, M., Chen, Z., Marquis, M., Averyt, K.B., Tignor, M., Miller, H.L. (Eds.), Climate Change 2007: The Physical Science Basis, 131-136, Cambridge University Press, Cambridge, UK.

Goudriaan, J., Ketner, P., 1984. A simulation study for the global carbon cycle, including man's impact on the biosphere. Climate Change, 6, 167-192.

Hansen, J., Nazarenko, L., Ruedy, R., Sato, M., Willis, J., Del Genio, A., Koch, D., Lacis, A., Lo, K., Menon, S., Novakov, T., Perlwitz, J., Russell, G., Schmidt, G.A., Tausnev, N., 2005. Earth's energy imbalance: confirmation and implications. Science, 308, 1431-1435.

Hansen, J., Sato, M., Ruedy, R., Lo, K., Lea, D.W., Elizade, M. M., 2006. Global Temperature Change. Proceedings of the National Academy of Sciences of the United States of America, 103/39, 14288-14293.

Hansen, J., Sato, M., Kharecha, P., Russell, G., Lea, D.W., Siddall, M., 2007. Climate change and trace gases. Philosophical Transactions of the Royal Society, A 365, 1925-1954.

Hansen, J., Sato, M., Ruedy, R., Kharecha, P., Lacis, A., Miller, R., Nazarenko, L., Lo, K., Schmidt, G.A., Russell, G., Aleinov, I., Bauer, S., Baum, E., Cairns, B., Canuto, V., Chandler, M., Cheng, Y., Cohen, A., Del Genio, A., Faluvegi, G., Fleming, E., Friend, A., Hall, T., Jackman, C., Jonas, J., Kelley, M., Kiang, N.Y., Koch, D., Labow, G., Lerner, J., Menon, S., Novakov, T., Oinas, V., Perlwitz, Ja., Perlwitz, Ju., Rind, D., Romanou, A., Schmunk, R., Shindell, D., Stone, P., Sun, S., Streets, D., Tausnev, N., Thresher, D., Unger, N., Yao, M., Zhang, S., 2007. Dangerous human-made interference with climate: a GISS modelE study. Atmospheric Chemistry and Physics, 7, 2287-2312.

Hansen, J., Sato, M., Kharecha, P., Beerling, D., Delmotte, V.M., Pagani, M., Raymo, M., Royer, D.L., Zachos, J.C., 2008. Target atmospheric CO_2: where should humanity aim?. Open Atmospheric Science Journal, 2, 217-231.

Hoff van't, JH., 1898. Lectures on the theoretical and physical chemistry, Part: Chemical dynamics, Edward Arnold, London, UK, 224-229.

Houghton, J.T., Jenkins, G.J., Ephraums, J.J. (Eds.), 1990. Climate Change 1990: The Scientific Assessment, Cambridge University Press, Cambridge, UK.

Houghton(1), J.T., Filho, L.G.M., Callander, B.A., Harris, N., Kattenberg, A., Maskell, K. Technical Summary. In Climate Change 1995: The Science of Climate Change, 9-49, Cambridge University Press, Cambridge, UK.

Houghton(2), J.T., Filho, L.G.M., Griggs, D.J., Maskell, K. (Eds.), 1997. IPCC Technical Paper II: An introduction to simple climate models used in the IPCC second assessment report.

Houweling, S., 2000. Global modeling of atmospheric methane sources and sinks, Ph.D. Thesis, Utrecht University.

Kaetterer, T., Reichstein, M., Andrén, O., Lomander, A., 1998. Temperature dependence of organic matter decomposition: a critical review using literature data analyzed with different models. Biology and Fertility of Soils, 27, 258-262.

Khvorostyanov, D.V., Krinner, G., Ciais, P., Heimann, M., Zimov, S.A., 2008. Vulnerability of permafrost carbon to global warming. Part I: model description and role of heat generated by organic matter decomposition. Tellus, 60B, 250-264.

Köhler, P., Fischer, H., 2004. Simulating changes in the terrestrial biosphere during the last glacial/interglacial transition. Global and Planetary Change, 43, 33-55.

Kwon, O.Y., Schnoor, J.L., 1994. Simple global carbon model: The atmosphere-terrestrial biosphere-ocean interaction. Global Biogeochemical Cycles, 8, 295-305.

Lawrence, D.M., Slater, A.G., 2005. A projection of severe near-surface permafrost degradation during the 21st century. Geophysical Research Letters, 32, L24401.

Lelieveld, J., Crutzen, P.J., Dentener, F.J., 1998. Changing concentration, lifetime and climate forcing of atmospheric methane. Tellus, 50B, 128-150.

Mastrandrea, M.D., Schneider, S.H., 2004. Probabilistic integrated assessment of "dangerous" climate change. Science, 304, 571-575.

Moxnes, E, Saysel, A.K., 2009. Misperceptions of basic climate change dynamics: information policies. Climatic Change, 93, 15-37.

Myhre G., Highwood E.J., Shine K.P., Stordal F., 1998. New estimates of radiative forcing due to well mixed greenhouse gases. Geophysical Research Letters, 25/14, 2715-2718

NASA-Goddard Institute for Space Studies home page. http://data.giss.nasa.gov/modelforce/ghgases/Fig1C.ext.txt. (accessed February 2009).

Nordhaud, W.D., 1992. “The “DICE” Model: Background and structure of a dynamic integrated climate-economy model of the economics of global warming”, http://cowles.econ.yale.edu/P/cd/d10a/d1009.pdf. (accessed December 2008).

Oeschger, H., Siegenthaler, U., Schotterer, U., Gugelmann, A., 1975. A box diffusion model to study the carbon dioxide exchange in nature. Tellus, XXVII(2), 168-192.

Peng, T.H., Takahashi, T., Broecker, W.S., Olafsson, J., 1987. Seasonal variability of carbon dioxide, nutrients and oxygen in the northern North Atlantic surface water: observations and a model. Tellus, 39B, 439-458.

Prentice, I.C., Farquhar, G.D., Fasham, M.J.R., Goulden, M.L., Heimann, M., Jaramillo, V.J., Kheshgi, H.S., Le Quéré, C., Scholes, R.J., Wallace, D.W.R., 2001. The carbon cycle and atmospheric carbon dioxide. In Watson, R.T. (Ed.), Climate Change 2001: The Scientific Basis, 183-237, Cambridge University Press, Cambridge, UK.

Ramaswamy, V., Boucher, O., Haigh, J., Hauglustaine, D., Haywood, J., Myhre, G., Nakajima, T., Shi, G.Y., Solomon, S., 2001. Radiative forcing of climate change. In Watson, R.T. (Ed.), Climate Change 2001: The Scientific Basis, 349-416, Cambridge University Press, Cambridge, UK.

Rasmussen, R.A., Khalil, M.A.K., 1981. Atmospheric methane: trends and seasonal cycles. Journal of Geophysical Research, 86, 9826-9832.

Raven, J.A., Falkowski, P.G., 1999. Oceanic sinks for atmospheric CO_2. Plant, Cell and Environment, 22, 741-755.

Schimel, D., Alves, D., Enting, I., Heimann, M., Joos, F., Raynaud, D., Wigley, T., Prather, M., Derwent, R., Ehhalt, D., Fraser, P., Sanhueza, E., Zhou, X., Jonas, P., Charlson, R., Rodhe, H., Sadasivan, S., Shine, K.P., Fouquart, Y., Ramaswamy, V., Solomon, S., Srinivasan, J., Albritton, D., Derwent, R., Isaksen, I., Lal, M., Wuebbles, D. Radiative forcing of climate change. In Houghton J.T., Meira Filho L.G., Callander B.A., Harris N., Kattenberg A., Maskell K. (Eds.), Climate Change 1995: The Science of Climate Change, 65-131, Cambridge University Press, Cambridge, UK.

Schneider, S.H., Rosencranz, A., Niles, J.O., (Eds.), 2002. Climate Change Policy/A Survey, Island Press, Washington DC, USA.

Siegenthaler, U., Sarmiento, J.L., 1993. Atmospheric carbon dioxide and the ocean. Nature, 365, 119-125.

Solomon, S.,Qin, D., Manning, M., Alley, R.B., Berntsen, T., Bindoff, N.L., Chen, Z., Chidthaisong, A., Gregory, J.M., Hegerl, G.C., Heimann, M., Hewitson, B., Hoskins, B.J., Joos, F., Jouzel, J., Kattsov, V., Lohmann, U., Matsuno, T., Molina, M., Nicholls, N., Overpeck, J., Raga ,G., Ramaswamy, V., Ren, J., Rusticucci, M., Somerville, R., Stocker, T.F., Whetton, P., Wood, R.A., Wratt, D., 2007. Technical Summary. In Solomon, S., Qin, D., Manning, M., Chen, Z., Marquis, M., Averyt, K.B., Tignor, M., Miller, H.L. (Eds.), Climate Change 2007: The Physical Science Basis, 19-91, Cambridge University Press, Cambridge, UK.

Sterman, J., 1994. Learning in and about Complex Systems. System Dynamics Review, 10-2/3, 291-330.

Sterman, J., Sweeney, L.B., 2006. Understanding public complacency about climate change. Climatic Change, 80-3/4, 213-238.

Stern, D., Kaufmann, R., 1995. "Annual Estimates of Global Anthropogenic Methane Emissions: 1860-1994", http://cdiac.ornl.gov/trends/meth/ch4.htm.

Sundqvist, E.T., Plummer, L.N. 1981. Carbon dioxide in the ocean surface layer: Some modeling considerations. In Bolin, B. (Ed.), Scope 16: Carbon Cycle Modelling, 259-269, John Wiley and Sons, NY.

Walter, B.P., Heimann, M., 2000. A process-based, climate-sensitive model to derive methane emissions from natural wetlands: Application to five wetland sites, sensitivity to model parameters, and climate. Global Biogeochemical Cycles, 14, 745-765.

Walter, B.P., Heimann, M., Matthews, E., 2001. Modeling modern methane emissions from natural wetlands 1. Model description and results. Journal of Geophysical Research, 106, 34189-34206.

Watson, R.T., Noble, I.R., Bolin, B., Ravindranath, H., Verardo, D.J., Dokken, D.J. (Eds.), 2000. Land Use, Land-Use Change and Forestry, Cambridge University Press, Cambridge, UK.

World Public Opinion homepage. http://www.worldpublicopinion.org/pipa/articles/btenvironmentra/79.php?nid=&id&pnt=79&lb=bte. (accessed September 2009).

Wuebbles, D.J., Hayhoe, K., 2002. Atmospheric methane and global change. Earth Science Reviews, 57, 177-210.

Zhang, T., Heginbottom, J. A., Barry, R. G., Brown, J., 2000. Further statistics on the distribution of permafrost and ground ice in the Northern Hemisphere. Polar Geography, 24, 126-131.

Zimov, S.A., Schuur, E.A.G., Chapin, F.S., 2006. Permafrost and the global carbon budget. Science, 312, 1612-1613.

APPENDIX A

LIST OF EQUATIONS FOR THE BASE RUN

ATMOSPHERIC CARBON

C_IN_ATM(t) = C_IN_ATM(t - dt) + (Resp_of_NW_tree_parts + anthropogenic_CO_2_emissions_2 + LUC_W_to_atm + LUC_NW_to_atm + Resp_of_active_soil_carbon + Resp_of_woody_tree_parts + Resp_of_ground_veg + Resp_of_det_decomp + LUC_GW_to_atm + LUC_det_to_atm + LUC_ActSC_to_atm + C_release_from_permafrost_as_CO_2 - Photosynt_of_trees - Photosynt_of_ground_veg - flux_atmosphere_to_ocean) * dtINIT C_IN_ATM = Preindustrial_C_in_atmosphere

INFLOWS:

Resp_of_NW_tree_parts (IN SECTOR: TERRESTRIAL CARBON)

anthropogenic_CO_2_emissions_2 = control_1*anthropogenic_CO_2_emissions

LUC_W_to_atm = if C_IN_W_TREE > LUC_emissions_2 then LUC_emissions_2*(C_IN_W_TREE/terrestrial_sum) else 0

LUC_NW_to_atm = if C_IN_NW_TREE>LUC_emissions_2 then LUC_emissions_2*(C_IN_NW_TREE/terrestrial_sum) else 0

Resp_of_active_soil_carbon (IN SECTOR: TERRESTRIAL CARBON)

Resp_of_woody_tree_parts = C_IN_W_TREE*Rate_coef_05*Q_{10resp}^(atm_mixed_layer_temperature_change/10)

Resp_of_ground_veg = C_IN_GRND_VEG*Rate_coef_06*Q_{10resp}^(atm_mixed_layer_temperature_change/10)

Resp_of_det_decomp = C_IN_DET_DECOMP*Rate_coef_02*Q_{10resp}^(atm_mixed_layer_temperature_change/10)

LUC_GW_to_atm = if C_IN_GRND_VEG>LUC_emissions_2 then
LUC_emissions_2*(C_IN_GRND_VEG/terrestrial_sum) else 0

LUC_det_to_atm = if C_IN_DET_DECOMP>LUC_emissions_2 then
LUC_emissions_2*(C_IN_DET_DECOMP/terrestrial_sum) else 0

LUC_ActSC_to_atm (IN SECTOR: TERRESTRIAL CARBON)

C_release_from_permafrost_as_CO_2 (Not in a sector)

OUTFLOWS:

Photosynt_of_trees (IN SECTOR: TERRESTRIAL CARBON)

Photosynt_of_ground_veg =
INIT_GPP_01*(1+Bcoef*LOGN(C_IN_ATM/Preindustrial_C_in_atmosphere))*
$Q_{10photsynth}$^(atm_mixed_layer_temperature_change/10)

flux_atmosphere_to_ocean (IN SECTOR: OCEANIC CARBON)

UNATTACHED:

anthropogenic_CO_2_emissions = GRAPH(TIME)
(1860, 0.091), (1861, 0.095), (1862, 0.097), (1863, 0.104), (1864, 0.112), (1865, 0.119), (1866, 0.122), (1867, 0.13), (1868, 0.135), (1869, 0.142), (1870, 0.147), (1871, 0.156), (1872, 0.173), (1873, 0.184), (1874, 0.174), (1875, 0.188), (1876, 0.191), (1877, 0.194), (1878, 0.196), (1879, 0.21), (1880, 0.236), (1881, 0.243), (1882, 0.256), (1883, 0.272), (1884, 0.275), (1885, 0.277), (1886, 0.281), (1887, 0.295), (1888, 0.327), (1889, 0.327), (1890, 0.356), (1891, 0.372), (1892, 0.374), (1893, 0.37), (1894, 0.383), (1895, 0.406), (1896, 0.419), (1897, 0.44), (1898, 0.465), (1899, 0.507), (1900, 0.534), (1901, 0.552), (1902, 0.566), (1903, 0.617), (1904, 0.624), (1905, 0.663), (1906, 0.707), (1907, 0.784), (1908, 0.75), (1909, 0.785), (1910, 0.819), (1911, 0.836), (1912, 0.879), (1913, 0.943), (1914, 0.85), (1915, 0.838), (1916, 0.901), (1917, 0.955), (1918, 0.936), (1919, 0.806), (1920, 0.932), (1921, 0.803), (1922, 0.845), (1923, 0.97), (1924, 0.963), (1925, 0.975), (1926, 0.983), (1927, 1.06), (1928, 1.06), (1929, 1.15), (1930, 1.05), (1931, 0.94), (1932, 0.847), (1933, 0.893), (1934, 0.973), (1935, 1.03), (1936, 1.13), (1937, 1.21), (1938, 1.14), (1939, 1.19), (1940, 1.30), (1941, 1.33), (1942, 1.34), (1943, 1.39), (1944, 1.38), (1945, 1.16), (1946, 1.24), (1947, 1.39), (1948, 1.47), (1949, 1.42), (1950, 1.63), (1951, 1.77),

(1952, 1.79), (1953, 1.84), (1954, 1.87), (1955, 2.04), (1956, 2.18), (1957, 2.27), (1958, 2.33), (1959, 2.46), (1960, 2.58), (1961, 2.59), (1962, 2.70), (1963, 2.85), (1964, 3.01), (1965, 3.15), (1966, 3.31), (1967, 3.41), (1968, 3.59), (1969, 3.80), (1970, 4.08), (1971, 4.23), (1972, 4.40), (1973, 4.63), (1974, 4.64), (1975, 4.62), (1976, 4.88), (1977, 5.03), (1978, 5.11), (1979, 5.39), (1980, 5.33), (1981, 5.17), (1982, 5.13), (1983, 5.11), (1984, 5.29), (1985, 5.44), (1986, 5.61), (1987, 5.75), (1988, 5.96), (1989, 6.09), (1990, 6.14), (1991, 6.24), (1992, 6.12), (1993, 6.12), (1994, 6.24), (1995, 6.37), (1996, 6.51), (1997, 6.62), (1998, 6.59), (1999, 6.57), (2000, 6.74), (2001, 6.90), (2002, 6.95), (2003, 7.29), (2004, 7.67), (2005, 7.97), (2006, 8.23), (2007, 8.34), (2008, 8.46), (2009, 8.57), (2010, 8.69), (2011, 8.84), (2012, 9.00), (2013, 9.16), (2014, 9.31), (2015, 9.47), (2016, 9.62), (2017, 9.78), (2018, 9.93), (2019, 10.1), (2020, 10.2), (2021, 10.4), (2022, 10.6), (2023, 10.8), (2024, 10.9), (2025, 11.1), (2026, 11.2), (2027, 11.3), (2028, 11.4), (2029, 11.5), (2030, 11.6), (2031, 11.7), (2032, 11.8), (2033, 11.9), (2034, 12.0), (2035, 12.2), (2036, 12.3), (2037, 12.4), (2038, 12.5), (2039, 12.6), (2040, 12.7), (2041, 12.8), (2042, 12.9), (2043, 13.0), (2044, 13.1), (2045, 13.2), (2046, 13.3), (2047, 13.4), (2048, 13.5), (2049, 13.6), (2050, 13.8), (2051, 13.9), (2052, 14.0), (2053, 14.0), (2054, 14.1), (2055, 14.2), (2056, 14.3), (2057, 14.4), (2058, 14.5), (2059, 14.6), (2060, 14.7), (2061, 14.8), (2062, 14.9), (2063, 15.0), (2064, 15.1), (2065, 15.2), (2066, 15.3), (2067, 15.4), (2068, 15.5), (2069, 15.6), (2070, 15.7), (2071, 15.8), (2072, 15.9), (2073, 16.0), (2074, 16.1), (2075, 16.2), (2076, 16.3), (2077, 16.5), (2078, 16.7), (2079, 16.9), (2080, 17.0), (2081, 17.2), (2082, 17.4), (2083, 17.5), (2084, 17.7), (2085, 17.9), (2086, 18.1), (2087, 18.2), (2088, 18.4), (2089, 18.6), (2090, 18.7), (2091, 18.9), (2092, 19.1), (2093, 19.2), (2094, 19.4), (2095, 19.6), (2096, 19.8), (2097, 19.9), (2098, 20.1), (2099, 20.3), (2100, 20.4)

control_1 = 1

Preindustrial_C_in_atmosphere = 607

Rate_coef_05 = 0.035

terrestrial_sum = ACTIVE_SOIL_C + C_IN_DET_DECOMP + C_IN_GRND_VEG + C_IN_NW_TREE + C_IN_W_TREE

ATMOSPHERIC METHANE

Atmospheric_Methane(t) = Atmospheric_Methane(t - dt) + (Waste_decomposition + Rice_cultivation + Domestic_ruminants + Biomass_burning + Fossil_fuels + Wetland_emissions + Termites_Oceans_&_other + C_release_from_permafrost_as_CH_4 - Methane_removal) * dtINIT Atmospheric_Methane = 2.4724

INFLOWS:

Waste_decomposition = GRAPH(if control_10=1 then TIME else 0)
(1860, 0.0016), (1865, 0.0019), (1870, 0.0021), (1875, 0.0024), (1880, 0.0027), (1885, 0.003), (1890, 0.0034), (1895, 0.0039), (1900, 0.0044), (1905, 0.005), (1910, 0.0056), (1915, 0.0064), (1920, 0.0072), (1925, 0.0082), (1930, 0.0093), (1935, 0.0105), (1940, 0.0119), (1945, 0.0134), (1950, 0.0152), (1955, 0.0172), (1960, 0.0194), (1965, 0.022), (1970, 0.0249), (1975, 0.0281), (1980, 0.0318), (1985, 0.036), (1990, 0.04), (1995, 0.0395), (2000, 0.0416), (2005, 0.0447), (2010, 0.0481), (2015, 0.0524), (2020, 0.0572), (2025, 0.0628), (2030, 0.0689), (2035, 0.075), (2040, 0.081), (2045, 0.0871), (2050, 0.0934), (2055, 0.0954), (2060, 0.0975), (2065, 0.0995), (2070, 0.102), (2075, 0.104), (2080, 0.105), (2085, 0.106), (2090, 0.107), (2095, 0.108), (2100, 0.109)

Rice_cultivation = GRAPH(if control_10=1 then TIME else 0)
(1860, 0.0401), (1865, 0.0404), (1870, 0.0407), (1875, 0.041), (1880, 0.0421), (1885, 0.0432), (1890, 0.0443), (1895, 0.0454), (1900, 0.0466), (1905, 0.0477), (1910, 0.0489), (1915, 0.0501), (1920, 0.0512), (1925, 0.0524), (1930, 0.0539), (1935, 0.0553), (1940, 0.0568), (1945, 0.0582), (1950, 0.0596), (1955, 0.0638), (1960, 0.0681), (1965, 0.0734), (1970, 0.0791), (1975, 0.0848), (1980, 0.0897), (1985, 0.095), (1990, 0.1), (1995, 0.09), (2000, 0.0953), (2005, 0.101), (2010, 0.105), (2015, 0.109), (2020, 0.114), (2025, 0.118), (2030, 0.121), (2035, 0.125), (2040, 0.128), (2045, 0.132), (2050, 0.135), (2055, 0.135), (2060, 0.135), (2065, 0.136), (2070, 0.136), (2075, 0.136), (2080, 0.136), (2085, 0.136), (2090, 0.137), (2095, 0.137), (2100, 0.137)

Domestic_ruminants = GRAPH(if control_10=1 then TIME else 0)
(1860, 0.0256), (1865, 0.0261), (1870, 0.0266), (1875, 0.0271), (1880, 0.0282), (1885, 0.0294), (1890, 0.0305), (1895, 0.0318), (1900, 0.033), (1905, 0.0344), (1910, 0.0358), (1915, 0.0373), (1920, 0.0388), (1925, 0.0404), (1930, 0.0423), (1935, 0.0443), (1940, 0.0464), (1945, 0.0486), (1950, 0.0509), (1955, 0.0557), (1960, 0.061), (1965, 0.0674), (1970, 0.0746),

(1975, 0.0823), (1980, 0.0897), (1985, 0.098), (1990, 0.107), (1995, 0.12), (2000, 0.13), (2005, 0.14), (2010, 0.149), (2015, 0.16), (2020, 0.17), (2025, 0.181), (2030, 0.191), (2035, 0.2), (2040, 0.209), (2045, 0.218), (2050, 0.227), (2055, 0.231), (2060, 0.235), (2065, 0.239), (2070, 0.243), (2075, 0.247), (2080, 0.249), (2085, 0.252), (2090, 0.255), (2095, 0.258), (2100, 0.261)

Biomass_burning = GRAPH(if control_10=1 then TIME else 0)
(1860, 0.0098), (1865, 0.0105), (1870, 0.0108), (1875, 0.0113), (1880, 0.0116), (1885, 0.0128), (1890, 0.013), (1895, 0.0131), (1900, 0.0131), (1905, 0.0157), (1910, 0.0162), (1915, 0.0138), (1920, 0.014), (1925, 0.0163), (1930, 0.016), (1935, 0.0159), (1940, 0.0155), (1945, 0.0149), (1950, 0.0169), (1955, 0.0243), (1960, 0.024), (1965, 0.0295), (1970, 0.0297), (1975, 0.027), (1980, 0.0312), (1985, 0.036), (1990, 0.038), (1995, 0.0282), (2000, 0.0288), (2005, 0.0294), (2010, 0.03), (2015, 0.0307), (2020, 0.0312), (2025, 0.0318), (2030, 0.0322), (2035, 0.0326), (2040, 0.0331), (2045, 0.0335), (2050, 0.0339), (2055, 0.0337), (2060, 0.0335), (2065, 0.0334), (2070, 0.0332), (2075, 0.033), (2080, 0.033), (2085, 0.033), (2090, 0.033), (2095, 0.0329), (2100, 0.0329)

Fossil_fuels = GRAPH(if control_10=1 then TIME else 0)
(1860, 0.0022), (1865, 0.0029), (1870, 0.0034), (1875, 0.0045), (1880, 0.0054), (1885, 0.0065), (1890, 0.0081), (1895, 0.0092), (1900, 0.0121), (1905, 0.0147), (1910, 0.0182), (1915, 0.0187), (1920, 0.0212), (1925, 0.022), (1930, 0.0234), (1935, 0.0209), (1940, 0.027), (1945, 0.0241), (1950, 0.0304), (1955, 0.036), (1960, 0.0446), (1965, 0.051), (1970, 0.0641), (1975, 0.0708), (1980, 0.074), (1985, 0.073), (1990, 0.081), (1995, 0.0923), (2000, 0.0938), (2005, 0.0982), (2010, 0.101), (2015, 0.103), (2020, 0.105), (2025, 0.11), (2030, 0.116), (2035, 0.122), (2040, 0.128), (2045, 0.134), (2050, 0.141), (2055, 0.146), (2060, 0.153), (2065, 0.159), (2070, 0.165), (2075, 0.171), (2080, 0.181), (2085, 0.191), (2090, 0.202), (2095, 0.212), (2100, 0.222)

Wetland_emissions = if control_10 = 1 then methane_production_rate*
(1-CH_4_oxidation_fraction)*Wetland_area else 0

Termites_Oceans_&_other = if control_10=1 then 0.04 else 0

C_release_from_permafrost_as_CH_4 (IN SECTOR: PERMAFROST)

OUTFLOWS:

Methane_removal = Atmospheric_Methane/Methane_residence_time

CH_4_oxidation_fraction = 0.4

Gt_ppbv_conversion_parameter_for_CH_4 = 326

methane_in_atm_as_ppbv=Atmospheric_Methane*Gt_ppbv_conversion_parameter_for_CH_4

methane_production_rate = Ref_CH_4_production_rate*$Q_{10\_CH4\_production}$^(atm_mixed_layer_temperature_change/10)*(NPP/HISTORY(NPP,TIME-1))

methane_radiative_forcing = rad_for_coef_CH_4*(SQRT(methane_in_atm_as_ppbv)-SQRT(Preind_CH_4_level))-0.47*LOGN(1+0.6356*(methane_in_atm_as_ppbv*Preind_N_2O_level/10E6)^0.75+0.007*(methane_in_atm_as_ppbv/1000)*(methane_in_atm_as_ppbv*Preind_N_2O_level/10E6)^1.52)-0.47*LOGN(1+0.6356*(Preind_CH_4_level*Preind_N_2O_level/10E6)^0.75+0.007*(Preind_CH_4_level/1000)*(Preind_CH_4_level*Preind_N_2O_level/10E6)^1.52)

Methane_residence_time = Ref_methane_residence_time/((100-percent_decrease_in_CH_4_loss_frequency)/100)

percent_decrease_in_CH_4_loss_frequency = percent_increase_in_CH_4*sensitivity_of_CH_4_loss_frequency_to_increase_in_CH_4

percent_increase_in_CH_4 = (methane_in_atm_as_ppbv-Preind_CH_4_level)/Preind_CH_4_level*100

Preind_CH_4_level = 806

$Q_{10\_CH4\_production}$ = IF control_7=1 then 6 else 1

rad_for_coef_CH_4 = 0.036

Ref_CH_4_production_rate = 5.13E-8

Ref_methane_residence_time = 9

Wetland_area = 5.3E6

CH_4_in_atm_as_ppbv_hist_data_&_IS92a_scenario = GRAPH(TIME)
(1860, 806), (1862, 809), (1864, 812), (1866, 815), (1868, 818), (1870, 821), (1872, 824), (1874, 827), (1876, 830), (1878, 833), (1880, 837), (1882, 841), (1884, 845), (1886, 849), (1888, 853), (1890, 857), (1892, 861), (1894, 866), (1896, 870), (1898, 875), (1900, 879), (1902, 888), (1904, 897), (1906, 905), (1908, 914), (1910, 924), (1912, 934), (1914, 944), (1916, 955), (1918, 966), (1920, 978), (1922, 990), (1924, 1002), (1926, 1014), (1928, 1025), (1930, 1036), (1932, 1047), (1934, 1058), (1936, 1069), (1938, 1079), (1940, 1089), (1942, 1099), (1944, 1109), (1946, 1121), (1948, 1133), (1950, 1148), (1952, 1164), (1954, 1182), (1956, 1202), (1958, 1224), (1960, 1248), (1962, 1272), (1964, 1298), (1966, 1326), (1968, 1355), (1970, 1386), (1972, 1418), (1974, 1449), (1976, 1482), (1978, 1514), (1980, 1547), (1982, 1581), (1984, 1614), (1986, 1645), (1988, 1672), (1990, 1694), (1992, 1714), (1994, 1730), (1996, 1750), (1998, 1764), (2000, 1773), (2002, 1771), (2004, 1780), (2006, 1898), (2008, 1931), (2010, 1964), (2012, 1999), (2014, 2034), (2016, 2071), (2018, 2108), (2020, 2145), (2022, 2184), (2024, 2223), (2026, 2262), (2028, 2303), (2030, 2343), (2032, 2386), (2034, 2429), (2036, 2472), (2038, 2517), (2040, 2561), (2042, 2607), (2044, 2653), (2046, 2699), (2048, 2746), (2050, 2793), (2052, 2838), (2054, 2883), (2056, 2925), (2058, 2964), (2060, 3003), (2062, 3039), (2064, 3074), (2066, 3109), (2068, 3142), (2070, 3175), (2072, 3206), (2074, 3237), (2076, 3268), (2078, 3298), (2080, 3328), (2082, 3358), (2084, 3387), (2086, 3416), (2088, 3445), (2090, 3474), (2092, 3502), (2094, 3531), (2096, 3559), (2098, 3588), (2100, 3616)

sensitivity_of_CH_4_loss_frequency_to_increase_in_CH_4=GRAPH(percent_increase_in_CH_4)
(0.00, 0.24), (25.0, 0.114), (50.0, 0.08), (75.0, 0.067), (100, 0.06), (125, 0.057), (150, 0.054), (175, 0.053), (200, 0.052), (225, 0.051), (250, 0.0507), (275, 0.0505), (300, 0.0502), (325, 0.0499), (350, 0.0497), (375, 0.0494), (400, 0.0491), (425, 0.0488), (450, 0.0486), (475, 0.0483), (500, 0.048), (525, 0.0478), (550, 0.0475), (575, 0.0472), (600, 0.0469), (625, 0.0467), (650, 0.0464), (675, 0.0461), (700, 0.0459), (725, 0.0456), (750, 0.0453), (775, 0.0451), (800, 0.0448), (825, 0.0445), (850, 0.0442), (875, 0.044), (900, 0.0437), (925, 0.0434), (950, 0.0432), (975, 0.0429), (1000, 0.0426), (1025, 0.0424), (1050, 0.0421), (1075, 0.0418), (1100, 0.0415), (1125, 0.0413), (1150, 0.041), (1175, 0.0407), (1200, 0.0405), (1225,

0.0402), (1250, 0.0399), (1275, 0.0397), (1300, 0.0394), (1325, 0.0391), (1350, 0.0389), (1375, 0.0386), (1400, 0.0383), (1425, 0.038), (1450, 0.0378), (1475, 0.0375), (1500, 0.0372), (1525, 0.037), (1550, 0.0367), (1575, 0.0364), (1600, 0.0362), (1625, 0.0359), (1650, 0.0356), (1675, 0.0353), (1700, 0.0351), (1725, 0.0348), (1750, 0.0345), (1775, 0.0343), (1800, 0.034), (1825, 0.0337), (1850, 0.0335), (1875, 0.0332), (1900, 0.0329), (1925, 0.0326), (1950, 0.0324), (1975, 0.0321), (2000, 0.0318), (2025, 0.0316), (2050, 0.0313), (2075, 0.031), (2100, 0.0308), (2125, 0.0305), (2150, 0.0302), (2175, 0.0299), (2200, 0.0297), (2225, 0.0294), (2250, 0.0291), (2275, 0.0289), (2300, 0.0286), (2325, 0.0283), (2350, 0.028), (2375, 0.0278), (2400, 0.0275), (2425, 0.0272), (2450, 0.027), (2475, 0.0267), (2500, 0.0264), (2525, 0.0262), (2550, 0.0259), (2575, 0.0256), (2600, 0.0254), (2625, 0.0251), (2650, 0.0248), (2675, 0.0245), (2700, 0.0243), (2725, 0.024), (2750, 0.0237), (2775, 0.0235), (2800, 0.0232), (2825, 0.0229), (2850, 0.0227), (2875, 0.0224), (2900, 0.0221), (2925, 0.0218), (2950, 0.0216), (2975, 0.0213), (3000, 0.021), (3025, 0.0208), (3050, 0.0205), (3075, 0.0202), (3100, 0.0199), (3125, 0.0197), (3150, 0.0194), (3175, 0.0191), (3200, 0.0189), (3225, 0.0186), (3250, 0.0183), (3275, 0.0181), (3300, 0.0178), (3325, 0.0175), (3350, 0.0173), (3375, 0.017), (3400, 0.0167), (3425, 0.0164), (3450, 0.0162), (3475, 0.0159), (3500, 0.0156), (3525, 0.0154), (3550, 0.0151), (3575, 0.0148), (3600, 0.0146), (3625, 0.0143), (3650, 0.014), (3675, 0.0137), (3700, 0.0135), (3725, 0.0132), (3750, 0.0129), (3775, 0.0127), (3800, 0.0124), (3825, 0.0121), (3850, 0.0118), (3875, 0.0116), (3900, 0.0113), (3925, 0.011), (3950, 0.0108), (3975, 0.0105), (4000, 0.0102), (4025, 0.00996), (4050, 0.00969), (4075, 0.00942), (4100, 0.00915), (4125, 0.00888), (4150, 0.00861), (4175, 0.00834), (4200, 0.00807), (4225, 0.0078), (4250, 0.00753), (4275, 0.00726), (4300, 0.00699), (4325, 0.00672), (4350, 0.00645), (4375, 0.00618), (4400, 0.00591), (4425, 0.00564), (4450, 0.00537), (4475, 0.0051), (4500, 0.00483)

ATMOSPHERIC NITROUS OXIDE

N_2O_in_atm(t) = N_2O_in_atm(t - dt) + (Other_Anthrop_N_2O_emissions + Natural_N_2O_emissions+N_2O_from_agriculture-N_2O_removal)*dt INIT N_2O_in_atm=1482

INFLOWS:

Other_Anthrop_N_2O_emissions = GRAPH(if control_11=1 then TIME else 0)
(1860, 0.213), (1865, 0.283), (1870, 0.353), (1875, 0.424), (1880, 0.494), (1885, 0.565), (1890, 0.635), (1895, 0.706), (1900, 0.776), (1905, 0.846), (1910, 0.917), (1915, 0.987), (1920, 1.06), (1925, 1.13), (1930, 1.20), (1935, 1.27), (1940, 1.34), (1945, 1.41), (1950, 1.48), (1955, 1.55), (1960, 1.62), (1965, 1.69), (1970, 1.76), (1975, 1.83), (1980, 1.90), (1985, 1.97), (1990, 2.18),

(1995, 2.31), (2000, 2.45), (2005, 2.65), (2010, 2.81), (2015, 2.97), (2020, 3.10), (2025, 3.27), (2030, 3.34), (2035, 3.41), (2040, 3.48), (2045, 3.55), (2050, 3.62), (2055, 3.62), (2060, 3.62), (2065, 3.61), (2070, 3.61), (2075, 3.61), (2080, 3.63), (2085, 3.64), (2090, 3.65), (2095, 3.67), (2100, 3.68)

Natural_N_2O_emissions = if control_11=1 then 13.043 else 0

N_2O_from_agriculture = GRAPH(if control_11=1 then TIME else 0)
(1860, 0.404), (1865, 0.464), (1870, 0.525), (1875, 0.585), (1880, 0.645), (1885, 0.705), (1890, 0.765), (1895, 0.826), (1900, 0.886), (1905, 0.946), (1910, 1.01), (1915, 1.07), (1920, 1.13), (1925, 1.19), (1930, 1.25), (1935, 1.31), (1940, 1.37), (1945, 1.43), (1950, 1.49), (1955, 1.55), (1960, 1.61), (1965, 1.67), (1970, 1.73), (1975, 1.79), (1980, 1.85), (1985, 1.91), (1990, 2.42), (1995, 2.73), (2000, 3.01), (2005, 3.19), (2010, 3.42), (2015, 3.63), (2020, 3.95), (2025, 4.20), (2030, 4.30), (2035, 4.40), (2040, 4.50), (2045, 4.60), (2050, 4.70), (2055, 4.72), (2060, 4.74), (2065, 4.76), (2070, 4.78), (2075, 4.80), (2080, 4.84), (2085, 4.88), (2090, 4.92), (2095, 4.96), (2100, 5.00)

OUTFLOWS:

N_2O_removal = N_2O_in_atm/N_2O_residence_time

N_2O_in_atm_as_ppbv = N_2O_in_atm*Tg_ppbv_conversion_parameter_for_N_2O

N_2O_radiative_forcing = rad_for_coef_N_2O*(SQRT(N_2O_in_atm_as_ppbv)-SQRT(Preind_N_2O_level))-0.47*LOGN(1+0.6356*(Preind_CH_4_level*N_2O_in_atm_as_ppbv/10E6)^0.75+0.007*(Preind_CH_4_level/1000)*(Preind_CH_4_level*N_2O_in_atm_as_ppbv/10E6)^1.52)-0.47*LOGN(1+0.6356*(Preind_CH_4_level*Preind_N_2O_level/10E6)^0.75+0.007*(Preind_CH_4_level/1000)*(Preind_CH_4_level*Preind_N_2O_level/10E6)^1.52)

N_2O_residence_time = 110

Preind_N_2O_level = 276.4

rad_for_coef_N_2O = 0.14

Tg_ppbv_conversion_parameter_for_N_2O = 0.1865

N_2O_in_atm_historical_data_&_IS92a_scenario = GRAPH(TIME)

(1860, 276), (1861, 277), (1862, 277), (1863, 277), (1864, 277), (1865, 277), (1866, 277), (1867, 277), (1868, 277), (1869, 277), (1870, 277), (1871, 277), (1872, 278), (1873, 278), (1874, 278), (1875, 278), (1876, 278), (1877, 278), (1878, 278), (1879, 278), (1880, 278), (1881, 278), (1882, 278), (1883, 279), (1884, 279), (1885, 279), (1886, 279), (1887, 279), (1888, 279), (1889, 279), (1890, 279), (1891, 279), (1892, 279), (1893, 279), (1894, 279), (1895, 280), (1896, 280), (1897, 280), (1898, 280), (1899, 280), (1900, 280), (1901, 280), (1902, 280), (1903, 280), (1904, 280), (1905, 280), (1906, 280), (1907, 281), (1908, 281), (1909, 281), (1910, 281), (1911, 281), (1912, 281), (1913, 282), (1914, 282), (1915, 282), (1916, 282), (1917, 282), (1918, 283), (1919, 283), (1920, 283), (1921, 283), (1922, 283), (1923, 284), (1924, 284), (1925, 284), (1926, 284), (1927, 285), (1928, 285), (1929, 285), (1930, 285), (1931, 285), (1932, 285), (1933, 286), (1934, 286), (1935, 286), (1936, 286), (1937, 286), (1938, 286), (1939, 287), (1940, 287), (1941, 287), (1942, 287), (1943, 287), (1944, 288), (1945, 288), (1946, 288), (1947, 288), (1948, 289), (1949, 289), (1950, 289), (1951, 289), (1952, 289), (1953, 290), (1954, 290), (1955, 290), (1956, 290), (1957, 291), (1958, 291), (1959, 291), (1960, 291), (1961, 292), (1962, 292), (1963, 292), (1964, 293), (1965, 293), (1966, 293), (1967, 294), (1968, 294), (1969, 295), (1970, 295), (1971, 296), (1972, 296), (1973, 297), (1974, 297), (1975, 298), (1976, 299), (1977, 299), (1978, 300), (1979, 301), (1980, 301), (1981, 302), (1982, 303), (1983, 304), (1984, 305), (1985, 305), (1986, 306), (1987, 306), (1988, 307), (1989, 309), (1990, 309), (1991, 310), (1992, 310), (1993, 311), (1994, 311), (1995, 312), (1996, 313), (1997, 314), (1998, 315), (1999, 315), (2000, 316), (2001, 317), (2002, 317), (2003, 318), (2004, 319), (2005, 319), (2006, 320), (2007, 321), (2008, 322), (2009, 325), (2010, 328), (2011, 329), (2012, 330), (2013, 331), (2014, 332), (2015, 333), (2016, 334), (2017, 335), (2018, 337), (2019, 338), (2020, 339), (2021, 340), (2022, 341), (2023, 342), (2024, 343), (2025, 344), (2026, 345), (2027, 346), (2028, 348), (2029, 349), (2030, 350), (2031, 351), (2032, 352), (2033, 353), (2034, 354), (2035, 355), (2036, 356), (2037, 357), (2038, 359), (2039, 360), (2040, 361), (2041, 362), (2042, 363), (2043, 364), (2044, 365), (2045, 366), (2046, 367), (2047, 368), (2048, 369), (2049, 370), (2050, 371), (2051, 372), (2052, 373), (2053, 374), (2054, 375), (2055, 376), (2056, 377), (2057, 378), (2058, 380), (2059, 381), (2060, 382), (2061, 383), (2062, 384), (2063, 384), (2064, 385), (2065, 386), (2066, 387), (2067, 388), (2068, 389), (2069, 390), (2070, 391), (2071, 392), (2072, 393), (2073, 394), (2074, 395), (2075, 396), (2076, 397), (2077, 398), (2078, 398), (2079, 399), (2080, 400), (2081, 401), (2082, 402), (2083, 402),

(2084, 403), (2085, 404), (2086, 405), (2087, 406), (2088, 407), (2089, 408), (2090, 409), (2091, 410), (2092, 411), (2093, 411), (2094, 412), (2095, 413), (2096, 414), (2097, 415), (2098, 415), (2099, 416), (2100, 417)

OCEANIC CARBON

C_in_mixed_layer(t) = C_in_mixed_layer(t - dt) + (flux_atmosphere_to_ocean - Flux_to_01) * dtINIT C_in_mixed_layer = Preindustrial_C_in_mixed_layer

INFLOWS:

flux_atmosphere_to_ocean = (Equil_C_in_mixed_layer-C_in_mixed_layer)/Mixing_time

OUTFLOWS:

Flux_to_01 = (C_in_mixed_layer/Mixed_layer_thickness-Concentration[conc_L01])* Eddy_diff_coeff*2/(Mixed_layer_thickness+Layer_thickness[Layer_01])

Layer_01(t) = Layer_01(t - dt) + (Flux_to_01 - Flux_to_02) * dtINIT Layer_01 = 2050

INFLOWS:

Flux_to_01 = (C_in_mixed_layer/Mixed_layer_thickness-Concentration[conc_L01])* Eddy_diff_coeff*2/(Mixed_layer_thickness+Layer_thickness[Layer_01])

OUTFLOWS:

Flux_to_02 = (Concentration[conc_L01]-Concentration[conc_L02])* Eddy_diff_coeff*2/(Layer_thickness[Layer_01]+Layer_thickness[Layer_02])

Layer_02(t) = Layer_02(t - dt) + (Flux_to_02 - Flux_to_03) * dtINIT Layer_02 = 2050

INFLOWS:

Flux_to_02 = (Concentration[conc_L01]-Concentration[conc_L02])* Eddy_diff_coeff*2/(Layer_thickness[Layer_01]+Layer_thickness[Layer_02])

OUTFLOWS:

Flux_to_03 = (Concentration[conc_L02]-Concentration[conc_L03])* Eddy_diff_coeff*2/(Layer_thickness[Layer_02]+Layer_thickness[Layer_03])

Layer_03(t) = Layer_03(t - dt) + (Flux_to_03 - Flux_to04) * dtINIT Layer_03 = 2050

INFLOWS:

Flux_to_03 = (Concentration[conc_L02]-Concentration[conc_L03])*
Eddy_diff_coeff*2/(Layer_thickness[Layer_02]+Layer_thickness[Layer_03])

OUTFLOWS:

Flux_to04 = (Concentration[conc_L03]-Concentration[conc_L04])*
Eddy_diff_coeff*2/(Layer_thickness[Layer_03]+Layer_thickness[Layer_04])

Layer_04(t) = Layer_04(t - dt) + (Flux_to04 - Flux_to_05) * dtINIT Layer_04 = 2050

INFLOWS:

Flux_to04 = (Concentration[conc_L03]-Concentration[conc_L04])*
Eddy_diff_coeff*2/(Layer_thickness[Layer_03]+Layer_thickness[Layer_04])

OUTFLOWS:

Flux_to_05 = (Concentration[conc_L04]-Concentration[conc_L05])*
Eddy_diff_coeff*2/(Layer_thickness[Layer_04]+Layer_thickness[Layer_05])

Layer_05(t) = Layer_05(t - dt) + (Flux_to_05 - Flux_to_06) * dtINIT Layer_05 = 2050

INFLOWS:

Flux_to_05 = (Concentration[conc_L04]-Concentration[conc_L05])*
Eddy_diff_coeff*2/(Layer_thickness[Layer_04]+Layer_thickness[Layer_05])

OUTFLOWS:

Flux_to_06 = (Concentration[conc_L05]-Concentration[conc_L06])*
Eddy_diff_coeff*2/(Layer_thickness[Layer_05]+Layer_thickness[Layer_06])

Layer_06(t) = Layer_06(t - dt) + (Flux_to_06 - Flux_to_07) * dtINIT Layer_06 = 5730

INFLOWS:

Flux_to_06 = (Concentration[conc_L05]-Concentration[conc_L06])*
Eddy_diff_coeff*2/(Layer_thickness[Layer_05]+Layer_thickness[Layer_06])

OUTFLOWS:

Flux_to_07 = (Concentration[conc_L06]-Concentration[conc_L07])*
Eddy_diff_coeff*2/(Layer_thickness[Layer_06]+Layer_thickness[Layer_07])

Layer_07(t) = Layer_07(t - dt) + (Flux_to_07 - Flux_to_08) * dtINIT Layer_07 = 5730

INFLOWS:

Flux_to_07 = (Concentration[conc_L06]-Concentration[conc_L07])*
Eddy_diff_coeff*2/(Layer_thickness[Layer_06]+Layer_thickness[Layer_07])

OUTFLOWS:

Flux_to_08 = (Concentration[conc_L07]-Concentration[conc_L08])*
Eddy_diff_coeff*2/(Layer_thickness[Layer_07]+Layer_thickness[Layer_08])

Layer_08(t) = Layer_08(t - dt) + (Flux_to_08 - Flux_to_09) * dtINIT Layer_08 = 5730

INFLOWS:

Flux_to_08 = (Concentration[conc_L07]-Concentration[conc_L08])*
Eddy_diff_coeff*2/(Layer_thickness[Layer_07]+Layer_thickness[Layer_08])

OUTFLOWS:

Flux_to_09 = (Concentration[conc_L08]-Concentration[conc_L09])*
Eddy_diff_coeff*2/(Layer_thickness[Layer_08]+Layer_thickness[Layer_09])

Layer_09(t) = Layer_09(t - dt) + (Flux_to_09 - Flux_to_10) * dtINIT Layer_09 = 5730

INFLOWS:

Flux_to_09 = (Concentration[conc_L08]-Concentration[conc_L09])*
Eddy_diff_coeff*2/(Layer_thickness[Layer_08]+Layer_thickness[Layer_09])

OUTFLOWS:

Flux_to_10 = (Concentration[conc_L09]-Concentration[conc_L10])*
Eddy_diff_coeff*2/(Layer_thickness[Layer_09]+Layer_thickness[Layer_10])

Layer_10(t) = Layer_10(t - dt) + (Flux_to_10) * dtINIT Layer_10 = 5730

INFLOWS:

Flux_to_10 = (Concentration[conc_L09]-Concentration[conc_L10])*
Eddy_diff_coeff*2/(Layer_thickness[Layer_09]+Layer_thickness[Layer_10])

Buffer_CO_2_coefficient = 4.05

Buffer_factor =
Ref_buffer_factor+Buffer_CO_2_coefficient*LOGN(C_IN_ATM/Ref_buffer_Carbon)

Concentration[conc_L01] = Layer_01/Layer_thickness[Layer_01]

Concentration[conc_L02] = Layer_02/Layer_thickness[Layer_02]

Concentration[conc_L03] = Layer_03/Layer_thickness[Layer_03]

Concentration[conc_L04] = Layer_04/Layer_thickness[Layer_04]

Concentration[conc_L05] = Layer_05/Layer_thickness[Layer_05]

Concentration[conc_L06] = Layer_06/Layer_thickness[Layer_06]

Concentration[conc_L07] = Layer_07/Layer_thickness[Layer_07]

Concentration[conc_L08] = Layer_08/Layer_thickness[Layer_08]

Concentration[conc_L09] = Layer_09/Layer_thickness[Layer_09]

Concentration[conc_L10] = Layer_10/Layer_thickness[Layer_10]

Eddy_diff_coeff = 4000

Equil_C_in_mixed_layer = Preindustrial_C_in_mixed_layer*(1+(C_IN_ATM-
Preindustrial_C_in_atmosphere)/(Preindustrial_C_in_atmosphere*Buffer_factor))

Layer_thickness[Layer_01] = 200

Layer_thickness[Layer_02] = 200

Layer_thickness[Layer_03] = 200

Layer_thickness[Layer_04] = 200

Layer_thickness[Layer_05] = 200

Layer_thickness[Layer_06] = 560

Layer_thickness[Layer_07] = 560

Layer_thickness[Layer_08] = 560

Layer_thickness[Layer_09] = 560

Layer_thickness[Layer_10] = 560

Mixed_layer_thickness = 75

Mixing_time = 9.5

Preindustrial_C_in_mixed_layer = 795

Ref_buffer_Carbon = 760

Ref_buffer_factor = 10

PERMAFROST

C_in_permafrost(t) = C_in_permafrost(t - dt) + (-C_release_from_permafrost_as_CH_4 - C_release_from_permafrost_as_CO_2) * dtINIT C_in_permafrost = 375

OUTFLOWS:

C_release_from_permafrost_as_CH_4 = Carbon_density_of_permafrost* (thawing-freezing)*CH_4_release_fraction*(16/12)

C_release_from_permafrost_as_CO_2 (Not in a sector)

Permafrost_Area(t) = Permafrost_Area(t - dt) + (freezing - thawing) * dt
INIT Permafrost_Area = 11E6

INFLOWS:

freezing = freezing_fraction*Permafrost_Area

OUTFLOWS:

thawing = actual_thawing_fraction*Permafrost_Area

actual_thawing_fraction =
preindustrial_thawing_fraction*thawing_fraction_multiplier_extreme_scenario

Carbon_density_of_permafrost = INIT(C_in_permafrost)/INIT(Permafrost_Area)

CH_4_release_fraction = 0.5

CO_2_release_fraction = 1-CH_4_release_fraction

control_8 = 0

critical_heat_for_devastating_melting = heat_capacity_of_permafrost*
(0-initial_average_temperature_of_permafrost)*time_conversion_parameter

freezing_fraction = 0.1

heat_capacity_of_permafrost = Heat_capacity_of_atm_&_mixed_layer

initial_average_temperature_of_permafrost = -1

preindustrial_thawing_fraction = 0.1

ratio_of_heat_difference_to_critical_heat =
control_8*(Atm_mixed_layer_heat_difference/critical_heat_for_devastating_melting)

thawing_fraction_multiplier_extreme_scenario =
GRAPH(ratio_of_heat_difference_to_critical_heat)
(0.00, 1.00), (0.25, 1.00), (0.5, 1.00), (0.75, 1.00), (1.00, 1.01), (1.25, 1.01), (1.50, 1.03), (1.75, 1.05), (2.00, 1.08), (2.25, 1.12), (2.50, 1.15), (2.75, 1.19), (3.00, 1.23), (3.25, 1.27), (3.50, 1.31), (3.75, 1.36), (4.00, 1.40), (4.25, 1.45), (4.50, 1.50), (4.75, 1.56), (5.00, 1.63)

thawing_fraction_multiplier_mild_scenario =
GRAPH(ratio_of_heat_difference_to_critical_heat)
(0.00, 1.00), (0.25, 1.01), (0.5, 1.01), (0.75, 1.02), (1.00, 1.02), (1.25, 1.03), (1.50, 1.03), (1.75, 1.04), (2.00, 1.04), (2.25, 1.05), (2.50, 1.06), (2.75, 1.07), (3.00, 1.08), (3.25, 1.09), (3.50, 1.10), (3.75, 1.11), (4.00, 1.13), (4.25, 1.14), (4.50, 1.16), (4.75, 1.17), (5.00, 1.19), (5.25, 1.21), (5.50, 1.23), (5.75, 1.26), (6.00, 1.29)

RADIATIVE FORCING & TEMPERATURE CHANGE

Atm_mixed_layer_heat_difference(t) = Atm_mixed_layer_heat_difference(t - dt) +
(Radiative_forcing - Feedback_cooling - Heat_transfer_to_deep_ocean) * dt
INIT Atm_mixed_layer_heat_difference = 0

INFLOWS:

Radiative_forcing = total_radiative_forcing*time_conversion_parameter

OUTFLOWS:

Feedback_cooling = Climate_feedback_parameter*atm_mixed_layer_temperature_change*
time_conversion_parameter

Heat_transfer_to_deep_ocean = Heat_capacity_of_deep_ocean*
Temp_dif_btw_atm_mixed_lay_&_deep_ocean/Heat_transfer_time_constant*
time_conversion_parameter

Deep_ocean_heat_difference(t) = Deep_ocean_heat_difference(t - dt) +
(Heat_transfer_to_deep_ocean) * dt
INIT Deep_ocean_heat_difference = 0

INFLOWS:

Heat_transfer_to_deep_ocean =
Heat_capacity_of_deep_ocean*Temp_dif_btw_atm_mixed_lay_&_deep_ocean/
Heat_transfer_time_constant*time_conversion_parameter

atm_mixed_layer_temperature_change = Atm_mixed_layer_heat_difference/
Heat_capacity_of_atm_&_mixed_layer/time_conversion_parameter

avg_temp_change_1951_1980 = 0.33133

Climate_feedback_parameter = (rad_for_coef_CO_2/Climate_sensitivity)*LOGN(2)

Climate_sensitivity = 2.908

CO_2_radiative_forcing =
rad_for_coef_CO_2*LOGN(C_IN_ATM/Preindustrial_C_in_atmosphere)

deep_ocean_temp_change =
Deep_ocean_heat_difference/Heat_capacity_of_deep_ocean/time_conversion_parameter

global_temperature_anomaly = atm_mixed_layer_temperature_change-
avg_temp_change_1951_1980

Heat_capacity_of_atm_&_mixed_layer = 44.248

Heat_capacity_of_deep_ocean = 220

Heat_transfer_time_constant = 500

rad_for_coef_CO_2 = 5.35

Temp_dif_btw_atm_mixed_lay_&_deep_ocean = atm_mixed_layer_temperature_change-
deep_ocean_temp_change

time_conversion_parameter = 31536000

total_radiative_forcing = CO_2_radiative_forcing*control_4+methane_radiative_forcing*
control_5+N_2O_radiative_forcing*control_6

TERRESTRIAL CARBON

ACTIVE_SOIL_C(t) = ACTIVE_SOIL_C(t - dt) + (Death_of_below_ground_of_GW +
Transport_of_decomp_matter_to_ASC + Death_of_below_ground_of_WT –
Fossilisation - Resp_of_active_soil_carbon - LUC_ActSC_to_atm) * dt
INIT ACTIVE_SOIL_C = 1041

INFLOWS:

Death_of_below_ground_of_GW = C_IN_GRND_VEG*Rate_coef_08

Transport_of_decomp_matter_to_ASC = C_IN_DET_DECOMP*Rate_coef_15

Death_of_below_ground_of_WT = C_IN_W_TREE*Rate_coef_14

OUTFLOWS:

Fossilisation = 0

Resp_of_active_soil_carbon =
ACTIVE_SOIL_C*Rate_coef_04*Q_{10resp}^(atm_mixed_layer_temperature_change/10)

LUC_ActSC_to_atm = if ACTIVE_SOIL_C>LUC_emissions_2 then
LUC_emissions_2*(ACTIVE_SOIL_C/terrestrial_sum) else 0

C_IN_DET_DECOMP(t)=C_IN_DET_DECOMP(t-dt)+(Death_of_above_ground_of_GW +
Death_of_above_ground_of_WT +Death_of_above_ground_of_NW-
Resp_of_det_decomp-Transport_of_decomp_matter_to_ASC-LUC_det_to_atm)*dt
INIT C_IN_DET_DECOMP = 75

INFLOWS:

Death_of_above_ground_of_GW = C_IN_GRND_VEG*Rate_coef_09

Death_of_above_ground_of_WT = C_IN_W_TREE*Rate_coef_13

Death_of_above_ground_of_NW = C_IN_NW_TREE*Rate_coef_10

OUTFLOWS:

Resp_of_det_decomp (IN SECTOR: ATMOSPHERIC CARBON)

Transport_of_decomp_matter_to_ASC = C_IN_DET_DECOMP*Rate_coef_15

LUC_det_to_atm (IN SECTOR: ATMOSPHERIC CARBON)

C_IN_GRND_VEG(t) = C_IN_GRND_VEG(t - dt) + (Photosynt_of_ground_veg -
Death_of_below_ground_of_GW - Resp_of_ground_veg -
Death_of_above_ground_of_GW - LUC_GW_to_atm) * dt
INIT C_IN_GRND_VEG = 64

INFLOWS:

Photosynt_of_ground_veg (IN SECTOR: ATMOSPHERIC CARBON)

OUTFLOWS:

Death_of_below_ground_of_GW = C_IN_GRND_VEG*Rate_coef_08

Resp_of_ground_veg (IN SECTOR: ATMOSPHERIC CARBON)

Death_of_above_ground_of_GW = C_IN_GRND_VEG*Rate_coef_09

LUC_GW_to_atm (IN SECTOR: ATMOSPHERIC CARBON)

C_IN_NW_TREE(t) = C_IN_NW_TREE(t - dt) + (Photosynt_of_trees - Resp_of_NW_tree_parts - LUC_NW_to_atm - Death_of_above_ground_of_NW - Aging_of_NW_trees) * dt

INIT C_IN_NW_TREE = 34

INFLOWS:

Photosynt_of_trees = INIT_GPP_03*(1+Bcoef*LOGN(C_IN_ATM/Preindustrial_C_in_atmosphere))* $Q_{10photsynth}$^(atm_mixed_layer_temperature_change/10)

OUTFLOWS:

Resp_of_NW_tree_parts = C_IN_NW_TREE*Rate_coef_07*Q_{10resp}^(atm_mixed_layer_temperature_change/10)

LUC_NW_to_atm (IN SECTOR: ATMOSPHERIC CARBON)

Death_of_above_ground_of_NW = C_IN_NW_TREE*Rate_coef_10

Aging_of_NW_trees = C_IN_NW_TREE*Rate_coef_11

C_IN_W_TREE(t) = C_IN_W_TREE(t - dt) + (Aging_of_NW_trees - LUC_W_to_atm - Resp_of_woody_tree_parts - Death_of_below_ground_of_WT - Death_of_above_ground_of_WT) * dt

INIT C_IN_W_TREE = 420

INFLOWS:

Aging_of_NW_trees = C_IN_NW_TREE*Rate_coef_11

OUTFLOWS:

LUC_W_to_atm (IN SECTOR: ATMOSPHERIC CARBON)

Resp_of_woody_tree_parts (IN SECTOR: ATMOSPHERIC CARBON)

Death_of_below_ground_of_WT = C_IN_W_TREE*Rate_coef_14

Death_of_above_ground_of_WT = C_IN_W_TREE*Rate_coef_13

Bcoef = 0.5

control_3 = 1

INIT_GPP_01 = 38

INIT_GPP_03 = 82

LUC_emissions_2 = LUC_emissions*control_3

$Q_{10photsynth}$ = IF control_2=1 then 1.37 else 1

Q_{10resp} = IF control_9=1 then 2 ELSE 1

Rate_coef_02 = 0.6408

Rate_coef_04 = 0.0125

Rate_coef_06 = 0.296

Rate_coef_07 = 0.757

Rate_coef_08 = 0.087

Rate_coef_09 = 0.174

Rate_coef_10 = 0.57

Rate_coef_11 = 0.84

Rate_coef_13 = 0.033

Rate_coef_14 = 0.004425

Rate_coef_15 = 0.037

LUC_emissions = GRAPH(TIME)
(1860, 0.569), (1861, 0.58), (1862, 0.521), (1863, 0.521), (1864, 0.522), (1865, 0.522), (1866, 0.522), (1867, 0.521), (1868, 0.519), (1869, 0.517), (1870, 0.516), (1871, 0.537), (1872, 0.623), (1873, 0.634), (1874, 0.641), (1875, 0.648), (1876, 0.655), (1877, 0.662), (1878, 0.669), (1879, 0.676), (1880, 0.683), (1881, 0.719), (1882, 0.673), (1883, 0.678), (1884, 0.683), (1885, 0.688), (1886, 0.69), (1887, 0.69), (1888, 0.689), (1889, 0.687), (1890, 0.686), (1891, 0.681), (1892, 0.695), (1893, 0.696), (1894, 0.713), (1895, 0.718), (1896, 0.719), (1897, 0.723), (1898, 0.725), (1899, 0.726), (1900, 0.727), (1901, 0.793), (1902, 0.797), (1903, 0.826), (1904, 0.852), (1905, 0.878), (1906, 0.909), (1907, 0.919), (1908, 0.928), (1909, 0.935), (1910, 0.941), (1911, 0.883), (1912, 0.846), (1913, 0.816), (1914, 0.805), (1915, 0.793), (1916, 0.795), (1917, 0.798), (1918, 0.801), (1919, 0.807), (1920, 0.809), (1921, 0.857), (1922, 0.849), (1923, 0.857), (1924, 0.863), (1925, 0.866), (1926, 0.871), (1927, 0.91), (1928, 0.913), (1929, 0.94), (1930, 1.02), (1931, 1.03), (1932, 0.931), (1933, 0.928), (1934, 0.915), (1935, 0.914), (1936, 0.922), (1937, 0.899), (1938, 0.902), (1939, 0.9), (1940, 0.887), (1941, 0.87), (1942, 0.891), (1943, 0.886), (1944, 0.892), (1945, 0.894), (1946, 0.977), (1947, 1.01), (1948, 1.02), (1949, 1.02), (1950, 1.04), (1951, 1.26), (1952, 1.28), (1953, 1.28), (1954, 1.34), (1955, 1.38), (1956, 1.44), (1957, 1.47), (1958, 1.52), (1959, 1.40), (1960, 1.39), (1961, 1.46), (1962, 1.46), (1963, 1.47), (1964, 1.49), (1965, 1.50), (1966, 1.54), (1967, 1.55), (1968, 1.48), (1969, 1.48), (1970, 1.44), (1971, 1.29), (1972, 1.26), (1973, 1.25), (1974, 1.25), (1975, 1.25), (1976, 1.31), (1977, 1.32), (1978, 1.31), (1979, 1.28), (1980, 1.24), (1981, 1.26), (1982, 1.46), (1983, 1.51), (1984, 1.56), (1985, 1.58), (1986, 1.60), (1987, 1.61), (1988, 1.64), (1989, 1.65), (1990, 1.64), (1991, 1.71), (1992, 1.61), (1993, 1.59), (1994, 1.58), (1995, 1.56), (1996, 1.53), (1997, 1.49), (1998, 1.49), (1999, 1.45), (2000, 1.41), (2001, 1.39), (2002, 1.52), (2003, 1.51), (2004, 1.53), (2005, 1.47), (2006, 1.41), (2007, 1.36), (2008, 1.31), (2009, 1.25), (2010, 1.20), (2011, 1.19), (2012, 1.19), (2013, 1.18), (2014, 1.18), (2015, 1.17), (2016, 1.16), (2017,

1.15), (2018, 1.15), (2019, 1.14), (2020, 1.13), (2021, 1.13), (2022, 1.13), (2023, 1.14), (2024, 1.14), (2025, 1.14), (2026, 1.13), (2027, 1.11), (2028, 1.10), (2029, 1.08), (2030, 1.06), (2031, 1.05), (2032, 1.03), (2033, 1.02), (2034, 1.00), (2035, 0.99), (2036, 0.97), (2037, 0.96), (2038, 0.94), (2039, 0.93), (2040, 0.92), (2041, 0.9), (2042, 0.89), (2043, 0.87), (2044, 0.85), (2045, 0.84), (2046, 0.82), (2047, 0.81), (2048, 0.8), (2049, 0.78), (2050, 0.77), (2051, 0.75), (2052, 0.72), (2053, 0.69), (2054, 0.67), (2055, 0.65), (2056, 0.62), (2057, 0.59), (2058, 0.57), (2059, 0.55), (2060, 0.52), (2061, 0.5), (2062, 0.47), (2063, 0.45), (2064, 0.42), (2065, 0.4), (2066, 0.37), (2067, 0.34), (2068, 0.32), (2069, 0.29), (2070, 0.27), (2071, 0.25), (2072, 0.22), (2073, 0.2), (2074, 0.17), (2075, 0.14), (2076, 0.13), (2077, 0.12), (2078, 0.11), (2079, 0.1), (2080, 0.09), (2081, 0.07), (2082, 0.06), (2083, 0.05), (2084, 0.04), (2085, 0.03), (2086, 0.02), (2087, 0.01), (2088, 0.00), (2089, -0.01), (2090, -0.03), (2091, -0.04), (2092, -0.05), (2093, -0.06), (2094, -0.07), (2095, -0.08), (2096, -0.09), (2097, -0.1), (2098, -0.11), (2099, -0.12), (2100, -0.14)

TEST

emission_sum(t) = emission_sum(t - dt) + (anthrop_emis + LUC_emis) * dt

INIT emission_sum = 0.000001

INFLOWS:

anthrop_emis = anthropogenic_CO_2_emissions_2

LUC_emis = LUC_emissions_2

atm_CO_2_as_ppm = C_IN_ATM/Gt_ppm_conversion_factor

Atm_CO_2_hist_data_&_IS92a_scenario_as_ppm = Atm_CO_2_historical_data_&_IS92a_scenario/Gt_ppm_conversion_factor

atm_C_increase = (C_IN_ATM-HISTORY(C_IN_ATM,TIME-1))*unit_correct_param

atm_C_increase_hist_data = Atm_CO_2_historical_data_&_IS92a_scenario-HISTORY(Atm_CO_2_historical_data_&_IS92a_scenario,TIME-1)

Aut_R = Resp_of_woody_tree_parts+Resp_of_ground_veg+Resp_of_NW_tree_parts

carbon_total = C_IN_ATM + ocean_sum + terrestrial_sum

control_10 = 1

control_11 = 1

control_2 = 1

control_4 = 1

control_5 = 1

control_6 = 1

control_7 = 1

control_9 = 1

GPP = Photosynt_of_ground_veg+Photosynt_of_trees

GPP_as_ppm = GPP/Gt_ppm_conversion_factor

Gt_ppm_conversion_factor = 2.123

Het_R = Resp_of_det_decomp+Resp_of_active_soil_carbon

NBP = NPP-Het_R

NPP = GPP-Aut_R

NPP_as_ppm = NPP/Gt_ppm_conversion_factor

NPP_GPP_ratio = NPP/GPP

ocean_sum = C_in_mixed_layer+Layer_01+Layer_02+Layer_03+Layer_04 + Layer_05 + Layer_06 + Layer_07 + Layer_08 + Layer_09 + Layer_10

ocean_uptake = Flux_atmosphere_to_ocean

terrestrial_uptake = anthropogenic_CO_2_emissions_2+ + LUC_emissions_2-atm_C_increase-Flux_atmosphere_to_ocean

total_respiration = Aut_R+Het_R

total_respiration_as_ppm = total_respiration/Gt_ppm_conversion_factor

unit_correct_param = 1

Atm_CO_2_historical_data_&_IS92a_scenario = GRAPH(TIME)
(1860, 608), (1861, 608), (1862, 608), (1863, 608), (1864, 609), (1865, 609), (1866, 609), (1867, 610), (1868, 610), (1869, 610), (1870, 610), (1871, 611), (1872, 611), (1873, 612), (1874, 612), (1875, 613), (1876, 614), (1877, 614), (1878, 615), (1879, 616), (1880, 617), (1881, 618), (1882, 619), (1883, 620), (1884, 621), (1885, 622), (1886, 623), (1887, 623), (1888, 624), (1889, 624), (1890, 625), (1891, 625), (1892, 625), (1893, 625), (1894, 626), (1895, 626), (1896, 626), (1897, 626), (1898, 627), (1899, 627), (1900, 628), (1901, 629), (1902, 629), (1903, 630), (1904, 631), (1905, 632), (1906, 633), (1907, 634), (1908, 635), (1909, 635), (1910, 636), (1911, 637), (1912, 638), (1913, 639), (1914, 639), (1915, 640), (1916, 641), (1917, 641), (1918, 642), (1919, 643), (1920, 643), (1921, 644), (1922, 645), (1923, 646), (1924, 646), (1925, 648), (1926, 648), (1927, 649), (1928, 650), (1929, 651), (1930, 652), (1931, 653), (1932, 654), (1933, 655), (1934, 656), (1935, 657), (1936, 658), (1937, 658), (1938, 659), (1939, 659), (1940, 659), (1941, 659), (1942, 659), (1943, 659), (1944, 658), (1945, 658), (1946, 658), (1947, 659), (1948, 659), (1949, 659), (1950, 660), (1951, 660), (1952, 661), (1953, 662), (1954, 663), (1955, 665), (1956, 666), (1957, 667), (1958, 669), (1959, 671), (1960, 673), (1961, 674), (1962, 676), (1963, 677), (1964, 679), (1965, 679), (1966, 682), (1967, 684), (1968, 686), (1969, 689), (1970, 691), (1971, 693), (1972, 695), (1973, 700), (1974, 701), (1975, 703), (1976, 705), (1977, 709), (1978, 712), (1979, 715), (1980, 719), (1981, 722), (1982, 724), (1983, 728), (1984, 731), (1985, 734), (1986, 737), (1987, 741), (1988, 746), (1989, 749), (1990, 752), (1991, 755), (1992, 756), (1993, 758), (1994, 761), (1995, 766), (1996, 769), (1997, 772), (1998, 778), (1999, 782), (2000, 784), (2001, 788), (2002, 792), (2003, 798), (2004, 801), (2005, 806), (2006, 811), (2007, 815), (2008, 818), (2009, 826), (2010, 830), (2011, 835), (2012, 839), (2013, 844), (2014, 849), (2015, 854), (2016, 859), (2017, 864), (2018, 869), (2019, 874), (2020, 879), (2021, 885), (2022, 890), (2023, 896), (2024, 901), (2025, 907), (2026, 913), (2027, 918), (2028, 924), (2029, 930), (2030, 936), (2031, 941), (2032, 947), (2033, 953), (2034, 959), (2035, 965), (2036, 971), (2037, 977), (2038, 983), (2039, 988),

(2040, 994), (2041, 1000), (2042, 1006), (2043, 1013), (2044, 1019), (2045, 1025), (2046, 1031), (2047, 1037), (2048, 1043), (2049, 1050), (2050, 1056), (2051, 1062), (2052, 1069), (2053, 1075), (2054, 1082), (2055, 1088), (2056, 1094), (2057, 1101), (2058, 1107), (2059, 1114), (2060, 1120), (2061, 1127), (2062, 1134), (2063, 1140), (2064, 1147), (2065, 1154), (2066, 1161), (2067, 1167), (2068, 1174), (2069, 1181), (2070, 1188), (2071, 1195), (2072, 1202), (2073, 1209), (2074, 1216), (2075, 1223), (2076, 1230), (2077, 1237), (2078, 1245), (2079, 1252), (2080, 1260), (2081, 1267), (2082, 1275), (2083, 1283), (2084, 1291), (2085, 1300), (2086, 1308), (2087, 1316), (2088, 1325), (2089, 1333), (2090, 1342), (2091, 1351), (2092, 1360), (2093, 1369), (2094, 1378), (2095, 1388), (2096, 1397), (2097, 1407), (2098, 1417), (2099, 1426), (2100, 1436)

Global_temp_anomaly_5_year_mean_Hansen = GRAPH(TIME)
(1882, -0.24), (1883, -0.25), (1884, -0.26), (1885, -0.29), (1886, -0.29), (1887, -0.26), (1888, -0.28), (1889, -0.28), (1890, -0.28), (1891, -0.29), (1892, -0.32), (1893, -0.3), (1894, -0.28), (1895, -0.24), (1896, -0.23), (1897, -0.2), (1898, -0.16), (1899, -0.16), (1900, -0.19), (1901, -0.2), (1902, -0.23), (1903, -0.26), (1904, -0.27), (1905, -0.3), (1906, -0.3), (1907, -0.3), (1908, -0.32), (1909, -0.35), (1910, -0.34), (1911, -0.34), (1912, -0.29), (1913, -0.25), (1914, -0.24), (1915, -0.25), (1916, -0.25), (1917, -0.26), (1918, -0.28), (1919, -0.25), (1920, -0.22), (1921, -0.19), (1922, -0.2), (1923, -0.19), (1924, -0.17), (1925, -0.14), (1926, -0.13), (1927, -0.13), (1928, -0.11), (1929, -0.11), (1930, -0.1), (1931, -0.11), (1932, -0.07), (1933, -0.08), (1934, -0.08), (1935, -0.06), (1936, 0.00), (1937, 0.02), (1938, 0.05), (1939, 0.08), (1940, 0.07), (1941, 0.06), (1942, 0.1), (1943, 0.1), (1944, 0.07), (1945, 0.07), (1946, 0.04), (1947, -0.01), (1948, -0.06), (1949, -0.05), (1950, -0.05), (1951, -0.02), (1952, -0.03), (1953, -0.02), (1954, -0.05), (1955, -0.04), (1956, -0.04), (1957, -0.01), (1958, 0.01), (1959, 0.06), (1960, 0.05), (1961, 0.05), (1962, 0.00), (1963, -0.02), (1964, -0.05), (1965, -0.06), (1966, -0.08), (1967, -0.02), (1968, 0.01), (1969, -0.01), (1970, -0.01), (1971, 0.03), (1972, 0.00), (1973, -0.02), (1974, -0.03), (1975, 0.00), (1976, -0.03), (1977, 0.00), (1978, 0.05), (1979, 0.13), (1980, 0.12), (1981, 0.17), (1982, 0.17), (1983, 0.14), (1984, 0.12), (1985, 0.16), (1986, 0.17), (1987, 0.19), (1988, 0.26), (1989, 0.3), (1990, 0.27), (1991, 0.24), (1992, 0.25), (1993, 0.25), (1994, 0.24), (1995, 0.29), (1996, 0.38), (1997, 0.39), (1998, 0.38), (1999, 0.42), (2000, 0.45), (2001, 0.45), (2002, 0.48), (2003, 0.54), (2004, 0.55), (2005, 0.55), (2006, 0.53)

Global_temp_anomaly_annual_mean_Hansen = GRAPH(TIME)

(1880, -0.25), (1881, -0.19), (1882, -0.22), (1883, -0.24), (1884, -0.3), (1885, -0.3), (1886, -0.25), (1887, -0.35), (1888, -0.26), (1889, -0.15), (1890, -0.37), (1891, -0.28), (1892, -0.32), (1893, -0.32), (1894, -0.33), (1895, -0.27), (1896, -0.17), (1897, -0.13), (1898, -0.25), (1899, -0.17), (1900, -0.1), (1901, -0.16), (1902, -0.27), (1903, -0.31), (1904, -0.34), (1905, -0.25), (1906, -0.2), (1907, -0.39), (1908, -0.34), (1909, -0.35), (1910, -0.33), (1911, -0.34), (1912, -0.34), (1913, -0.31), (1914, -0.15), (1915, -0.09), (1916, -0.3), (1917, -0.4), (1918, -0.32), (1919, -0.2), (1920, -0.19), (1921, -0.13), (1922, -0.24), (1923, -0.21), (1924, -0.21), (1925, -0.16), (1926, -0.01), (1927, -0.13), (1928, -0.11), (1929, -0.25), (1930, -0.07), (1931, -0.01), (1932, -0.06), (1933, -0.17), (1934, -0.05), (1935, -0.1), (1936, -0.03), (1937, 0.08), (1938, 0.12), (1939, 0.03), (1940, 0.05), (1941, 0.11), (1942, 0.04), (1943, 0.1), (1944, 0.2), (1945, 0.07), (1946, -0.04), (1947, 0.01), (1948, -0.04), (1949, -0.06), (1950, -0.15), (1951, -0.04), (1952, -0.03), (1953, -0.11), (1954, -0.1), (1955, -0.1), (1956, -0.17), (1957, 0.08), (1958, 0.08), (1959, 0.06), (1960, -0.01), (1961, 0.08), (1962, 0.04), (1963, 0.08), (1964, -0.21), (1965, -0.11), (1966, -0.03), (1967, 0.00), (1968, -0.04), (1969, 0.08), (1970, 0.03), (1971, -0.1), (1972, 0.00), (1973, 0.14), (1974, -0.08), (1975, -0.05), (1976, -0.16), (1977, 0.13), (1978, 0.02), (1979, 0.09), (1980, 0.18), (1981, 0.26), (1982, 0.05), (1983, 0.26), (1984, 0.09), (1985, 0.05), (1986, 0.13), (1987, 0.27), (1988, 0.31), (1989, 0.2), (1990, 0.38), (1991, 0.35), (1992, 0.12), (1993, 0.14), (1994, 0.24), (1995, 0.38), (1996, 0.3), (1997, 0.4), (1998, 0.57), (1999, 0.33), (2000, 0.33), (2001, 0.48), (2002, 0.56), (2003, 0.55), (2004, 0.48), (2005, 0.62), (2006, 0.55), (2007, 0.57), (2008, 0.44)

Ocean_uptake_historical_data = GRAPH(TIME)

(1861, 0.279), (1862, 0.279), (1863, 0.28), (1864, 0.281), (1865, 0.283), (1866, 0.286), (1867, 0.29), (1868, 0.294), (1869, 0.298), (1870, 0.304), (1871, 0.309), (1872, 0.315), (1873, 0.322), (1874, 0.329), (1875, 0.336), (1876, 0.344), (1877, 0.353), (1878, 0.361), (1879, 0.37), (1880, 0.38), (1881, 0.389), (1882, 0.399), (1883, 0.408), (1884, 0.417), (1885, 0.426), (1886, 0.435), (1887, 0.444), (1888, 0.452), (1889, 0.461), (1890, 0.468), (1891, 0.475), (1892, 0.482), (1893, 0.487), (1894, 0.492), (1895, 0.496), (1896, 0.499), (1897, 0.501), (1898, 0.503), (1899, 0.506), (1900, 0.509), (1901, 0.512), (1902, 0.517), (1903, 0.522), (1904, 0.528), (1905, 0.536), (1906, 0.544), (1907, 0.553), (1908, 0.562), (1909, 0.571), (1910, 0.58), (1911, 0.588), (1912, 0.596), (1913, 0.604), (1914, 0.611), (1915, 0.618), (1916, 0.625), (1917, 0.632), (1918, 0.638), (1919, 0.644), (1920, 0.649), (1921, 0.654), (1922, 0.659), (1923, 0.664), (1924,

0.668), (1925, 0.672), (1926, 0.675), (1927, 0.678), (1928, 0.679), (1929, 0.68), (1930, 0.681), (1931, 0.68), (1932, 0.68), (1933, 0.68), (1934, 0.68), (1935, 0.68), (1936, 0.68), (1937, 0.681), (1938, 0.683), (1939, 0.685), (1940, 0.688), (1941, 0.693), (1942, 0.698), (1943, 0.705), (1944, 0.713), (1945, 0.723), (1946, 0.734), (1947, 0.746), (1948, 0.759), (1949, 0.773), (1950, 0.789), (1951, 0.805), (1952, 0.823), (1953, 0.842), (1954, 0.862), (1955, 0.884), (1956, 0.906), (1957, 0.931), (1958, 0.956), (1959, 0.983), (1960, 1.01), (1961, 1.04), (1962, 1.07), (1963, 1.10), (1964, 1.12), (1965, 1.15), (1966, 1.19), (1967, 1.23), (1968, 1.27), (1969, 1.32), (1970, 1.38), (1971, 1.44), (1972, 1.49), (1973, 1.55), (1974, 1.60), (1975, 1.65), (1976, 1.69), (1977, 1.74), (1978, 1.79), (1979, 1.84), (1980, 1.90), (1981, 1.95), (1982, 1.99), (1983, 2.03), (1984, 2.08), (1985, 2.12), (1986, 2.16), (1987, 2.21), (1988, 2.26), (1989, 2.30), (1990, 2.34), (1991, 2.38)

terrestrial_uptake_historical_data = GRAPH(TIME)
(1960, 0.41), (1961, 0.98), (1962, 1.29), (1963, 1.49), (1964, 1.58), (1965, 1.67), (1966, 0.83), (1967, 0.69), (1968, 1.69), (1969, 0.93), (1970, 0.83), (1971, 2.33), (1972, 2.16), (1973, 0.36), (1974, 1.24), (1975, 2.87), (1976, 2.18), (1977, 1.54), (1978, 0.76), (1979, 1.27), (1980, 1.50), (1981, 1.02), (1982, 1.84), (1983, 1.48), (1984, 0.94), (1985, 1.62), (1986, 2.02), (1987, 1.68), (1988, 0.65), (1989, 1.52), (1990, 2.97), (1991, 2.94), (1992, 3.47), (1993, 3.95), (1994, 2.95), (1995, 1.86), (1996, 1.92), (1997, 2.95), (1998, 1.46), (1999, 0.61), (2000, 2.94), (2001, 3.13), (2002, 2.51), (2003, 0.98), (2004, 1.78), (2005, 2.71), (2006, 2.46), (2007, 3.16), (2008, 3.16)

<u>Not in a sector</u>
C_release_from_permafrost_as_CO_2 = Carbon_density_of_permafrost*
(thawing-freezing)*CO_2_release_fraction*(44/12)

OUTFLOW FROM: C_in_permafrost (IN SECTOR: PERMAFROST)

INFLOW TO: C_IN_ATM (IN SECTOR: ATMOSPHERIC CARBON)

APPENDIX B: LIST OF EQUATIONS FOR THE TEST RUNS

Only the equations of the variables that were changed for the relevant test runs are presented in this Appendix.

Test 01: No Anthropogenic CO_2 Emissions

control_1 = 0

control_3 = 0

Test 02: No Radiative Forcing

control_4 = 0

control_5 = 0

control_6 = 0

Test 03: No Photosynthesis

Photosynt_of_ground_veg = INIT_GPP_01*
(1+Bcoef*LOGN(C_IN_ATM/Preindustrial_C_in_atmosphere))*
$Q_{10photsynth}$^(atm_mixed_layer_temperature_change/10)*0

Photosynt_of_trees =
INIT_GPP_03*(1+Bcoef*LOGN(C_IN_ATM/Preindustrial_C_in_atmosphere))*
$Q_{10photsynth}$^(atm_mixed_layer_temperature_change/10)*0

control_1 = 0

control_3 = 0

Test 04: No Buffer Factor

Equil_C_in_mixed_layer = Preindustrial_C_in_mixed_layer*
(1+(C_IN_ATM-Preindustrial_C_in_atmosphere)/
(Preindustrial_C_in_atmosphere*Buffer_factor/Buffer_factor))

Test 06: Sensitivity of Photosynthesis to Temperature Coefficient, $Q_{10photsynth}$

$Q_{10photsynth}$ = 1.37

Test 07: Sensitivity of Respiration to Temperature Coefficient, Q_{10resp}

Q_{10resp} = 2

Test 08: Sensitivity of Wetland Methane Emissions to Temperature Coefficient of Methane Production Rate, $Q_{10\ CH4\ production}$

$Q_{10\_CH4\_production}$ = 6

Scenario 01: Abrupt Anthropogenic CO_2 Emissions Cut in 2010

control_5 = 0

control_6 = 0

anthropogenic_CO_2_emissions = GRAPH(TIME)
(1860, 0.091), (1861, 0.095), (1862, 0.097), (1863, 0.104), (1864, 0.112), (1865, 0.119), (1866, 0.122), (1867, 0.13), (1868, 0.135), (1869, 0.142), (1870, 0.147), (1871, 0.156), (1872, 0.173), (1873, 0.184), (1874, 0.174), (1875, 0.188), (1876, 0.191), (1877, 0.194), (1878, 0.196), (1879, 0.21), (1880, 0.236), (1881, 0.243), (1882, 0.256), (1883, 0.272), (1884, 0.275), (1885, 0.277), (1886, 0.281), (1887, 0.295), (1888, 0.327), (1889, 0.327), (1890, 0.356), (1891, 0.372), (1892, 0.374), (1893, 0.37), (1894, 0.383), (1895, 0.406), (1896, 0.419), (1897, 0.44), (1898, 0.465), (1899, 0.507), (1900, 0.534), (1901, 0.552), (1902, 0.566), (1903, 0.617), (1904, 0.624), (1905, 0.663), (1906, 0.707), (1907, 0.784), (1908, 0.75), (1909, 0.785), (1910, 0.819), (1911, 0.836), (1912, 0.879), (1913, 0.943), (1914, 0.85), (1915, 0.838), (1916, 0.901), (1917, 0.955), (1918, 0.936), (1919, 0.806), (1920, 0.932), (1921, 0.803), (1922, 0.845), (1923, 0.97), (1924, 0.963), (1925, 0.975), (1926, 0.983), (1927, 1.06), (1928, 1.06), (1929, 1.15), (1930, 1.05), (1931,

0.94), (1932, 0.847), (1933, 0.893), (1934, 0.973), (1935, 1.03), (1936, 1.13), (1937, 1.21), (1938, 1.14), (1939, 1.19), (1940, 1.30), (1941, 1.33), (1942, 1.34), (1943, 1.39), (1944, 1.38), (1945, 1.16), (1946, 1.24), (1947, 1.39), (1948, 1.47), (1949, 1.42), (1950, 1.63), (1951, 1.77), (1952, 1.79), (1953, 1.84), (1954, 1.87), (1955, 2.04), (1956, 2.18), (1957, 2.27), (1958, 2.33), (1959, 2.46), (1960, 2.58), (1961, 2.59), (1962, 2.70), (1963, 2.85), (1964, 3.01), (1965, 3.15), (1966, 3.31), (1967, 3.41), (1968, 3.59), (1969, 3.80), (1970, 4.08), (1971, 4.23), (1972, 4.40), (1973, 4.63), (1974, 4.64), (1975, 4.62), (1976, 4.88), (1977, 5.03), (1978, 5.11), (1979, 5.39), (1980, 5.33), (1981, 5.17), (1982, 5.13), (1983, 5.11), (1984, 5.29), (1985, 5.44), (1986, 5.61), (1987, 5.75), (1988, 5.96), (1989, 6.09), (1990, 6.14), (1991, 6.24), (1992, 6.12), (1993, 6.12), (1994, 6.24), (1995, 6.37), (1996, 6.51), (1997, 6.62), (1998, 6.59), (1999, 6.57), (2000, 6.74), (2001, 6.90), (2002, 6.95), (2003, 7.29), (2004, 7.67), (2005, 7.97), (2006, 8.23), (2007, 8.34), (2008, 8.46), (2009, 8.57), (2010, 0.00), (2011, 0.00), (2012, 0.00), (2013, 0.00), (2014, 0.00), (2015, 0.00), (2016, 0.00), (2017, 0.00), (2018, 0.00), (2019, 0.00), (2020, 0.00), (2021, 0.00), (2022, 0.00), (2023, 0.00), (2024, 0.00), (2025, 0.00), (2026, 0.00), (2027, 0.00), (2028, 0.00), (2029, 0.00), (2030, 0.00), (2031, 0.00), (2032, 0.00), (2033, 0.00), (2034, 0.00), (2035, 0.00), (2036, 0.00), (2037, 0.00), (2038, 0.00), (2039, 0.00), (2040, 0.00), (2041, 0.00), (2042, 0.00), (2043, 0.00), (2044, 0.00), (2045, 0.00), (2046, 0.00), (2047, 0.00), (2048, 0.00), (2049, 0.00), (2050, 0.00), (2051, 0.00), (2052, 0.00), (2053, 0.00), (2054, 0.00), (2055, 0.00), (2056, 0.00), (2057, 0.00), (2058, 0.00), (2059, 0.00), (2060, 0.00), (2061, 0.00), (2062, 0.00), (2063, 0.00), (2064, 0.00), (2065, 0.00), (2066, 0.00), (2067, 0.00), (2068, 0.00), (2069, 0.00), (2070, 0.00), (2071, 0.00), (2072, 0.00), (2073, 0.00), (2074, 0.00), (2075, 0.00), (2076, 0.00), (2077, 0.00), (2078, 0.00), (2079, 0.00), (2080, 0.00), (2081, 0.00), (2082, 0.00), (2083, 0.00), (2084, 0.00), (2085, 0.00), (2086, 0.00), (2087, 0.00), (2088, 0.00), (2089, 0.00), (2090, 0.00), (2091, 0.00), (2092, 0.00), (2093, 0.00), (2094, 0.00), (2095, 0.00), (2096, 0.00), (2097, 0.00), (2098, 0.00), (2099, 0.00), (2100, 0.00)

LUC_emissions = GRAPH(TIME)

(1860, 0.569), (1861, 0.58), (1862, 0.521), (1863, 0.521), (1864, 0.522), (1865, 0.522), (1866, 0.522), (1867, 0.521), (1868, 0.519), (1869, 0.517), (1870, 0.516), (1871, 0.537), (1872, 0.623), (1873, 0.634), (1874, 0.641), (1875, 0.648), (1876, 0.655), (1877, 0.662), (1878, 0.669), (1879, 0.676), (1880, 0.683), (1881, 0.719), (1882, 0.673), (1883, 0.678), (1884, 0.683), (1885, 0.688), (1886, 0.69), (1887, 0.69), (1888, 0.689), (1889, 0.687), (1890, 0.686), (1891, 0.681), (1892, 0.695), (1893, 0.696), (1894, 0.713), (1895, 0.718), (1896, 0.719), (1897,

0.723), (1898, 0.725), (1899, 0.726), (1900, 0.727), (1901, 0.793), (1902, 0.797), (1903, 0.826), (1904, 0.852), (1905, 0.878), (1906, 0.909), (1907, 0.919), (1908, 0.928), (1909, 0.935), (1910, 0.941), (1911, 0.883), (1912, 0.846), (1913, 0.816), (1914, 0.805), (1915, 0.793), (1916, 0.795), (1917, 0.798), (1918, 0.801), (1919, 0.807), (1920, 0.809), (1921, 0.857), (1922, 0.849), (1923, 0.857), (1924, 0.863), (1925, 0.866), (1926, 0.871), (1927, 0.91), (1928, 0.913), (1929, 0.94), (1930, 1.02), (1931, 1.03), (1932, 0.931), (1933, 0.928), (1934, 0.915), (1935, 0.914), (1936, 0.922), (1937, 0.899), (1938, 0.902), (1939, 0.9), (1940, 0.887), (1941, 0.87), (1942, 0.891), (1943, 0.886), (1944, 0.892), (1945, 0.894), (1946, 0.977), (1947, 1.01), (1948, 1.02), (1949, 1.02), (1950, 1.04), (1951, 1.26), (1952, 1.28), (1953, 1.28), (1954, 1.34), (1955, 1.38), (1956, 1.44), (1957, 1.47), (1958, 1.52), (1959, 1.40), (1960, 1.39), (1961, 1.46), (1962, 1.46), (1963, 1.47), (1964, 1.49), (1965, 1.50), (1966, 1.54), (1967, 1.55), (1968, 1.48), (1969, 1.48), (1970, 1.44), (1971, 1.29), (1972, 1.26), (1973, 1.25), (1974, 1.25), (1975, 1.25), (1976, 1.31), (1977, 1.32), (1978, 1.31), (1979, 1.28), (1980, 1.24), (1981, 1.26), (1982, 1.46), (1983, 1.51), (1984, 1.56), (1985, 1.58), (1986, 1.60), (1987, 1.61), (1988, 1.64), (1989, 1.65), (1990, 1.64), (1991, 1.71), (1992, 1.61), (1993, 1.59), (1994, 1.58), (1995, 1.56), (1996, 1.53), (1997, 1.49), (1998, 1.49), (1999, 1.45), (2000, 1.41), (2001, 1.39), (2002, 1.52), (2003, 1.51), (2004, 1.53), (2005, 1.47), (2006, 1.41), (2007, 1.36), (2008, 1.31), (2009, 1.25), (2010, 0.00), (2011, 0.00), (2012, 0.00), (2013, 0.00), (2014, 0.00), (2015, 0.00), (2016, 0.00), (2017, 0.00), (2018, 0.00), (2019, 0.00), (2020, 0.00), (2021, 0.00), (2022, 0.00), (2023, 0.00), (2024, 0.00), (2025, 0.00), (2026, 0.00), (2027, 0.00), (2028, 0.00), (2029, 0.00), (2030, 0.00), (2031, 0.00), (2032, 0.00), (2033, 0.00), (2034, 0.00), (2035, 0.00), (2036, 0.00), (2037, 0.00), (2038, 0.00), (2039, 0.00), (2040, 0.00), (2041, 0.00), (2042, 0.00), (2043, 0.00), (2044, 0.00), (2045, 0.00), (2046, 0.00), (2047, 0.00), (2048, 0.00), (2049, 0.00), (2050, 0.00), (2051, 0.00), (2052, 0.00), (2053, 0.00), (2054, 0.00), (2055, 0.00), (2056, 0.00), (2057, 0.00), (2058, 0.00), (2059, 0.00), (2060, 0.00), (2061, 0.00), (2062, 0.00), (2063, 0.00), (2064, 0.00), (2065, 0.00), (2066, 0.00), (2067, 0.00), (2068, 0.00), (2069, 0.00), (2070, 0.00), (2071, 0.00), (2072, 0.00), (2073, 0.00), (2074, 0.00), (2075, 0.00), (2076, 0.00), (2077, 0.00), (2078, 0.00), (2079, 0.00), (2080, 0.00), (2081, 0.00), (2082, 0.00), (2083, 0.00), (2084, 0.00), (2085, 0.00), (2086, 0.00), (2087, 0.00), (2088, 0.00), (2089, 0.00), (2090, 0.00), (2091, 0.00), (2092, 0.00), (2093, 0.00), (2094, 0.00), (2095, 0.00), (2096, 0.00), (2097, 0.00), (2098, 0.00), (2099, 0.00), (2100, 0.00)

Scenario 02: Anthropogenic CO_2 Emissions Halved in 2010

control_5 = 0

control_6 = 0

anthropogenic_CO_2_emissions = GRAPH(TIME)
(1860, 0.091), (1861, 0.095), (1862, 0.097), (1863, 0.104), (1864, 0.112), (1865, 0.119), (1866, 0.122), (1867, 0.13), (1868, 0.135), (1869, 0.142), (1870, 0.147), (1871, 0.156), (1872, 0.173), (1873, 0.184), (1874, 0.174), (1875, 0.188), (1876, 0.191), (1877, 0.194), (1878, 0.196), (1879, 0.21), (1880, 0.236), (1881, 0.243), (1882, 0.256), (1883, 0.272), (1884, 0.275), (1885, 0.277), (1886, 0.281), (1887, 0.295), (1888, 0.327), (1889, 0.327), (1890, 0.356), (1891, 0.372), (1892, 0.374), (1893, 0.37), (1894, 0.383), (1895, 0.406), (1896, 0.419), (1897, 0.44), (1898, 0.465), (1899, 0.507), (1900, 0.534), (1901, 0.552), (1902, 0.566), (1903, 0.617), (1904, 0.624), (1905, 0.663), (1906, 0.707), (1907, 0.784), (1908, 0.75), (1909, 0.785), (1910, 0.819), (1911, 0.836), (1912, 0.879), (1913, 0.943), (1914, 0.85), (1915, 0.838), (1916, 0.901), (1917, 0.955), (1918, 0.936), (1919, 0.806), (1920, 0.932), (1921, 0.803), (1922, 0.845), (1923, 0.97), (1924, 0.963), (1925, 0.975), (1926, 0.983), (1927, 1.06), (1928, 1.06), (1929, 1.15), (1930, 1.05), (1931, 0.94), (1932, 0.847), (1933, 0.893), (1934, 0.973), (1935, 1.03), (1936, 1.13), (1937, 1.21), (1938, 1.14), (1939, 1.19), (1940, 1.30), (1941, 1.33), (1942, 1.34), (1943, 1.39), (1944, 1.38), (1945, 1.16), (1946, 1.24), (1947, 1.39), (1948, 1.47), (1949, 1.42), (1950, 1.63), (1951, 1.77), (1952, 1.79), (1953, 1.84), (1954, 1.87), (1955, 2.04), (1956, 2.18), (1957, 2.27), (1958, 2.33), (1959, 2.46), (1960, 2.58), (1961, 2.59), (1962, 2.70), (1963, 2.85), (1964, 3.01), (1965, 3.15), (1966, 3.31), (1967, 3.41), (1968, 3.59), (1969, 3.80), (1970, 4.08), (1971, 4.23), (1972, 4.40), (1973, 4.63), (1974, 4.64), (1975, 4.62), (1976, 4.88), (1977, 5.03), (1978, 5.11), (1979, 5.39), (1980, 5.33), (1981, 5.17), (1982, 5.13), (1983, 5.11), (1984, 5.29), (1985, 5.44), (1986, 5.61), (1987, 5.75), (1988, 5.96), (1989, 6.09), (1990, 6.14), (1991, 6.24), (1992, 6.12), (1993, 6.12), (1994, 6.24), (1995, 6.37), (1996, 6.51), (1997, 6.62), (1998, 6.59), (1999, 6.57), (2000, 6.74), (2001, 6.90), (2002, 6.95), (2003, 7.29), (2004, 7.67), (2005, 7.97), (2006, 8.23), (2007, 8.34), (2008, 8.46), (2009, 8.57), (2010, 4.29), (2011, 4.29), (2012, 4.29), (2013, 4.29), (2014, 4.29), (2015, 4.29), (2016, 4.29), (2017, 4.29), (2018, 4.29), (2019, 4.29), (2020, 4.29), (2021, 4.29), (2022, 4.29), (2023, 4.29), (2024, 4.29), (2025, 4.29), (2026, 4.29), (2027, 4.29), (2028, 4.29), (2029, 4.29), (2030, 4.29), (2031, 4.29), (2032, 4.29), (2033, 4.29), (2034, 4.29), (2035, 4.29), (2036, 4.29), (2037, 4.29), (2038, 4.29), (2039, 4.29), (2040, 4.29), (2041, 4.29), (2042, 4.29),

(2043, 4.29), (2044, 4.29), (2045, 4.29), (2046, 4.29), (2047, 4.29), (2048, 4.29), (2049, 4.29), (2050, 4.29), (2051, 4.29), (2052, 4.29), (2053, 4.29), (2054, 4.29), (2055, 4.29), (2056, 4.29), (2057, 4.29), (2058, 4.29), (2059, 4.29), (2060, 4.29), (2061, 4.29), (2062, 4.29), (2063, 4.29), (2064, 4.29), (2065, 4.29), (2066, 4.29), (2067, 4.29), (2068, 4.29), (2069, 4.29), (2070, 4.29), (2071, 4.29), (2072, 4.29), (2073, 4.29), (2074, 4.29), (2075, 4.29), (2076, 4.29), (2077, 4.29), (2078, 4.29), (2079, 4.29), (2080, 4.29), (2081, 4.29), (2082, 4.29), (2083, 4.29), (2084, 4.29), (2085, 4.29), (2086, 4.29), (2087, 4.29), (2088, 4.29), (2089, 4.29), (2090, 4.29), (2091, 4.29), (2092, 4.29), (2093, 4.29), (2094, 4.29), (2095, 4.29), (2096, 4.29), (2097, 4.29), (2098, 4.29), (2099, 4.29), (2100, 4.29)

LUC_emissions = GRAPH(TIME)
(1860, 0.569), (1861, 0.58), (1862, 0.521), (1863, 0.521), (1864, 0.522), (1865, 0.522), (1866, 0.522), (1867, 0.521), (1868, 0.519), (1869, 0.517), (1870, 0.516), (1871, 0.537), (1872, 0.623), (1873, 0.634), (1874, 0.641), (1875, 0.648), (1876, 0.655), (1877, 0.662), (1878, 0.669), (1879, 0.676), (1880, 0.683), (1881, 0.719), (1882, 0.673), (1883, 0.678), (1884, 0.683), (1885, 0.688), (1886, 0.69), (1887, 0.69), (1888, 0.689), (1889, 0.687), (1890, 0.686), (1891, 0.681), (1892, 0.695), (1893, 0.696), (1894, 0.713), (1895, 0.718), (1896, 0.719), (1897, 0.723), (1898, 0.725), (1899, 0.726), (1900, 0.727), (1901, 0.793), (1902, 0.797), (1903, 0.826), (1904, 0.852), (1905, 0.878), (1906, 0.909), (1907, 0.919), (1908, 0.928), (1909, 0.935), (1910, 0.941), (1911, 0.883), (1912, 0.846), (1913, 0.816), (1914, 0.805), (1915, 0.793), (1916, 0.795), (1917, 0.798), (1918, 0.801), (1919, 0.807), (1920, 0.809), (1921, 0.857), (1922, 0.849), (1923, 0.857), (1924, 0.863), (1925, 0.866), (1926, 0.871), (1927, 0.91), (1928, 0.913), (1929, 0.94), (1930, 1.02), (1931, 1.03), (1932, 0.931), (1933, 0.928), (1934, 0.915), (1935, 0.914), (1936, 0.922), (1937, 0.899), (1938, 0.902), (1939, 0.9), (1940, 0.887), (1941, 0.87), (1942, 0.891), (1943, 0.886), (1944, 0.892), (1945, 0.894), (1946, 0.977), (1947, 1.01), (1948, 1.02), (1949, 1.02), (1950, 1.04), (1951, 1.26), (1952, 1.28), (1953, 1.28), (1954, 1.34), (1955, 1.38), (1956, 1.44), (1957, 1.47), (1958, 1.52), (1959, 1.40), (1960, 1.39), (1961, 1.46), (1962, 1.46), (1963, 1.47), (1964, 1.49), (1965, 1.50), (1966, 1.54), (1967, 1.55), (1968, 1.48), (1969, 1.48), (1970, 1.44), (1971, 1.29), (1972, 1.26), (1973, 1.25), (1974, 1.25), (1975, 1.25), (1976, 1.31), (1977, 1.32), (1978, 1.31), (1979, 1.28), (1980, 1.24), (1981, 1.26), (1982, 1.46), (1983, 1.51), (1984, 1.56), (1985, 1.58), (1986, 1.60), (1987, 1.61), (1988, 1.64), (1989, 1.65), (1990, 1.64), (1991, 1.71), (1992, 1.61), (1993, 1.59), (1994, 1.58), (1995, 1.56), (1996, 1.53), (1997, 1.49), (1998, 1.49), (1999, 1.45), (2000, 1.41), (2001, 1.39), (2002, 1.52), (2003, 1.51), (2004, 1.53), (2005, 1.47), (2006, 1.41),

(2007, 1.36), (2008, 1.31), (2009, 1.25), (2010, 0.6), (2011, 0.6), (2012, 0.6), (2013, 0.6), (2014, 0.6), (2015, 0.6), (2016, 0.6), (2017, 0.6), (2018, 0.6), (2019, 0.6), (2020, 0.6), (2021, 0.6), (2022, 0.6), (2023, 0.6), (2024, 0.6), (2025, 0.6), (2026, 0.6), (2027, 0.6), (2028, 0.6), (2029, 0.6), (2030, 0.6), (2031, 0.6), (2032, 0.6), (2033, 0.6), (2034, 0.6), (2035, 0.6), (2036, 0.6), (2037, 0.6), (2038, 0.6), (2039, 0.6), (2040, 0.6), (2041, 0.6), (2042, 0.6), (2043, 0.6), (2044, 0.6), (2045, 0.6), (2046, 0.6), (2047, 0.6), (2048, 0.6), (2049, 0.6), (2050, 0.6), (2051, 0.6), (2052, 0.6), (2053, 0.6), (2054, 0.6), (2055, 0.6), (2056, 0.6), (2057, 0.6), (2058, 0.6), (2059, 0.6), (2060, 0.6), (2061, 0.6), (2062, 0.6), (2063, 0.6), (2064, 0.6), (2065, 0.6), (2066, 0.6), (2067, 0.6), (2068, 0.6), (2069, 0.6), (2070, 0.6), (2071, 0.6), (2072, 0.6), (2073, 0.6), (2074, 0.6), (2075, 0.6), (2076, 0.6), (2077, 0.6), (2078, 0.6), (2079, 0.6), (2080, 0.6), (2081, 0.6), (2082, 0.6), (2083, 0.6), (2084, 0.6), (2085, 0.6), (2086, 0.6), (2087, 0.6), (2088, 0.6), (2089, 0.6), (2090, 0.6), (2091, 0.6), (2092, 0.6), (2093, 0.6), (2094, 0.6), (2095, 0.6), (2096, 0.6), (2097, 0.6), (2098, 0.6), (2099, 0.6), (2100, 0.6)

Scenario 03: Attempts for Target CO_2 Levels

anthropogenic_CO_2_emissions = GRAPH(TIME)
(1860, 0.09), (1861, 0.1), (1862, 0.1), (1863, 0.1), (1864, 0.11), (1865, 0.12), (1866, 0.12), (1867, 0.13), (1868, 0.14), (1869, 0.14), (1870, 0.15), (1871, 0.16), (1872, 0.17), (1873, 0.18), (1874, 0.17), (1875, 0.19), (1876, 0.19), (1877, 0.19), (1878, 0.2), (1879, 0.21), (1880, 0.24), (1881, 0.24), (1882, 0.26), (1883, 0.27), (1884, 0.28), (1885, 0.28), (1886, 0.28), (1887, 0.29), (1888, 0.33), (1889, 0.33), (1890, 0.36), (1891, 0.37), (1892, 0.37), (1893, 0.37), (1894, 0.38), (1895, 0.41), (1896, 0.42), (1897, 0.44), (1898, 0.47), (1899, 0.51), (1900, 0.53), (1901, 0.55), (1902, 0.57), (1903, 0.62), (1904, 0.62), (1905, 0.66), (1906, 0.71), (1907, 0.78), (1908, 0.75), (1909, 0.79), (1910, 0.82), (1911, 0.84), (1912, 0.88), (1913, 0.94), (1914, 0.85), (1915, 0.84), (1916, 0.9), (1917, 0.95), (1918, 0.94), (1919, 0.81), (1920, 0.93), (1921, 0.8), (1922, 0.84), (1923, 0.97), (1924, 0.96), (1925, 0.97), (1926, 0.98), (1927, 1.06), (1928, 1.06), (1929, 1.15), (1930, 1.05), (1931, 0.94), (1932, 0.85), (1933, 0.89), (1934, 0.97), (1935, 1.03), (1936, 1.13), (1937, 1.21), (1938, 1.14), (1939, 1.19), (1940, 1.30), (1941, 1.33), (1942, 1.34), (1943, 1.39), (1944, 1.38), (1945, 1.16), (1946, 1.24), (1947, 1.39), (1948, 1.47), (1949, 1.42), (1950, 1.63), (1951, 1.77), (1952, 1.79), (1953, 1.84), (1954, 1.87), (1955, 2.04), (1956, 2.18), (1957, 2.27), (1958, 2.33), (1959, 2.46), (1960, 2.58), (1961, 2.59), (1962, 2.70), (1963, 2.85), (1964, 3.01), (1965, 3.15), (1966, 3.31), (1967, 3.41), (1968, 3.59), (1969, 3.80), (1970, 4.08), (1971, 4.23), (1972, 4.40), (1973, 4.63), (1974, 4.64), (1975, 4.62), (1976, 4.88), (1977, 5.03), (1978, 5.11),

(1979, 5.39), (1980, 5.33), (1981, 5.17), (1982, 5.13), (1983, 5.11), (1984, 5.29), (1985, 5.44), (1986, 5.61), (1987, 5.75), (1988, 5.96), (1989, 6.09), (1990, 6.14), (1991, 6.24), (1992, 6.12), (1993, 6.12), (1994, 6.24), (1995, 6.37), (1996, 6.51), (1997, 6.62), (1998, 6.59), (1999, 6.57), (2000, 6.74), (2001, 6.90), (2002, 6.95), (2003, 7.29), (2004, 7.67), (2005, 7.97), (2006, 8.23), (2007, 8.34), (2008, 8.46), (2009, 8.57), (2010, 8.25), (2011, 7.93), (2012, 7.61), (2013, 7.29), (2014, 6.97), (2015, 6.65), (2016, 6.33), (2017, 6.01), (2018, 5.69), (2019, 5.37), (2020, 5.05), (2021, 4.73), (2022, 4.41), (2023, 4.09), (2024, 3.77), (2025, 3.45), (2026, 3.38), (2027, 3.31), (2028, 3.24), (2029, 3.17), (2030, 3.10), (2031, 3.03), (2032, 2.96), (2033, 2.89), (2034, 2.82), (2035, 2.75), (2036, 2.68), (2037, 2.61), (2038, 2.54), (2039, 2.47), (2040, 2.40), (2041, 2.33), (2042, 2.26), (2043, 2.19), (2044, 2.12), (2045, 2.05), (2046, 1.98), (2047, 1.91), (2048, 1.84), (2049, 1.77), (2050, 1.70), (2051, 1.67), (2052, 1.64), (2053, 1.61), (2054, 1.58), (2055, 1.55), (2056, 1.52), (2057, 1.49), (2058, 1.46), (2059, 1.43), (2060, 1.40), (2061, 1.37), (2062, 1.34), (2063, 1.31), (2064, 1.28), (2065, 1.25), (2066, 1.22), (2067, 1.19), (2068, 1.16), (2069, 1.13), (2070, 1.10), (2071, 1.07), (2072, 1.04), (2073, 1.01), (2074, 0.98), (2075, 0.95), (2076, 0.93), (2077, 0.91), (2078, 0.89), (2079, 0.87), (2080, 0.85), (2081, 0.83), (2082, 0.81), (2083, 0.79), (2084, 0.77), (2085, 0.75), (2086, 0.73), (2087, 0.71), (2088, 0.69), (2089, 0.67), (2090, 0.65), (2091, 0.63), (2092, 0.61), (2093, 0.59), (2094, 0.57), (2095, 0.55), (2096, 0.53), (2097, 0.51), (2098, 0.49), (2099, 0.47), (2100, 0.45), (2101, 0.445), (2102, 0.44), (2103, 0.435), (2104, 0.43), (2105, 0.425), (2106, 0.42), (2107, 0.415), (2108, 0.41), (2109, 0.405), (2110, 0.4), (2111, 0.395), (2112, 0.39), (2113, 0.385), (2114, 0.38), (2115, 0.375), (2116, 0.37), (2117, 0.365), (2118, 0.36), (2119, 0.355), (2120, 0.35), (2121, 0.345), (2122, 0.34), (2123, 0.335), (2124, 0.33), (2125, 0.325), (2126, 0.32), (2127, 0.315), (2128, 0.31), (2129, 0.305), (2130, 0.3), (2131, 0.295), (2132, 0.29), (2133, 0.285), (2134, 0.28), (2135, 0.275), (2136, 0.27), (2137, 0.265), (2138, 0.26), (2139, 0.255), (2140, 0.25), (2141, 0.245), (2142, 0.24), (2143, 0.235), (2144, 0.23), (2145, 0.225), (2146, 0.22), (2147, 0.215), (2148, 0.21), (2149, 0.205), (2150, 0.2)

Waste_decomposition = GRAPH(if control_10=1 then TIME else 0)
(1860, 0.0016), (1865, 0.0019), (1870, 0.0021), (1875, 0.0024), (1880, 0.0027), (1885, 0.003), (1890, 0.0034), (1895, 0.0039), (1900, 0.0044), (1905, 0.005), (1910, 0.0056), (1915, 0.0064), (1920, 0.0072), (1925, 0.0082), (1930, 0.0093), (1935, 0.0105), (1940, 0.0119), (1945, 0.0134), (1950, 0.0152), (1955, 0.0172), (1960, 0.0194), (1965, 0.022), (1970, 0.0249), (1975, 0.0281), (1980, 0.0318), (1985, 0.036), (1990, 0.04), (1995, 0.0395), (2000, 0.0416), (2005,

0.048), (2010, 0.048), (2015, 0.048), (2020, 0.048), (2025, 0.048), (2030, 0.048), (2035, 0.048), (2040, 0.048), (2045, 0.048), (2050, 0.048), (2055, 0.048), (2060, 0.048), (2065, 0.048), (2070, 0.048), (2075, 0.048), (2080, 0.048), (2085, 0.048), (2090, 0.048), (2095, 0.048), (2100, 0.048)

Rice_cultivation = GRAPH(if control_10=1 then TIME else 0)
(1860, 0.0401), (1865, 0.0404), (1870, 0.0407), (1875, 0.041), (1880, 0.0421), (1885, 0.0432), (1890, 0.0443), (1895, 0.0454), (1900, 0.0466), (1905, 0.0477), (1910, 0.0489), (1915, 0.0501), (1920, 0.0512), (1925, 0.0524), (1930, 0.0539), (1935, 0.0553), (1940, 0.0568), (1945, 0.0582), (1950, 0.0596), (1955, 0.0638), (1960, 0.0681), (1965, 0.0734), (1970, 0.0791), (1975, 0.0848), (1980, 0.0897), (1985, 0.095), (1990, 0.1), (1995, 0.09), (2000, 0.0953), (2005, 0.101), (2010, 0.105), (2015, 0.105), (2020, 0.105), (2025, 0.105), (2030, 0.105), (2035, 0.105), (2040, 0.105), (2045, 0.105), (2050, 0.105), (2055, 0.105), (2060, 0.105), (2065, 0.105), (2070, 0.105), (2075, 0.105), (2080, 0.105), (2085, 0.105), (2090, 0.105), (2095, 0.105), (2100, 0.105)

Domestic_ruminants = GRAPH(if control_10=1 then TIME else 0)
(1860, 0.0256), (1865, 0.0261), (1870, 0.0266), (1875, 0.0271), (1880, 0.0282), (1885, 0.0294), (1890, 0.0305), (1895, 0.0318), (1900, 0.033), (1905, 0.0344), (1910, 0.0358), (1915, 0.0373), (1920, 0.0388), (1925, 0.0404), (1930, 0.0423), (1935, 0.0443), (1940, 0.0464), (1945, 0.0486), (1950, 0.0509), (1955, 0.0557), (1960, 0.061), (1965, 0.0674), (1970, 0.0746), (1975, 0.0823), (1980, 0.0897), (1985, 0.098), (1990, 0.107), (1995, 0.12), (2000, 0.13), (2005, 0.14), (2010, 0.149), (2015, 0.149), (2020, 0.149), (2025, 0.149), (2030, 0.149), (2035, 0.149), (2040, 0.149), (2045, 0.149), (2050, 0.149), (2055, 0.149), (2060, 0.149), (2065, 0.149), (2070, 0.149), (2075, 0.149), (2080, 0.149), (2085, 0.149), (2090, 0.149), (2095, 0.149), (2100, 0.149)

Biomass_burning = GRAPH(if control_10=1 then TIME else 0)
(1860, 0.0098), (1865, 0.0105), (1870, 0.0108), (1875, 0.0113), (1880, 0.0116), (1885, 0.0128), (1890, 0.013), (1895, 0.0131), (1900, 0.0131), (1905, 0.0157), (1910, 0.0162), (1915, 0.0138), (1920, 0.014), (1925, 0.0163), (1930, 0.016), (1935, 0.0159), (1940, 0.0155), (1945, 0.0149), (1950, 0.0169), (1955, 0.0243), (1960, 0.024), (1965, 0.0295), (1970, 0.0297), (1975, 0.027), (1980, 0.0312), (1985, 0.036), (1990, 0.038), (1995, 0.0282), (2000, 0.0288), (2005, 0.0294), (2010, 0.03), (2015, 0.03), (2020, 0.03), (2025, 0.03), (2030, 0.03), (2035, 0.03),

(2040, 0.03), (2045, 0.03), (2050, 0.03), (2055, 0.03), (2060, 0.03), (2065, 0.03), (2070, 0.03), (2075, 0.03), (2080, 0.03), (2085, 0.03), (2090, 0.03), (2095, 0.03), (2100, 0.03)

Fossil_fuels = GRAPH(if control_10=1 then TIME else 0)
(1860, 0.0022), (1865, 0.0029), (1870, 0.0034), (1875, 0.0045), (1880, 0.0054), (1885, 0.0065), (1890, 0.0081), (1895, 0.0092), (1900, 0.0121), (1905, 0.0147), (1910, 0.0182), (1915, 0.0187), (1920, 0.0212), (1925, 0.022), (1930, 0.0234), (1935, 0.0209), (1940, 0.027), (1945, 0.0241), (1950, 0.0304), (1955, 0.036), (1960, 0.0446), (1965, 0.051), (1970, 0.0641), (1975, 0.0708), (1980, 0.074), (1985, 0.073), (1990, 0.081), (1995, 0.0923), (2000, 0.0938), (2005, 0.0982), (2010, 0.101), (2015, 0.101), (2020, 0.101), (2025, 0.101), (2030, 0.101), (2035, 0.101), (2040, 0.101), (2045, 0.101), (2050, 0.101), (2055, 0.101), (2060, 0.101), (2065, 0.101), (2070, 0.101), (2075, 0.101), (2080, 0.101), (2085, 0.101), (2090, 0.101), (2095, 0.101), (2100, 0.101)

N_2O_from_agriculture = GRAPH(if control_11=1 then TIME else 0)
(1860, 0.404), (1865, 0.464), (1870, 0.525), (1875, 0.585), (1880, 0.645), (1885, 0.705), (1890, 0.765), (1895, 0.826), (1900, 0.886), (1905, 0.946), (1910, 1.01), (1915, 1.07), (1920, 1.13), (1925, 1.19), (1930, 1.25), (1935, 1.31), (1940, 1.37), (1945, 1.43), (1950, 1.49), (1955, 1.55), (1960, 1.61), (1965, 1.67), (1970, 1.73), (1975, 1.79), (1980, 1.85), (1985, 1.91), (1990, 2.42), (1995, 2.73), (2000, 3.01), (2005, 3.19), (2010, 3.42), (2015, 3.42), (2020, 3.42), (2025, 3.42), (2030, 3.42), (2035, 3.42), (2040, 3.42), (2045, 3.42), (2050, 3.42), (2055, 3.42), (2060, 3.42), (2065, 3.42), (2070, 3.42), (2075, 3.42), (2080, 3.42), (2085, 3.42), (2090, 3.42), (2095, 3.42), (2100, 3.42)

Other_Anthrop_N_2O_emissions = GRAPH(if control_11=1 then TIME else 0)
(1860, 0.213), (1865, 0.283), (1870, 0.353), (1875, 0.424), (1880, 0.494), (1885, 0.565), (1890, 0.635), (1895, 0.706), (1900, 0.776), (1905, 0.846), (1910, 0.917), (1915, 0.987), (1920, 1.06), (1925, 1.13), (1930, 1.20), (1935, 1.27), (1940, 1.34), (1945, 1.41), (1950, 1.48), (1955, 1.55), (1960, 1.62), (1965, 1.69), (1970, 1.76), (1975, 1.83), (1980, 1.90), (1985, 1.97), (1990, 2.18), (1995, 2.31), (2000, 2.45), (2005, 2.65), (2010, 2.81), (2015, 2.81), (2020, 2.81), (2025, 2.81), (2030, 2.81), (2035, 2.81), (2040, 2.81), (2045, 2.81), (2050, 2.81), (2055, 2.81), (2060, 2.81), (2065, 2.81), (2070, 2.81), (2075, 2.81), (2080, 2.81), (2085, 2.81), (2090, 2.81), (2095, 2.81), (2100, 2.81)

APPENDIX C:
CALCULATION OF THE GHG RADIATIVE FORCINGS

The formulas used for radiative forcings of the greenhouse gases are taken from Houghton et. al. (1990) and arranged. For the radiative forcing coefficient of CO_2, the value proposed by Myhre et al. (1998) and then used in subsequent IPCC reports is adopted.

Table C.1 Equations for GHG radiative forcings

Greenhouse Gas	Radiative Forcing, RF (W/m^2)	Radiative Forcing Coefficient, α
CO_2	$RF = \alpha * \ln\left({}^{C}/_{C_0}\right)^*$	5.35
CH_4	$RF = \alpha * \left(\sqrt{M} - \sqrt{M_0}\right) - \left(f(M, N_0) - f(M_0, N_0)\right)^*$	0.036
N_2O	$RF = \alpha * \left(\sqrt{N} - \sqrt{N_0}\right) - \left(f(M_0, N) - f(M_0, N_0)\right)^*$	0.12

** The subscript 0 denotes the unperturbed concentration*

$$f(M,N)=0.47\ln[1+2.01*10^{-5}(MN)^{0.75}+5.31*10^{-15}M(MN)^{1.52}] \quad \text{(C.1.)}$$

C is CO_2 in ppmv

M is CH_4 in ppbv

N is N_2O in ppbv

APPENDIX D: LIST OF CONTROL SWITCHES

Table D.1 Description of purposes and functions of the control switches

Name	Purpose	State	
		1	0
Control 1	Testing the effects of anthropogenic CO_2 emissions	anthropogenic CO_2 emissions are on	anthropogenic CO_2 emissions are off
Control 2	Observing the temperature-photosynthesis feedback	The feedback is active	The feedback is inactive
Control 3	Testing the effects of LUC emissions	LUC emissions are on	LUC emissions are off
Control 4	Testing the effect of CO_2 RF to total RF	CO_2 RF exists	CO_2 RF does not exist
Control 5	Testing the effect of CH_4 RF to total RF	CH_4 RF exists	CH_4 RF does not exist
Control 6	Testing the effect of N_2O RF to total RF	N_2O RF exists	N_2O RF does not exist
Control 7	Observing the temperature-wetland emissions feedback	The feedback is active	The feedback is inactive
Control 8	Observing the temperature-permafrost melting feedback	The feedback is active	The feedback is inactive
Control 9	Observing the temperature-respiration feedback	The feedback is active	The feedback is inactive
Control 10	Testing the effects of CH_4 emissions	CH_4 emissions are on	CH_4 emissions are off
Control 11	Testing the effects of N_2O emissions	N_2O emissions are on	N_2O emissions are off